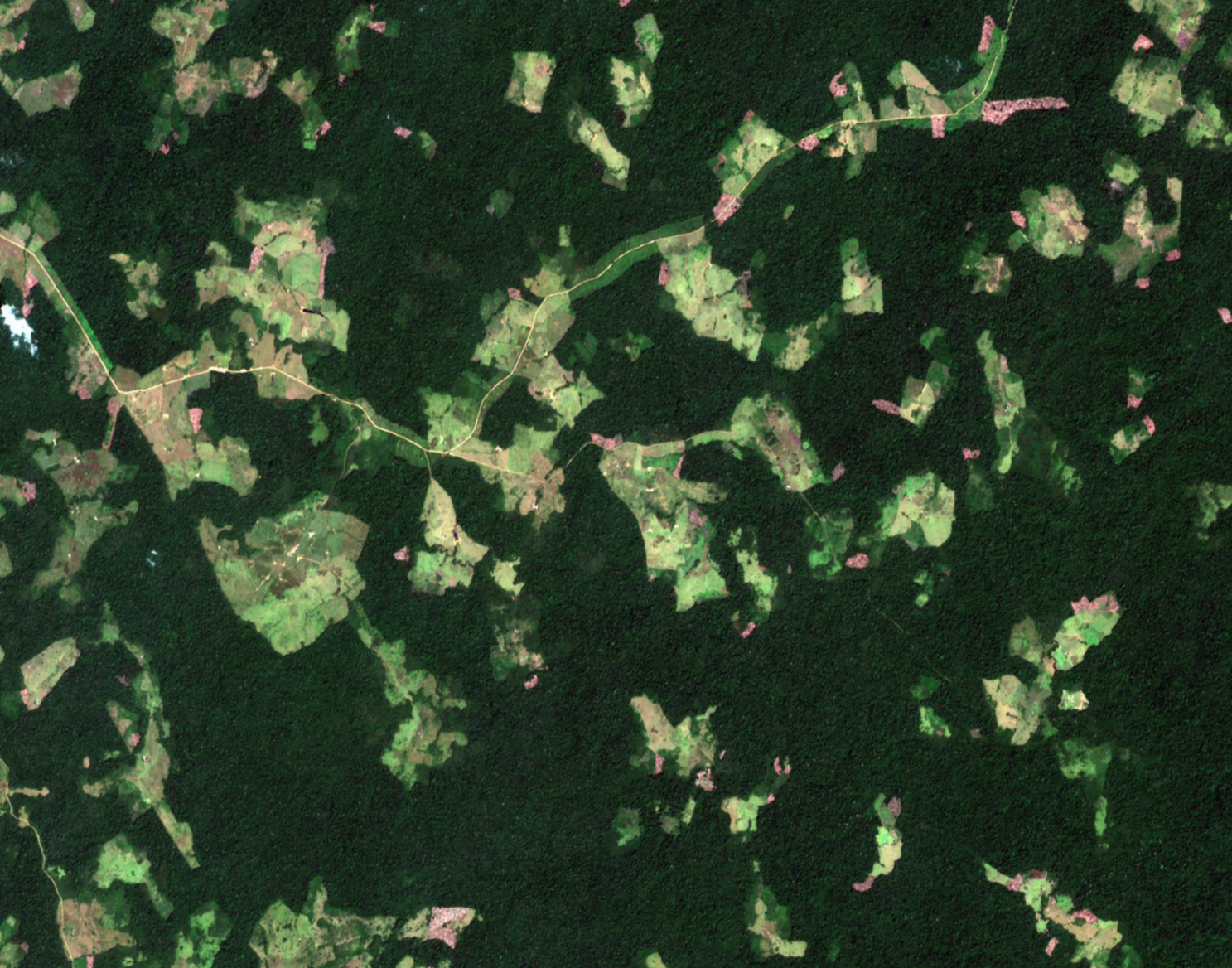


Open Source Guide to Earth Observation in Development Corporation

Methods & Guidance



MapTailor
Geospatial Consulting GbR



Version 0.9.1

Open Source Guide to Earth Observation in Development Corporation



MapTailor Geospatial Consulting GbR, KfW Development Bank, Agence Française de Développement (AFD)

About MAPME: Leveraging the potential of remote sensing for planning, monitoring and evaluating projects is MAPME's primary objective. It is a joint initiative by KfW, MapTailor Geospatial Consulting GbR, and Agence Française de Développement (AFD). MAPME is an open framework that develops and promotes open source data and tools for the relevant project management stages. It consists of the following core components: (i) Good practice guidance (this document) that describes workflows for using remote sensing data and products for planning, monitoring and evaluation; (ii) Project-related support with remote sensing analyses. Open source code and tools provided via open code repositories such as GitLab or GitHub; (iii) User-tailored trainings. More information can be found on the MAPME project homepage.

Cover image: Satellite Image: ESA, CC BY-SA 3.0 IGO, Sentinel-2, edited by MapTailor Geospatial Consulting

Recommended citation: MAPME (2021). Open Source Guide to Earth Observation in Development Corporation version 0.9.1.

Contact: contact@mapme-initiative.org

Table of contents

1.	General introduction	18
2.	Purpose of this guideline	19
3.	Who should read this study?	20
4.	Indicator #1 – forest cover.....	21
4.1.	Name and short description of the indicator	21
4.2.	Background and rationale behind indicator #1	21
4.3.	Analysis approach and tools.....	21
4.3.1.	Name of the approach.....	21
4.3.2.	The degree of processing required to achieve the desired product	22
4.3.3.	Previous applications in the scientific context.....	22
4.3.4.	Brief technical and content description of a recommended workflow	24
4.3.4.1.	Object-based supervised classification	24
4.3.4.2.	Trajectory analysis	27
4.3.5.	Required expertise	29
4.3.5.1.	Further statistics?	29
4.3.5.2.	Geodata processing and/or handling GIS?.....	29
4.3.5.3.	Technical expertise in remote sensing?.....	29
4.3.5.4.	Programming knowledge?	29
4.3.6.	How to validate the indicator maps?	29
4.3.7.	Required input data	30
4.3.7.1.	Suitable data sources for the approach	30
4.3.7.1.1.	OBIA-based supervised classification	30
4.3.7.1.2.	Trajectory-based workflow ($\Delta rNBR$)	31
4.3.7.1.3.	What limitations must be expected without in-situ data, and to what extent are other data sources suitable as substitutes for in-situ data?	32
4.3.8.	Cost benefit:.....	32
5.	Indicator #2 – forest fragmentation	34
5.1.	Name and short description of the indicator	34
5.2.	Background and rationale behind indicator #2	34
5.3.	Analysis approach and tools.....	35
5.3.1.	Name of the approach.....	35
5.3.2.	The degree of processing required to achieve the desired product	35
5.3.3.	Previous applications in the scientific context.....	35
5.3.4.	Brief technical and content description of a recommended workflow	36
5.3.5.	Required expertise	39

5.3.5.1.	Further statistics?	39
5.3.5.2.	Geodata processing and/or handling GIS?.....	39
5.3.5.3.	Technical expertise in remote sensing?.....	39
5.3.5.4.	Programming knowledge?	39
5.3.6.	How to validate the indicator maps?	39
5.3.7.	Required input data	39
5.3.7.1.	Suitable data sources for the approach	39
5.3.7.2.	What limitations must be expected without in-situ data, and to what extent are other data sources suitable as substitutes for in-situ data?.....	40
5.3.8.	Cost benefit.....	40
6.	Indicator #3 – tree types.....	42
6.1.	Name and short description of the indicator	42
6.2.	Background and rationale behind indicator #3	42
6.3.	Analysis approach and tools.....	42
6.3.1.	Name of the approach.....	42
6.3.2.	The degree of processing required to achieve the desired product	42
6.3.3.	Previous applications in the scientific context.....	42
6.3.4.	Brief technical and content description of a recommended workflow	43
6.3.5.	Required expertise	44
6.3.5.1.	Further statistics	44
6.3.5.2.	Geodata processing and/or handling GIS.....	44
6.3.5.3.	Technical expertise in remote sensing.....	45
6.3.5.4.	Programming knowledge	45
6.3.6.	How to validate the indicator maps?	45
6.3.7.	Required input data	45
6.3.7.1.	Suitable data sources for the approach	45
6.3.7.2.	What limitations must be expected without in-situ data, and to what extent are other data sources suitable as substitutes for in-situ data?.....	46
6.3.8.	Cost benefit.....	47
7.	Indicator #4 – forest biomass	48
7.1.	Name and short description of the indicator	48
7.2.	Background and rationale behind indicator #4	48
7.3.	Analysis approach and tools.....	48
7.3.1.	Name of the approach.....	48
7.3.2.	The degree of processing required to achieve the desired product	48
7.3.3.	Previous applications in the scientific context.....	49
7.3.4.	Brief technical and content description of a recommended workflow	50

7.3.4.1. RS time series metrics	50
7.3.4.2. 3D Modelling from stereo imagery.....	51
7.3.4.3. SAR Interferometry (InSAR).....	53
7.3.4.4. Multisource SAR	54
7.3.5. Required expertise	55
7.3.5.1. Further statistics	55
7.3.5.2. Geodata processing and/or handling GIS.....	55
7.3.5.3. Technical expertise in remote sensing.....	55
7.3.5.4. Programming knowledge	56
7.3.6. How to validate the indicator maps?	56
7.3.7. Required input data	56
7.3.7.1. Suitable data sources for the approach	56
7.3.7.2. What limitations must be expected without in-situ data, and to what extent are other data sources suitable as substitutes for in-situ data?.....	57
7.3.8. Cost benefit.....	57
8. Indicator #5 – individual tree crowns	59
8.1. Name and short description of the indicator	59
8.2. Background and rationale behind indicator #5	59
8.3. Analysis approach and tools.....	59
8.3.1. Name of the approach.....	59
8.3.2. The degree of processing required to achieve the desired product.....	59
8.3.3. Previous applications in the scientific context.....	59
8.3.4. Brief technical and content description of a recommended workflow	61
8.3.5. Required expertise	62
8.3.5.1. Further statistics?	62
8.3.5.2. Geodata processing and/or handling GIS?.....	62
8.3.5.3. Technical expertise in remote sensing?.....	62
8.3.5.4. Programming knowledge?	63
8.3.6. How to validate the indicator maps?	63
8.3.7. Required input data	63
8.3.7.1. Suitable data sources for the approach	63
8.3.7.2. What limitations must be expected without in-situ data, and to what extent are other data sources suitable as substitutes for in-situ data?.....	64
8.3.8. Cost benefit.....	64
9. Indicator #6 – soil erosion	65
9.1. Name and short description of the indicator	65
9.2. Background and rationale behind indicator #6	65

9.3.	Analysis approach and tools.....	65
9.3.1.	Name of the approach.....	66
9.3.2.	The degree of processing required to achieve the desired product	66
9.3.3.	Previous applications in the scientific context.....	66
9.3.4.	Brief technical and content description of a recommended workflow	67
9.3.4.1.	Mapping soil (gully) erosion using OBIA and LiDAR derivates.....	67
9.3.4.2.	Modelling the soil erosion quantity and/or risk	68
9.3.5.	Required expertise	69
9.3.5.1.	Further statistics	69
9.3.5.2.	Geodata processing and/or handling GIS.....	69
9.3.5.3.	Technical expertise in remote sensing.....	70
9.3.5.4.	Programming knowledge	70
9.3.6.	How to validate the indicator maps?	70
9.3.7.	Required input data	70
9.3.7.1.	Suitable data sources for the approach	70
9.3.7.1.1.	Mapping soil (gully) erosion using OBIA and LiDAR derivates	70
9.3.7.1.2.	Soil erosion modelling and risk assessment.....	70
9.3.7.2.	What limitations must be expected without in-situ data, and to what extent are other data sources suitable as substitutes for in-situ data?.....	71
9.3.8.	Cost benefit.....	72
10.	Indicator #7 – afforestation and reforestation	74
10.1.	Name and short description of the indicator	74
10.2.	Background and rationale behind indicator #7	74
10.3.	Analysis approach and tools	75
10.4.	Name of the approach.....	75
10.5.	The degree of processing required to achieve the desired product	76
10.6.	Previous applications in the scientific context.....	76
10.6.1.1.	Quantifying the success rates.....	78
10.6.1.2.	Vegetation growth monitoring (as a proxy for afforestation success)	79
10.6.2.	Required expertise	81
10.6.2.1.	Further statistics?	81
10.6.2.2.	Geodata processing and/or handling GIS?.....	81
10.6.2.3.	Technical expertise in remote sensing?.....	81
10.6.2.4.	Programming knowledge?	81
10.6.3.	How to validate the indicator maps.....	82
10.6.4.	Required input data	82
10.6.4.1.	Suitable data sources for the approach	82

10.6.4.1.1. Quantifying the success rates.....	82
10.6.4.1.2. Vegetation growth monitoring.....	83
10.6.5. What limitations must be expected without in-situ data, and to what extent are other data sources suitable as substitutes for in-situ data?.....	84
10.6.6. Cost benefit	84
11. Indicator #8 – Assessment of vegetation cover change and land degradation	87
11.1. Name and short description of the indicator	87
11.2. Background and rationale behind indicator #8	87
11.3. Analysis approach and tools	87
11.4. Name of the approach.....	88
11.5. The degree of processing required to achieve the desired product	88
11.6. Previous applications in the scientific context.....	88
11.6.1.1. Mapping trends in vegetation cover using satellite-based vegetation index	89
11.6.2. Required expertise.....	92
11.6.2.1. Further statistics?	92
11.6.2.2. Geodata processing and/or handling GIS?.....	92
11.6.2.3. Technical expertise in remote sensing?.....	93
11.6.2.4. Programming knowledge?	93
11.6.3. How to validate the indicator maps?	93
11.6.4. Required input data	93
11.6.4.1. Suitable data sources for the approach.....	93
11.6.5. Cost-benefit:	95
12. Indicator #9 – Cropland / crop type mapping.....	96
12.1. Name and short description of the indicator	96
12.2. Background and rational for indicator #9.....	96
12.3. Definitions.....	97
12.4. Analysis approach and tools	97
12.4.1. Name of the approach	97
12.4.2. The degree of processing to the desired product.....	98
12.4.3. Previous applications in the scientific context	98
12.4.4. Brief technical and content description of a recommended workflow	100
12.4.4.1. Supervised image classification to create crop type maps	100
12.4.5. What expertise is required?	104
12.4.5.1. Further statistics?	104
12.4.5.2. Geodata processing and/or handling GIS?.....	105
12.4.5.3. Technical expertise remote sensing?.....	105
12.4.5.4. Programming knowledge?	105

12.4.6.	How to validate the indicator maps?	105
12.4.7.	Required input data	105
12.4.7.1.	Which data sources are suitable for the approach?.....	105
12.4.7.1.1.	What limitations must be expected without in-situ data, and to what extent are other data sources suitable as substitutes for in-situ data?.....	107
12.4.8.	Cost-benefit:.....	109
13.	General conclusion and recommendations	111
14.	References	114
15.	Annex (external documents).....	121

List of figures

Figure 1: Detailed flow chart and visualisation of the key processing steps used to derive canopy cover change maps based on supervised image classification to create one annual forest map.....	26
Figure 2: Detailed flow chart and visualisation of the key processing steps used to derive canopy cover disturbance ($\Delta rNBR$) maps based on change detection analysis from two periods.....	27
Figure 3: Overview of required data sets and information in object-based supervised image classification.....	30
Figure 4: Overview of required data sets and information in NBR analysis.....	31
Figure 5: Guide for selecting proper imagery and methods for assessing forest cover change. The "gold standard" is highlighted in yellow colours. It provides the best results in terms of spatial detail.....	33
Figure 6: Flow chart and visualisation of the key processing steps used to derive forest fragmentation statistics from two periods.....	38
Figure 7: Overview of required data sets and information in forest fragmentation analysis.....	40
Figure 8: Guidance for selecting proper imagery and methods for assessing forest fragmentation. The "gold standard" is highlighted in yellow colours. It provides the best results in terms of spatial detail.....	41
Figure 9: Flow chart and visualisation of the key processing steps used to derive tree type maps based on supervised image classification in one period. Note that object-based image analysis is not mandatory or even possible when using medium resolution satellite images.....	44
Figure 10: Very high-resolution images in Google Earth showing the development of plantations in Cambodia. Left: 2010, Right: 2018.....	46
Figure 11: Overview of required data sets and information for creating forest type maps.....	47
Figure 12: Flow chart for biomass estimation based on optical and SAR data fusion	51
Figure 13: Flow chart for biomass estimation based on optical stereo image analysis.....	52
Figure 14: A schematic depiction of the laser pulse and response within forest canopies (from: Leiterer et al. 2015 ¹).....	53
Figure 15: Flow chart for biomass estimation based on SAR Interferometry	54
Figure 16: Flow chart for biomass estimation based on SAR data analysis with different signal wavelengths.....	55
Figure 17: Very high-resolution images in Google Earth showing the development of plantations in Cambodia. Left: 2010, Right: 2018.....	56
Figure 18: Three Important LiDAR Data Products: DSM, DTM, CHM.....	61
Figure 19: Flow chart and visualisation of the key processing steps used to derive individual tree crown maps.....	62
Figure 20: Overview of required data sets and information for creating single tree crown maps.	64
Figure 21: Flow chart and visualisation of the key processing steps used to derive gully erosion maps.....	68
Figure 22: Flow chart and visualisation of the key processing steps used to model soil erosion using RUSLE.	69
Figure 23: Overview of required data sets and information for creating soil erosion (gully) maps....	72

Figure 24: Guidance for selecting proper imagery and methods for assessing soil erosion (especially gully erosion). The “gold standard” is highlighted in yellow colours. It provides the best results in terms of spatial and thematic detail.	73
Figure 25: Afforestation planting seen in a very high-resolution satellite image in the Aralkum desert, Central Asia. Source: Google Earth.	75
Figure 26: Left: Afforestation planting seen in a very high-resolution satellite image. Right: Assessment of afforestation success rate. Source: Google Earth, Analysis: MapTailor Geospatial Consulting GbR.	77
Figure 27: Schematic overview of remote sensing-based monitoring of vegetation growth.	78
Figure 28: Detailed flow chart and visualisation of the key processing steps used to assess the survival rate of seedlings in afforestation/reforestation locations.	79
Figure 29: Detailed flow chart and visualisation of the key processing steps used to assess changes in vegetation cover in afforestation/reforestation locations.	80
Figure 30: Overview of required data sets and information for creating vegetation change maps....	81
Figure 31: Overview of required data sets and information for creating survival rate maps.	82
Figure 32: Overview of required data sets and information in NBR analysis.	83
Figure 33: Guidance for selecting proper imagery and methods for assessing afforestation/reforestation success. The “gold standard” is highlighted in yellow colours. It provides the best results in terms of spatial and thematic detail.	85
Figure 34: Example of a map showing the trend in vegetation cover in Kenya the period 1997-2020. Source: MapTailor GbR.	87
Figure 35: Idealized and very simplified scheme of the vegetation cover trend assessment. Annual satellite image composites are used to calculate annual vegetation indices, which proxy biomass. The temporal change (trend) of these vegetation index values is used to identify regions with positive or negative vegetation index trends. Source: MapTailor GbR.....	88
Figure 36: Detailed flow chart and visualisation of the key processing steps used to assess changes in vegetation cover / land productivity (left: linear trend of vegetation index against time, right: linear trend of residuals against time).	92
Figure 37: Overview of required data sets and information in vegetation trend analysis.....	94
Figure 38: Example for crop type maps in different years in Senegal, which are the basis for quantifying crop specific area and change. Such maps are also the basis for other tasks in remote sensing, such as crop yield modelling. Source: MapTailor Geospatial Consulting GbR.....	97
Figure 39: General mapping workflow, first, cropland is identified, second, crop types are mapped. When such maps are created in different years, indicators of crop intensity can be calculated.....	98
Figure 46: Guidance to select a proper workflow for assessing cropland / crop type acreage. The “gold standard” is highlighted in yellow colours.	101
Figure 40: General scheme of temporal compositing.....	102
Figure 41: Detailed flow chart and visualization of the major processing steps to derive cropland and crop type maps based on supervised image classification.....	104
Figure 42: Overview of required data sets and information in supervised image classification.....	106
Figure 43: Examples of crop calendars by FAO.....	107
Figure 44: Examples of the Collect Earth platform used to collect reference data. Source: http://www.openforis.org/tools/collect-earth/case-study.html	108

Figure 45: Guidance to select proper and methods for assessing cropland / crop type acreage. The “gold standard” is highlighted in yellow colours.	110
Figure 47: Suitability of different spatial resolution systems for assessing six forest indicators.	112
Figure 48: Recommended workflows and data sets regarding observation frequency.	113

List of tables

Table 1: Set of project indicators and their definition.	19
Table 2: Summary of two approaches and the rationale behind selecting one of them.....	21
Table 3: Overview of projects, scientific publications and most important findings.....	23
Table 4: Freely available software and tools suitable for calculating indicator #1 – “forest cover” supervised image classification workflow.	26
Table 5: Freely available software and tools suitable for calculating indicator #1 “forest cover” – trajectory workflow.....	29
Table 6: Overview of projects, scientific publications and most important findings.....	35
Table 7: Recommended set of forest fragmentation metrics and their definition. The names in the first column are taken from the R package ‘SDMTools’	36
Table 8: Available and recommended software packages to calculate forest fragmentation metrics.	38
Table 9: Overview of projects, scientific publications and most important findings.....	43
Table 10: Overview of projects, scientific publications and most important findings.....	49
Table 11: Overview of projects, scientific publications and most important findings.....	60
Table 12: Freely available software and tools suitable for calculating indicator #5 “Single tree crowns”	61
Table 13: Summary of two approaches and the rationale behind selecting one of them.....	66
Table 14: Freely available software and tools suitable for calculating indicator #6 “soil erosion”. For LiDAR processing (e.g. creation of DEM), please refer to Table 12.	69
Table 15: Potentially useful data sources for deriving six parameters of the (R)USLE model.	71
Table 16: Summary of two approaches and the rationale behind selecting one of them.....	75
Table 17: Examples of freely available geodata that can be used to understand the impact of environmental and other conditions on afforestation/reforestation success or failure.....	85
Table 18: Set of potential indicators that can be computed based on seasonal and multi-seasonal cropland / crop type maps.	99
Table 19: Overview and description of some vegetation indices, that can be calculated based on the temporal aggregates and used as input for the classifier algorithm. The band names and the corresponding band identifier are at the example of Sentinel-2.	102
Table 20: Freely available software and tools that is suitable for calculating indicator #8 “Cropland / crop type mapping” – Supervised image classification workflow.	104
Table 21: Overview of some satellite system properties and crop mapping requirements. See Annex 1 for a detailed description of individual satellite systems.....	106
Table 22: Examples for crowd-sourced and/or freely available reference data sets (cropland and/or crop type specific)	108
Table 23: Examples for tools potentially suitable for on-screen collection of reference data.....	108

Abbreviations:

ABA	Area-Based Approaches
ALS	Airborne Laser Scanning
CHIRPS	Climate Hazards Group InfraRed Precipitation with Station data
CHM	Canopy Height Models
CRU	Climatic Research Unit
CTI	Compound Topographic Index
DEGRAD	Forest Degradation Mapping in the Brazilian Amazon (Project name)
DEM	Digital Elevation Model
DL	Deep Learning
DSM	Digital Surface Model
DTM	Digital Terrain Model
FAO	Food and Agricultural Organization of the United Nations
FFM	Forest Fragmentation Metrics
GEE	Google Earth Engine (cloud-based platform for processing and analysing geodata, e.g., satellite images)
GHG	Green House Gas
GIS	Geographic Information Systems
GPS	Global Position System
GUI	Graphical User Interface
ITC	Individual Tree Crown
ITD	Individual Tree Detection
IPCC	Intergovernmental Panel for Climate Change
LiDAR	Light Detection And Ranging
MR	Medium Resolution data (here: > 10m, usually freely available)
MUSLE	Modified Universal Soil Loss Equation
NASA	National Aeronautics and Space Administration
NBR	Normalized Burn Ratio (vegetation index, used as a value to assess forest cover change)
NIR	Near Infrared part of the electromagnetic spectrum
OBIA	Object-Based Image Analysis
PRODES	Projeto de Monitoramento do Desmatamento na Amazônia Brasileira por Satélite
REDD+	Reducing Emissions from Deforestation and Degradation
RF	Random Forest (non-parametric machine learning algorithm)
RUSLE	Revised Universal Soil Loss Equation
SFM	Sustainable Forest Management
SMA	Spectral Mixture Analysis
SVM	Support Vector Machines (non-parametric machine learning algorithm)
SWIR	Shortwave Infrared part of the electromagnetic spectrum
VHR	Very High Resolution (here: < 10m, usually not freely available)
TOA	Top Of Atmosphere (reflectance recorded in the sensor without atmospheric correction)
TOC	Top Of Canopy (reflectance recorded in the sensor, corrected for atmospheric effects)
USGS	United States Geological Survey
USLE	Universal Soil Loss Equation
VIS	Visible for human eyes, part of the electromagnetic spectrum between circa 400–700nm
WRI	World Resources Institute

Terminology:

Agricultural land: Total of cropland and permanent meadows and pastures.

Arable land: Land that is used in most years for growing temporary crops.

Afforestation: Afforestation is the conversion from other land uses into forest, or the increase of canopy cover to above a certain (e.g. nationally) predefined threshold (e.g. 10%). Afforestation is the reverse of deforestation and includes areas that are actively converted from other land uses into forest through silvicultural measures. Afforestation also includes natural transitions into forest, for example on abandoned agricultural land or in burnt-over areas that have not been classified as forest during the barren period.

Airborne: Remote sensing data can be collected from the ground, the air (using airplanes or helicopters) or from space. Airborne refers to instruments on-board of airplanes or helicopters.

Calibration: The calibration data set supports the training of algorithms to generate, for instance, a land cover map, a cropland mask or a crop type map.

Clearcutting: Also, occasionally known as clearfelling – is when every single marketable tree is cut down from a selected area.

Composites: Compositing refers to the process of combining spatially overlapping images into a single image based on an aggregation function.

Cropland: Arable land and land under permanent crops.

Crop calendar: Crop calendars describe the major phenological phases of crops during the growing season. Ground data collection should coincide with the period in crop growth during which the crop type can most easily be identified (e.g. during the periods of flowering, fruit development and reproduction). For regions with a simple single cropping season, one observation per field per season is usually adequate, while in regions with double cropping (intra-annual crop rotation), two visits – one per crop cycle – might be required on the same field).

Deforestation: Deforestation is the conversion of forested areas to non-forest land use such as arable land, urban use, logged area or wasteland. According to FAO¹, deforestation is the conversion of forest to another land use or the long-term reduction of tree canopy cover below a certain (e.g. nationally) pre-defined threshold (e.g. 10%). Deforestation can result from deliberate removal of forest cover for agriculture or urban development, or it can be an unintentional consequence of uncontrolled grazing (which can prevent the natural regeneration of young trees). The combined effect of grazing and fires can be a major cause of deforestation in dry areas.

Features: In the context of this study, this term will be used as any spectral, spatial, temporal, topographic or any other data used for performing image segmentation or to infer the classification function (e.g. input to supervised image classification through machine learning algorithms). In other words, features can be seen as input or predictive variables (more in a classification sense).

Forest cover: Forest cover is one category of terrestrial land cover. Land cover is the observed physical features, both natural and man-made, that occupy the Earth's immediate surface. For example, forest cover can

¹ <http://www.fao.org/3/a-ap163e> (last accessed 11 September 2020).

be defined as 25% or greater canopy closure at the Landsat pixel scale (30m × 30m spatial resolution) for trees >5m in height.

Forest fragmentation: Simply defined, forest fragmentation refers to any process that results in the conversion of formerly continuous forest into patches of forest separated by non-forested lands. The definitions of fragmentation are as diverse as the subject itself.

Forest degradation: Forest degradation is a process leading to a ‘temporary or permanent deterioration in the density or structure of vegetation cover or its species composition’. It is a change in forest attributes that leads to a lower productive capacity caused by an increase in disturbances. The time-scale of forest degradation processes is in the order of a few years to a few decades.

Ground survey: Collection of reference data by means of visiting locations on ground (*in situ*) and collecting and recording relevant information, such as GPS points.

Image segmentation: It can be tentatively defined as the process of partitioning an image into multiple segments (sets of pixels); or to decompose an input image into smaller non-overlapping parts (segments) that are meaningful with respect to a particular task.

(Image) segments: A set of pixels with similar spectral (or other) characteristics.

(Image) object: Image segments after being populated with spectral, spatial, temporal or other attributes/data.

Indicator map: In this study, this term refers to digital map products that contain information about one of the success indicators, such as forest cover or tree type.

In-situ data: Ground collected reference data are observations of some property of the Earth surface on the ground through observations in the field. To give one example, in-situ data used in crop type classification can be collected via agricultural field surveys. Operators inspect fields and make records of important information about the crop that is cultivated – such as crop type, growth stage, etc. – along with the geographic location of the observation with a GPS. It can be regarded as a particular type of -> *Reference data*.

Land cover: Observed (bio)physical cover on the earth’s surface, for example forests.

Land use: Describes the human-environment interaction and is characterized by the activities of people to maintain a certain land cover type, for example cropland or agroforestry.

LiDAR: LiDAR (Light Detection and Ranging) is a surveying technique that uses light in the form of pulsed laser to measure variable distances. It is used to make high-resolution point clouds of terrain, is also referred to as ‘laser scanning’ or ‘3D scanning’, and has terrestrial airborne and mobile applications. Like radar, a LiDAR instrument is an active remote sensing instrument.

Machine learning: is the scientific study of algorithms and statistical models that computer systems use to perform a specific task without using explicit instructions, relying on patterns and inference instead. It is seen as a subset of artificial intelligence. Machine learning algorithms build a mathematical model based on sample data, known as “training data”, in order to make predictions or decisions without being explicitly programmed to perform the task. In remote sensing, it is used to create thematic maps (supervised classification) or regression modelling.

Metadata: Metadata are data that describe data, i.e. information on other geodata. ISO standard 19115-1:2014 defines the schema required for describing geographic information and services by means of metadata.

Metadata should provide information on the identification, spatial extent, quality, spatial and temporal aspects, content, spatial cartographic reference, licensing policy, as well as other properties.

Multi-class: Here, it is defined as a type of supervised classification problem with multiple ($n \geq 2$) mutually exclusive classes. Typically used when mapping a whole region into discrete land cover classes (e.g., forest, agriculture, urban).

Multispectral: Here it refers to so-called “passive” or optical sensors on-board of satellites, aircraft or drones that capture light reflected or emitted from the earth surface.

Optical data: Sometimes it is also referred to as multi-spectral data. Unlike LiDAR or Radar, optical or multispectral data are acquired by passive remote sensing instruments.

Reference data: Information about land cover / land use or other biophysical parameters (such as plant biomass) unambiguously described (e.g. taking photographs and comprehensive description according to LCCS) and associated with a certain location and time through GPS (or other means such as Galileo). Reference data is used to calibrate and validate algorithms (e.g. -> *Supervised classification*) and can come from various sources: field trips (-> in-situ data or other VHR data such as Google Earth).

Reforestation: Reforestation is the re-establishment of forest formations after temporary conditions with canopy cover below a certain (e.g. nationally) predefined threshold (e.g. 10%) due to anthropogenic or natural perturbations.

Remote sensing: Remote sensing is the process of detecting and monitoring the physical characteristics of the Earth’s surface by measuring its reflected and emitted radiation from a remote platform (typically from satellite, airplane, or drones). Different sensors exist, such as optical, Synthetic Aperture Radar, or Lidar.

Sampling unit: The unit at which the reference data is collected. It forms the basis for the comparison of the reference data and map that was created with remote sensing analysis (e.g. a crop type map). It can be a pixel, polygon (segment), or pixel block. Usually, the pixel is chosen as the spatial unit, but any of the types can be used.

Selective logging: This is the logging practice of entering a forest and only removing some trees, usually those which are unhealthy or in dense areas.

Single-class: Here, it is defined as a type of supervised classification problem with only one class with two mutually exclusive levels (e.g., species presence/absence, burned/unburned, cut/uncut forest).

Space-borne: Remote sensing data can be collected from the ground, the air (using airplanes or helicopters) or from space. Space-borne refers to instruments on-board of satellites.

Stratification: Stratification is the process of subdividing the study area into smaller areas (strata), in which each assessment unit is assigned to a single stratum. One purpose of stratification is ensuring a sufficient representation of land use / land cover category, which only represent a small proportion of the study area.

Supervised classification: Supervised Classification is a fundamental task in remote sensing analysis; it attempts to categorize and label (“classify”) groups of pixels or vectors within a remote sensing image by assigning it to a specific class label (e.g. a crop type, or a land cover category such a forest), based on specific rules or machine learning algorithms.

Time series: A collection of remote sensing images from one location but different times (different acquisition dates). An example is a collection of 16-day Landsat images from January to December in any given year. Time series of remote sensing images are used as input in vegetation trend analysis or in -> *Supervised classification*.

Validation: The main objectives of validation are providing a concise accuracy assessment for map products that were created based on the analysis of remote sensing images, for example crop type maps or forest cover maps. Validation data set is a high-quality reference data set, to be used to assess the accuracy of a map.

Windshield: Windshield sampling is a jargon describing a reference data collection along the road infrastructure in a study area. It supports an easier and faster data collection, especially in badly assessible areas, yet, the diversity of the observed objects (e.g. crop diversity), and the spatial non-randomness data collected in this fashion, can introduce statistical bias that must be evaluated carefully before use

1. General introduction

The disadvantages of deforestation are increased carbon dioxide emissions and soil erosion as well as the destruction of forest habitat and the loss of biological diversity of both plants and animals. Deforestation, particularly in tropical countries, is widely acknowledged to account for as much as 20% of global greenhouse gas (GHG) emissions (Achard et al., 2007). In addition, any reduction in deforestation is estimated to have an immediate positive impact on reducing global GHG emissions. This has been recognised through various initiatives; the most widely studied of these initiatives was reducing emissions from deforestation and degradation (REDD+)².

Planting trees and REDD+ are considered as some of the potentially effective ways to avoid emissions and capture carbon from the atmosphere to mitigate climate change. While there is controversy about this measure's scale of usefulness, an increasing number of projects are being implemented to either protect standing forest or reforest degraded areas.

Evaluating the effectiveness of these and other projects is increasingly done with the help of satellite images, because they help to create before-and-after-treatment comparisons and transparently quantify the outcomes of an intervention. Satellite images facilitate back-tracing and monitoring forest cover changes in large and inaccessible areas. Currently, mainstream evaluation efforts in the area of REDD+ mainly address large-scale, clear-cut deforestation and forest-cover loss which is detectable in optical imagery, even with moderate spatial resolution and often available as a pre-processed product, e.g. a digital map or web application (Hansen et al., 2013; Souza et al., 2013).

However, assessing changes that occur on a smaller scale in forest areas is of paramount importance from a practical perspective because most forest related projects have success indicators that are only measurable on that scale (e.g. selective logging, forest management practices, biodiversity conservation and reforestation on small agricultural plots). Usually, this requires the acquisition and analysis of very high resolution images (VHR³) (Lima et al., 2019).

The current practice of mapping forest inventory and area cover gain/loss using traditional inventories (field surveys) can be challenging due to the large scale, inaccessible areas (e.g. due to conflicts) or can be prohibitively expensive. While remote sensing is a suitable asset in general and it does in fact provide archive data, existing sources of forest maps are not necessarily fit for this purpose because they do not consider the very specific definitions of "success indicators" in an evaluation context and the spatial scale of their implementation. Hence, new methods need to be developed and evaluated to improve good practice guidance.

Both forest resource managers and forest ecosystem scientists therefore need to develop new tools to take advantage of an ever-increasing number of satellite images with higher spatial and temporal resolution. A higher spatial resolution as found in satellite systems such as SPOT-6/-7 (@1.5m)⁴ and Pleiades 1A/1B (@0.5m) can contribute significantly to the success of the project evaluation process for thematic mapping of issues like forest cover loss and single tree logging, especially in dense forest areas (Dalagnol et al., 2019; Schepaschenko et al., 2019). VHR satellite imagery would also be useful for distinguishing between tree cover classes (forest area, riparian forests, shrubland, mixed forests, plantations, orchards) as the mixed pixel effects from lower resolution imagery, i.e. medium resolu-

² <https://redd.unfccc.int/> (last accessed 19 August 2019).

³ Throughout this study, we define very high-resolution imagery (VHR) as images with a ground sampling distance (GSD) smaller than 10m. This corresponds to the highest, freely available GSD recently provided by Sentinel-2. While remote sensing also encompasses carrier systems other than satellites (drones, aerial), in this report the term VHR refers to satellite images if not otherwise stated.

⁴ <https://www.satimagingcorp.com/satellite-sensors/> for a good overview (last accessed 30 November 2019).

tion (MR) (e.g. Sentinel-2 @10m, Landsat 8 @30m) are diminished or even eliminated (Li et al., 2015).

Impact evaluation requires a specific set of indicators, which often entail concise and sophisticated definitions (such as "area under sustainable forest management, SFM, including selective logging"). Standardised products are not yet available for these purposes, and the requirements in terms of optimal pixel size and temporal resolution still need to be specified in an operational context. Very few peer-reviewed studies report explicitly on the use of remote sensing in project evaluation (Panlasigui et al., 2018; Zhang et al., 2018).

2. Purpose of this guideline

While there are very sophisticated methods in remote sensing science, the approaches must be practical and easy to implement from the point of view of the users. Therefore, the focus of this study is on pragmatic approaches that deliver robust and accurate results that still meet scientific standards. As such, this study aims to provide the basis for good practice for the application of remote sensing in forest project evaluation.

This is designed as a systematic review that shows how a set of dedicated project indicators can be assessed and mapped by means of analysing remote sensing data, using geographic information systems (GIS) and non-proprietary programming languages (e.g. R tools or Python), and by applying existing, globally available and preferably free data (in particular satellite images) and products (i.e. information derived from satellite images). The review contains good practice guidance for assessing six project impacts according to six dedicated indicators (Table 1):

Table 1: Set of project indicators and their definition.

Indicator ID	Indicator name	Indicator description	Section
#1	Forest cover	Defined as the spatial coverage of treed vegetation, proxy for deforestation & reforestation activities, including area coverage vs individual tree coverage, e.g. transition from extensive deforestation to selective logging and deforestation from clearcutting	4
#2	Forest fragmentation	Defined as the spatial configuration of treed vegetation, quantified by spatial indicators of forest patch fragmentation, proxy for forest quality and forest/timber harvesting management	5
#3	Tree types	Defined as broad categories of treed vegetation (e.g. broad-leaved vs needle-leaved, natural vs plantations)	6
#4	Biomass	Defined as the quantity of woody biomass	7
#5	Individual tree crowns	Defined as the top part of the tree, which features branches that grow out from the main trunk and support the various leaves used for photosynthesis.	8
#6	Soil erosion	Deforestation-induced erosion (especially gully erosion, i.e. removal of soil along drainage lines by surface water runoff)	9
#7	Afforestation and reforestation	Establishment of a forest or stand of trees (forestation) in an area where there was no previous tree cover (e.g. due to previous deforestation, or conversion of land use)	10
#8	Vegetation cover change and land degradation	Defined as loss of vegetation cover, i.e. as a result of ongoing degradation due to overgrazing or other causes	11
#9	Cropland / crop type mapping	Defined as the area (e.g. in hectares) of specific land uses (crop types), and its change over time	12

Each section is introduced with general background information and explains the rationale for each indicator. It is followed by a proposal for a workflow, composed of a specific set of methods and data that are recommended for assessing and mapping each indicator. The choice for specific methods and data was guided by these priorities:

- Methods should be:
 - fully reproducible and – if possible – applicable globally
 - straightforward in their implementation
 - previously cited and published in peer-review journals
 - focused on open-source software
 - able to produce accurate results
- Data sets used should be:
 - freely available
 - able to allow back-tracing (archive data)
 - from missions with global coverage and continuity (long-term missions such as Land-sat or Sentinel) in ideal cases, and similar characteristics (e.g. multispectral bands) to foster comparability of evaluations

Priority was given to presenting one workflow per indicator that fulfils these requirements. Nevertheless, in some cases alternative workflows are proposed to provide a choice between a “gold standard” (i.e., yielding highest accuracy, yet often implemented using costly data sets) and a “quick win” approach (i.e., only using free but therefore sometime less spatially detailed data or approaches based on existing, value-added products).

As a general note of caution, it is strongly suggested that any important policy and management decision or conclusion in project evaluation should not be based on remote sensing maps alone that have not been either sufficiently validated (at best with in reliable situ information) or cross-checked, or evaluated in terms of their detection sensitivity in the manner described here or in other guidelines.

3. Who should read this study?

This document is written for experts in the field of project evaluation. It assumes that the reader already has some experience with GIS and a basic understanding of remote sensing, ideally in the form of a concrete application in the context of project evaluation.

Although remote sensing terms are explained and defined, it does not replace reading a general introduction to remote sensing of vegetation such as (Jones and Vaughan, 2010).

Please also note that although many recent studies in this field are cited for each indicator, this document is not meant to be a rigorous scientific review. Also the reader should be aware that this is a rather technical guideline that focusses on workflows.

4. Indicator #1 – forest cover

4.1. Name and short description of the indicator

"Forest cover" is defined as an indicator for deforestation & reforestation. It assesses the area of areal coverage vs individual tree coverage, and transition from extensive deforestation to selective logging and deforestation due to clearcutting.

4.2. Background and rationale behind indicator #1

During the last few decades, the world's tropical forests have faced extensive vegetation loss (Achard et al., 2014). Likewise, forests in temperate zones are subjected to logging or wild fires (Hermosilla et al., 2017). In addition, large areas are affected by forest degradation processes (Asner et al., 2005; Broadbent et al., 2008; Souza et al., 2013). Selective logging is a pervasive activity in tropical forests. In the Brazilian Amazon, for example, it is a major source of forest degradation, possibly encompassing an area larger than that reported as deforested based on large-scale clearings (Asner et al., 2005). Unlike deforestation due to clearcutting, which is readily observed from satellites, selective logging in the Brazilian Amazon causes a spatially diffuse thinning of large trees, which is challenging to monitor with moderate spatial resolution (>10m) satellite observations (Lima et al., 2019). Hence, many studies rely on VHR images with spatial resolution <10m, and they use object-based image analysis (OBIA) instead of pixel-based (Dalagnol et al., 2019). A very precise method for monitoring changes in forest cover is the analysis of airborne Light Detection and Ranging (LiDAR) data (Dalagnol et al., 2019). It can be used to accurately assess canopy height and height difference (e.g. by creating and comparing 3D digital surface models from different periods) which are indicative of selective logging (Asner et al., 2013; Ellis et al., 2016).

However, the use of freely available satellite imagery is currently the only feasible (and low-cost) way to map changes over large and/or conflict-prone areas of remote tropical forests, where drones or airplanes cannot operate or data collection is subject to financial constraints. Initially, studies employed visual interpretation techniques to assess the total logged area and to back-trace forest cover changes in satellite archives. Visual interpretation of satellite images is one straightforward and potentially accurate approach for detecting forest degradation. The DEGRAD (Forest Degradation Mapping in the Brazilian Amazonia) project from the Brazilian National Institute for Space Research (INPE) has developed a method to map degraded forest using a visual interpretation procedure (INPE, 2008), and another programme is devoted to map forest cover (PRODES)⁵. However, visual interpretation is time-consuming, and different operators might achieve different results, increasing the degree of uncertainty in the analysis.

4.3. Analysis approach and tools

4.3.1. Name of the approach

In broad terms, there are two ways to assess forest cover changes: (i) an object-based supervised image classification framework, and (ii) trajectory analysis using moderate spatial resolution data. Table 2 can serve as a user guide to choosing between these two approaches.

Table 2: Summary of two approaches and the rationale behind selecting one of them.

⁵ <http://www.obt.inpe.br/OBT/assuntos/programas/amazonia/prodes> (last accessed 15 November 2019).

Name	Object-based supervised image classification and change detection using very high resolution (VHR) data	Trajectory analysis using medium resolution (MR) data
Description	<ul style="list-style-type: none"> Classification of mono-temporal VHR images in two or more periods (years), before-after assessment 	<ul style="list-style-type: none"> Assessment of change in canopy cover based on vegetation indices from satellite images
Suitable data	<ul style="list-style-type: none"> VHR data (<10m) 	<ul style="list-style-type: none"> Moderate spatial resolution data ($\geq 10m$)
Preference	<ul style="list-style-type: none"> Focus is forest cover & selective logging, reducing uncertainties in the detection of selective logging is critical Funds for VHR image acquisition available 	<ul style="list-style-type: none"> Very high-resolution data (<10m) is either unavailable or unaffordable Focus lies on deforestation due to clearcutting, uncertainties in the detection of selective logging can be tolerated
Strengths	<ul style="list-style-type: none"> Allows detection of selective logging Allows detection of even logging infrastructure 	<ul style="list-style-type: none"> Allows assessment of subtle changes in vegetation cover that are characteristics for vegetation regrowth Assessment of large-scale deforestation due to clear-cutting or afforestation using freely available data (Sentinel, Landsat) Due to the availability of archived and repeated images, and global data acquisition MR satellite plans, monitoring is feasible without data costs
Limitations	<ul style="list-style-type: none"> Primary limitation is costly data Analysis impacted by the choice of image acquisition timing, which in turn can be limited by cloud cover Often only limited archive data available because VHR satellite sensors are not equipped/tasked for global coverage (compared to Landsat or Sentinel) Need to parameterise image segmentation, at best based on reference polygons 	<ul style="list-style-type: none"> Detection of small-scale selective logging can be limited due to the spatial resolution of the sensors (mixed pixels) Because this method is based on multitemporal images, large amounts of data need to be processed. This can potentially limit the use of Desktop PCs and might require cloud computing solutions

4.3.2. The degree of processing required to achieve the desired product

The desired product consists of thematic maps showing annual forest cover (forest vs non-forest) and change maps, i.e. maps containing information about where forest cover change occurred and why (e.g. selective logging vs clearcutting, or afforestation). It requires analysis of raw or already pre-processed satellite data using machine learning analysis (OBIA approach) or statistical analysis (trajectory approach).

4.3.3. Previous applications in the scientific context

Table 3 summarised the findings of some recent, peer-reviewed publications. Two rough concepts for mapping forest cover change emerge from literature research. The most commonly used approach is based on classifying VHR images in a baseline and post-project phase using machine learning algorithms, followed by a change detection analysis comparing conditions before and after (Dalagnol et al., 2019; Hethcoat et al., 2019; Sannier et al., 2011). It is most accurate when the focus is on small-scale forest cover changes, such as those caused by selective logging. While studies using VHR images usually rely on mono-temporal images taken during relevant time steps in a year (Dalagnol et al., 2019), sometimes MR images are used in the same fashion (Hethcoat et al., 2019). Freely available MR images such as those provided by the Copernicus Earth Observation Programme⁶ of the European Commission (Sentinel satellites, 10m) or the Landsat satellites⁷ (30m or 15m⁸) of the U.S. National Aerospace Agency (NASA) enable more sophisticated time series or trajectory analysis. Among the

⁶ <https://www.copernicus.eu/en> (last accessed 15 August 2019).

⁷ <https://landsat.gsfc.nasa.gov/> (last accessed 15 August 2019).

⁸ Most multispectral bands of Landsat-5/-7/-8 have a GSD of 30m, yet, since Landsat-7 introduced a PAN band with 15m, users have the option to increase the GSD of the 30m pixels to 15m.

most prominent is detecting subtle temporal differences of a modified normalized burn ratio (NBR) vegetation index (Langner et al., 2018).

The vast majority of previous studies relied on moderate spatial resolution satellite imagery (>10m), notably even from the Landsat program (30m). These studies generally report high accuracies of the created forest maps, however, the spatial resolution can be too coarse to map small-scale forest disturbances in tropical forests, such as those resulting from selective logging (Verhegghen et al., 2015; Zenkevich et al., 2015). Previous studies revealed that, on satellite imagery spatial resolutions of 10m (Sentinel satellites⁹) – 30 m (Landsat), forest disturbance processes (e.g., selective logging) typically result in spectral changes caused at the sub-pixel level. Therefore, the choice of satellite images must be based on the question being evaluated.

Table 3: Overview of projects, scientific publications and most important findings.

Name of the approach	Method	Citation	Image source	Pixel size	Pros	Cons	In-situ or reference data
Trajectory	$\Delta rNBR$	(Langner et al., 2018)	Landsat-8	30m	Allows assessment of changes in forest cover with free satellite data; the use of multitemporal data decreases the impact of clouds	Need to define optimum $\Delta rNBR$ thresholds for forest disturbance maps	Yes, taken from VHR (GeoEye-1, Pleiades, WorldView-2) images by visual interpretation; for defining $\Delta rNBR$ thresholds for forest disturbance maps, and accuracy assessment.
Trajectory	$\Delta rNBR$	(Lima et al., 2019)	Sentinel-2 MSI, Landsat-5/7/8	10m and 30m	Both satellites showed the same performance in terms of accuracy, with area-adjusted overall accuracies of 96.7% and 95.7% for Sentinel-2 and Landsat 8, respectively. Logging infrastructure was better detected from Sentinel-2 (43.2%) than Landsat 8 (35.5%) data, confirming its potential for mapping small-scale logging.	Need to define optimum $\Delta rNBR$ thresholds for forest disturbance maps. Logging infrastructure is difficult to detect: log landings (circa 80%), but less than 50% for felling gaps, logging roads, or skid trails.	Yes, for defining $\Delta rNBR$ thresholds for forest disturbance maps.
VHR image classification	Random Forest, mapping change classes directly (i.e., no change detection based on two or more	(Dalagnol et al., 2019)	LiDAR, WorldView-2, Geoeye-1	1m (only LiDAR and 0.5m DGM)	It is possible to use VHR satellite data to detect canopy tree loss associated with logging.	Image acquisition time affects results. Classification of VHR using RFForest to create change maps. only had 64% precision for detecting logging/disturbances. A caveat regarding the current mapping approach is the requirement of LiDAR data to calibrate the model before ex-	Yes, for calibrating Random Forest to create change maps.

⁹ The European Space Agency (ESA) recently launched the Sentinel-2A and Sentinel-2B satellites (in June 2015 and March 2017, respectively), making the data freely accessible. Sentinel-2A and 2B are “twin” satellites with the same optical sensor, providing multi-spectral imagery in 13 spectral bands at different spatial resolutions (10 to 60 m) with a revisiting time frequency of five days.

	years)				tending the VHR satellite estimates into larger areas.	
Moderate image classification	Random Forest	(Hethcoat et al. 2019)	Landsat-5/7/8	30m	Method could detect low-intensity selective logging across largely areas of the Amazon. Landsat imagery acquired before the cessation of logging activities (i.e. the final cloud-free image of the next dry season).	Detection rate of logged pixels was approximately 90% (with roughly 20% commission and 8% omission error rates). trained forest- models were re-measured by 20% and approximately 40% of the area inside the spatial location of each logging tract were marketable trees. Forest inventories were recorded by 20% and included the spatial location of each tree.

4.3.4. Brief technical and content description of a recommended workflow

4.3.4.1. Object-based supervised classification

This workflow consists of creating annual forest cover maps in two or more periods (years) with the help of machine learning algorithms. Based on these annual maps, forest cover change maps can be created and compared to assess changes in forest cover (Sannier et al., 2011). A variant of this approach is creating forest change maps directly, without the annual maps (Dalagnol et al., 2019). To map changes in forest cover, VHR images from different periods (most importantly in a baseline period before a project intervention, and a post-project phase) and some training data are required.

Some issues should be considered before acquiring the VHR images:

- First, they should fit the time period of a particular concession. Selecting the proper timing of the image acquisition is imperative, because in tropical evergreen forests for example, vegetation regrowth can cause quick recovery (within a few months) from small-scale forest disturbances. Images acquired during, or very soon after, active logging are needed to map low intensity selective logging. This is partly because logging activities typically occur in the dry season when cloud-free imagery is more likely to be available, but also because the spectral changes associated with low-intensity selective logging practices are subtle and short-lived and rapidly become obscured under even limited regrowth. Therefore, the use of a single image for a given year can underestimate the amount of forest disturbance if selected improperly;
 - Second, the spatial resolution should be high enough to discern individual tree crowns in the forest canopy, especially when tracking selective logging is a primary objective. This means it has to be around 1 metre per pixel or better (Zenkevich et al., 2015);
 - Third, in addition multispectral bands in the visible part of the electromagnetic spectrum, imagery should also include the near-infrared (NIR) band, which allows more accurate detection of changes in forest cover.

To create annual forest maps, an OBIA workflow should be set up. OBIA is a technique used to analyse digital images that was developed as a complement to conventional pixel-based image approaches (Blaschke, 2010). While pixel-based image analysis depends on spectral (or other) information from each image pixel, OBIA is based on information based on sets of pixels termed "objects". Put very simply, an object is a set of pixels with similar or relatively homogeneous spectral (or other) characteristics that are spatially connected (e.g. forest stands, or individual trees). Objects exhibit different shapes, sizes, scales and temporal properties. Currently, the following methods are available for image segmentation (not exclusively):

- ArcGIS Mean Shift ([link](#));
- eCognition Region Growing ([link](#))
- GRASS GIS Region Growing ([link](#));
- Orfeo ToolBox (OTB) Large-scale MeanShift ([link](#));
- RSGISLib Shepherd's k-means ([link](#));
- SAGA GIS Seeded Region Growing ([link](#)).

The **complete** OBIA-based workflow applies the following steps in sequential fashion (see Figure 1) using freely available software (see Table 4):

- **Preparation of training data:** Provide training data as points (e.g. from GPS) or polygons in a common digital format, such as ESRI Shapefile, Geopackage, or GeoJson. Training data consists of geolocated information about forest and non-forest land covers.
- **Imagery preprocessing** consists of the orthorectification of the VHR images using a digital elevation model (DEM) and ground control points (GCP)¹⁰. In most cases, orthorectified images can be ordered by the data provider (see Annex 1) and this step becomes obsolete. It is recommended but not mandatory to obtain surface reflectance values from the VHR data with atmospheric correction.
- **Selecting identical multi-spectral bands** in all periods is recommended (blue, green, red, and NIR bands, for example).
- **Run image segmentation** (e.g. meanshift segmentation implemented in Orfeo Toolbox in QGIS¹¹) to create objects representing single trees, groups of trees, or patches of forest vs non-forest land cover.
- **Load train data** into the segmented image, e.g. using a threshold rule. In this case, if segments consist of at least 50% training pixels, they can be considered "valid" cases and selected as training segments.
- **Calculate segment statistics** for classification features (response & predictors), at least area, shape-index, average and standard deviation from the multi-spectral image bands.
- **Optional:** If image segmentation is omitted, i.e. a pixel-based approach is used, texture measures could be calculated for each band (mean, variance, homogeneity, contrast, dissimilarity, entropy, and second moment) to provide a local context for each pixel (Kim et al., 2009). Since logging activities tend to be accompanied by surrounding disturbances (residual damage to neighbouring unharvested trees and skid trails along which logs are extracted),

¹⁰ Raw remotely sensed images contain geometric distortions and cannot be used directly for map-based applications, accurate locational information extraction or geospatial data integration. A geometric correction process must be conducted to minimise the errors related to distortions and achieve the desired location accuracy before further analysis. In most cases, providers of VHR data already perform preprocessing that includes at least basic orthorectification. For example, providers might apply automated orthorectification utilising a coarse digital elevation model (DEM). This is where the individual satellite scenes are geocorrected in an automated fashion with each scene processed independently. There is usually no additional cost for this service but please note that, because each scene is processed without regard for its neighbouring scene, there may be slight offsets in the areas of overlap between scenes. However, the amount of correction is a significant improvement over an unprocessed image, and the data is ready for use in any standard GIS software.

¹¹ https://www.orfeo-toolbox.org/CookBook/Applications/app_Segmentation.html (last accessed 21 August 2019).

these types of texture measures can improve the quality of the classification in pixel-based workflows.

- **Merge train and segment statistics** data (from previous steps).
- **Calibrate** a Random Forest (RF) classifier¹².
- Return the evaluation scores, confusion matrices and trained classifiers.
- **Apply the classifier to the entire VHR scene** and create a binary forest cover map (i.e., 1=forest vs 0=non-forest).
- **Repeat** these steps for every period (year) to create annual binary forest cover maps.
- **Finally, compare** the maps and create change classes, such as 1=forest gain, 2 = forest loss, 3=no change.

Object-based Image Analysis (OBIA) (supervised image classification) workflow

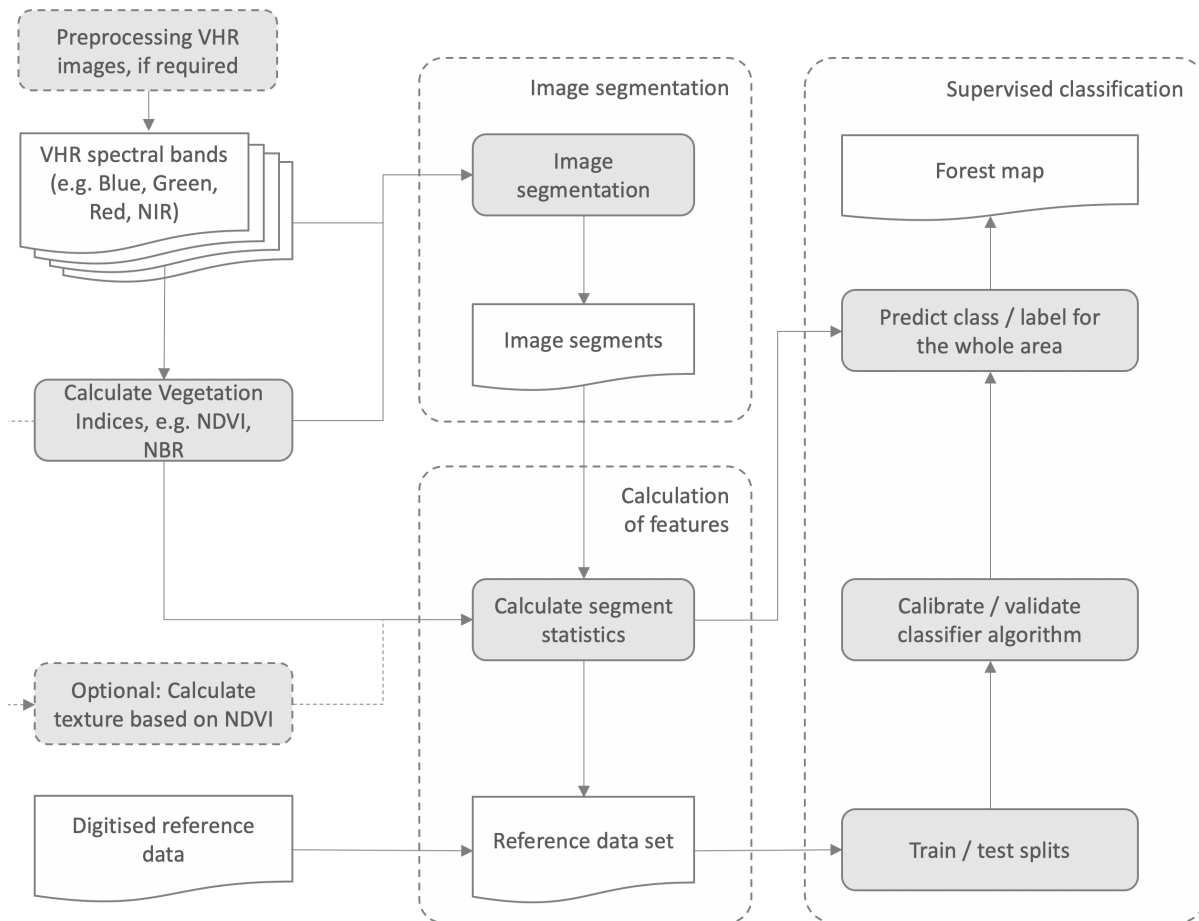


Figure 1: Detailed flow chart and visualisation of the key processing steps used to derive canopy cover change maps based on supervised image classification to create one annual forest map.

Table 4: Freely available software and tools suitable for calculating indicator #1 – “forest cover” supervised image classification workflow.

Name	Purpose	Most important functions
Orfeo Toolbox	Convert VHR data into top-of-canopy	<ul style="list-style-type: none"> Radiometric calibration and atmospheric corrections (TOA, Reflectance)

¹² Random Forest (RF) is a machine learning algorithm, which consists of an ensemble of decision trees (Breiman, 2001). RF reduces the prediction variance by using a large number of decision trees (Breiman et al., 1984).

QGIS ¹³	reflectance (6S radiative transfer model), apply orthorectification if necessary	TOC), orthorectification <ul style="list-style-type: none"> MeanShift with raster or vector results Object-based image classification
R	Random Forest classifier algorithm for creating forest cover and change maps	<ul style="list-style-type: none"> Raster processing: R package 'raster' Image segmentation: R package 'SegOptim' Image classification: R package 'randomForest'
Google Earth Engine (GEE) ¹⁴	Complete workflow (expect for the image preprocessing) can readily be implemented using existing functions in GEE	<ul style="list-style-type: none"> ee.Algorithms.Image.Segmentation.SNIC ee.Classifier.randomForest

4.3.4.2. Trajectory analysis

When working with MR images (e.g. Sentinel-2 and Landsat-8), the previously mentioned $\Delta rNBR$ method (Langner et al., 2018; Lima et al., 2019) is advisable because these satellite systems deliver frequent observations within a year, which can alleviate the impact of trees having different on-leaf seasons (which can lead to false or non-detection of logging events) and clouds (which might lead to only having VHR images available during a period that is not ideal for change detection). Using multitemporal data supports not only detecting the temporal change in the spectral signal as close as possible to the canopy disturbance events, i.e. increasing the chance of registering a "logging event". It also allows detection of subtle changes in the vegetation cover that could be indicative of reforestation. The $\Delta rNBR$ approach potentially works without training data, but at the cost of having ambiguous labels (e.g. "Forest gain") in the map, similar to supervised image classification.

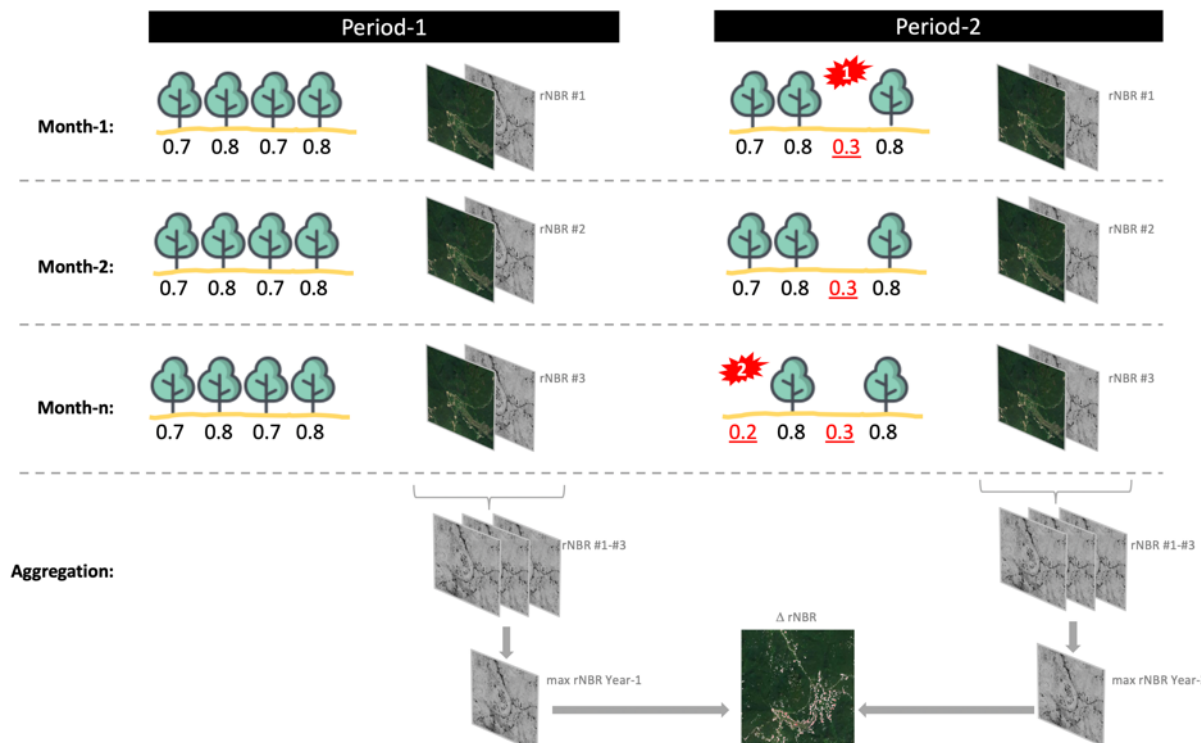


Figure 2: Detailed flow chart and visualisation of the key processing steps used to derive canopy cover disturbance ($\Delta rNBR$) maps based on change detection analysis from two periods.

¹³ <https://www.orfeo-toolbox.org/features-2/> (last accessed 30 November 2019)

¹⁴ https://developers.google.com/earth-engine/api_docs (last accessed 30 November 2019)

The ΔrNBR approach has frequently been tested (Langner et al., 2018; Senf et al., 2015) and its workflow applies the following steps in sequential fashion (see also Figure 2):

- **Imagery preprocessing** consists of the acquisition of top-of-canopy (TOC) reflectance Landsat¹⁵ and/or Sentinel-2¹⁶ satellite images in two periods (years). Images should be selected (i) to cover on-leaf seasons and – if known – periods of suspected or known logging activities.
- **Masking** clouds and cloud shadows (e.g. using the CFMask¹⁷ layers provided for Landsat images, or the cloud masks provided for Sentinel-2¹⁸).
- **Masking of non-forest areas in period 2** (this requires either an existing forest-non-forest map, or creating a new one following the same approach as outlined in section 4.3.4)
- **Calculation of the NBR index** for each cloud-free TOA image according to this formula:

$$NBR = \frac{NIR - SWIR2}{NIR + SWIR2}$$

where NIR is the near infrared band (Landsat-8: band 5, Sentinel-2: band 8), and SWIR2 the shortwave infrared band (Landsat-8: band 7, Sentinel-2: band 12)¹⁹.

- Calculation of **self-referencing NBR layers** (rNBR), i.e., apply a kernel window that calculates the median NBR for each pixel in the image, and then subtract the median NBR from the original value. For the kernel window, a 210m radius has previously been recommended as the value for Landsat images (Langner et al., 2018).
- **Create annual aggregates** of NBR values, e.g. by selecting the maximum numerical NBR value per pixel per year (max_rNBR).
- **Calculate the difference** ΔrNBR between the max_rNBR images in two periods:

$$\Delta rNBR = max_rNBR_year2 - max_rNBR_year1$$

- **Apply a threshold** to determine what the numerical difference actually means. This step is essential to determine whether or not a ΔrNBR is indicative of forest cover loss. A previous study recommends using a ΔrNBR of 0.035 (± 0.005) and 0.065 (± 0.009) for Landsat 8 and Sentinel-2 images, respectively (Lima et al., 2019). The result of this step can be a binary map (e.g. values larger than the threshold could be labelled "Potential Forest Loss", or a map with continuous values (i.e. the non-masked ΔrNBR values). The higher the values, the higher the likelihood that forest loss actually occurred.

A variant of this workflow is comparing consecutive pairs of observation years over a longer period, instead of only comparing a before- vs after-project period. Both variants have already been implemented in GEE (Table 5).

¹⁵ The USGS Landsat 8 Surface Reflectance Tier 2 dataset is the atmospherically corrected surface reflectance from the Landsat 8 OLI/TIRS sensors. These images contain 5 visible and near-infrared (VNIR) bands and 2 short-wave infrared (SWIR) bands processed to orthorectify surface reflectance, and two thermal infrared (TIR) bands processed to orthorectify brightness temperature. These data have been atmospherically corrected using LaSRC; this includes a cloud, shadow, water and snow mask produced using CFMASK, as well as a per-pixel saturation mask. For more information refer to: https://www.usgs.gov/land-resources/nli/landsat/landsat-collection-2?qt-science_support_page_related_con=1#qt-science_support_page_related_con (last accessed 19 August 2019).

¹⁶ The Level-2A product provides Top Of Canopy (TOC) reflectance images, using the Sen2Cor processor and derived from the associated Level-1C products. Each Level-2A product is composed of 100x100km² tiles in cartographic geometry (UTM/WGS84 projection). Level-2A products are systematically generated at the ground segment over Europe since March 2018, and the production was extended to global in December 2018. Level-2A generation can also be performed by the user using the Sentinel-2 Toolbox using the associated Level-1C product as input. For more information refer to: <https://earth.esa.int/web/sentinel/user-guides/sentinel-2-msi/product-types/level-2a> (last accessed 19 August 2019).

¹⁷ <https://www.usgs.gov/land-resources/nli/landsat/cfmak-algorithm> (last accessed 19 November 2019).

¹⁸ <https://sentinel.esa.int/web/sentinel/technical-guides/sentinel-2-msi/level-1c/cloud-masks> (last accessed 19 November 2019).

¹⁹ In order to have the same analysis scale, the spatial resolution of all input data should be rescaled to have the same size, e.g. 10m of Sentinel-2 NIR bands.

Table 5: Freely available software and tools suitable for calculating indicator #1 "forest cover" – trajectory workflow.

Name	Purpose	Most important functions
GEE (Code by Langner 2018)	Calculating ΔrNBR by comparing two years, based on Sentinel-2 and Landsat-8	<ul style="list-style-type: none">Define area of interest globallyDefine start and end period (year and months)Select Sentinel-2 or Landsat-8Determine Delta-NBR thresholds as described in (Langner et al., 2018)Compare two periodsPlot and export analysis results as maps or GeoTiff

4.3.5. Required expertise

4.3.5.1. Further statistics?

Spatial aggregation (such as the area of forests per project region or administrative unit) of information requires some knowledge to assess and understand statistics of central tendency.

4.3.5.2. Geodata processing and/or handling GIS?

The ability to handle a GUI- (graphical user interface) based GIS like QGIS²⁰ is necessary. For fast geodata processing, it is advisable to work in GEE, which requires JavaScript programming²¹, or other statistical programming languages with raster processing capabilities, such as R²² or Python²³. Working without any expertise in GIS or programming is possible using stand-alone, web-based tools, such as the Global Forest Watch²⁴ (for assessing forest cover change) or existing GEE codes (see Table 5).

4.3.5.3. Technical expertise in remote sensing?

Basic understanding of remote sensing image analysis is mandatory for creating new forest maps, such as image preprocessing and supervised image classification. A valid alternative is visual interpretation of VHR images and on-screen digitisation in GIS, which requires a solid understanding of image interpretation.

4.3.5.4. Programming knowledge?

Statistical programming languages with raster processing capabilities, such as R²⁵ or Python²⁶. For the implementation of the ΔrNBR, it is advisable to work in GEE, which requires JavaScript programming²⁷. Both methods, OBIA and ΔrNBR, can also be implemented without programming in QGIS (using GRASS GIS and Orfeo Toolbox).

4.3.6. How to validate the indicator maps?

The workflows create thematic maps of land covered by forest and forest cover change, which can be evaluated by an accuracy assessment, which is done based on so-called confusion matrices and

²⁰ <https://www.qgis.org/en/site/> (last accessed 19 August 2019).

²¹ <https://developers.google.com/earth-engine/tutorials> (last accessed 19 August 2019).

²² <https://www.r-project.org/> (last accessed 19 August 2019).

²³ <https://www.python.org/> (last accessed 19 August 2019).

²⁴ <https://data.globalforestwatch.org/> (last accessed 30 November 2019).

²⁵ <https://www.r-project.org/> (last accessed 19 August 2019).

²⁶ <https://www.python.org/> (last accessed 19 August 2019).

²⁷ <https://developers.google.com/earth-engine/tutorials> (last accessed 19 August 2019).

which usually requires the collection of so-called reference data, either in-situ during field surveys or on-screen. The good practices outlined by (Olofsson et al., 2014, 2013) should be considered to assess the map accuracy and to calculate error-corrected acreage estimates of forest / forest cover change. The required reference data can be used to adjust the area estimate as obtained from the map. In addition, a well-documented and good overview of this subject was prepared. Annex 4 provides more information about this comprehensive and important topic, which should be considered as a mandatory component of any remote sensing study. Forest change or selective logging maps can be validated visually on the basis of other VHR images instead of in-situ data (Zenkevich et al., 2015). In addition, existing forest cover maps could be used to cross-check newly created maps, e.g. the Global Forest Watch (Annex 2). Annex 4 provides details about how to acquire in-situ data. There exist several guidelines that have a focus on the collection of reference data in the context of forestry. A summary is given in Annex 6.

4.3.7. Required input data

4.3.7.1. Suitable data sources for the approach

4.3.7.1.1. OBIA-based supervised classification

Running the above workflows to implement an OBIA-based supervised classification method requires various basic data inputs (see also Figure 3).

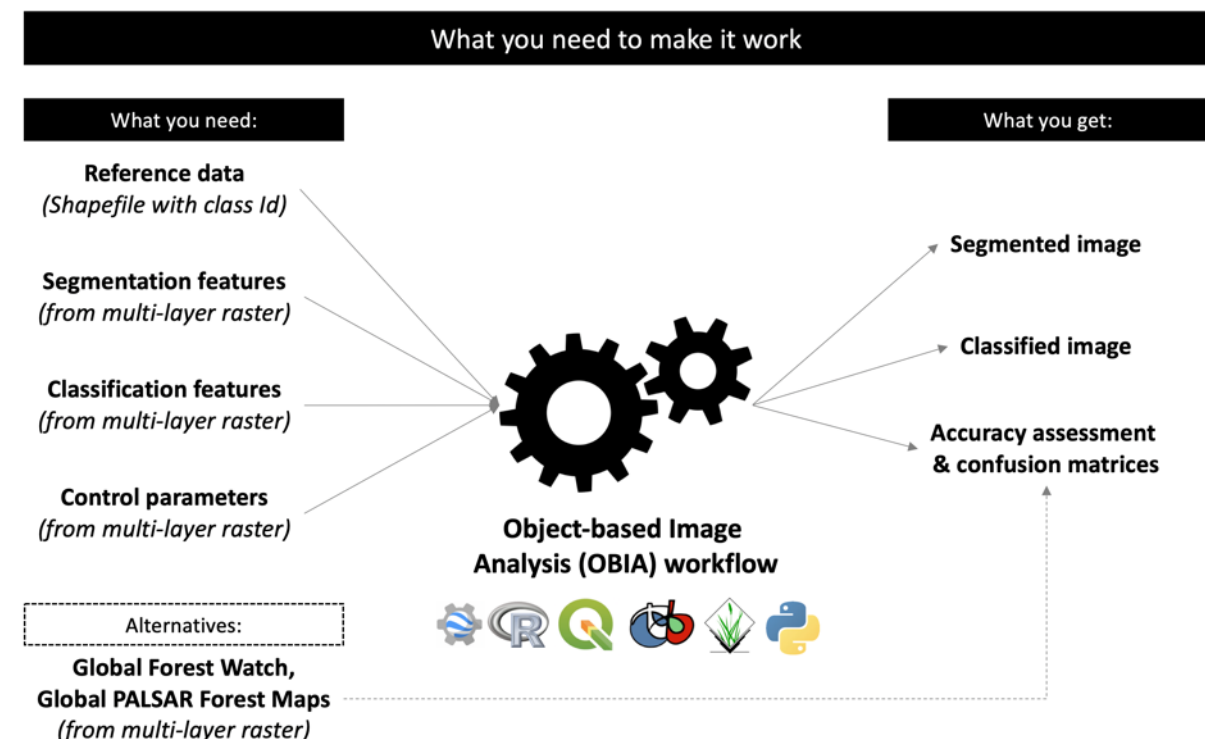


Figure 3: Overview of required data sets and information in object-based supervised image classification.

Reference data: Entails in-situ collected or hand-digitised patches of forest and non-forest land, delineated using VHR images, Google Earth, or after field visits to the site. If attributing the kind of deforestation is in the focus of the assessment, this training data set should contain information about the specific change category, e.g. "selective logging" vs "clear cut" vs "mining" vs "infrastructure

construction". Typically, reference data is provided in shapefile or GeoPackage format, or as a single-layer raster dataset containing samples for calibrating (training) a classifier. The labels, classes or categories should be coded as integers {0,1} for single-class problems (i.e. forest vs non-forest) or {1,2,...,n} for multi-class problems. Without reference data, forest maps cannot be created (missing calibration data for the classifier algorithm) or validated.

Remote sensing data: This is typically a multi-layer raster dataset recorded on one acquisition date per period (mono-temporal imagery) that needs to be acquired from a commercial provider (see Annex 1) when VHR data is needed. The most commonly used file format is GeoTIFF. Satellite data is the basis for extracting segmentation and classification features. Segmentation features are typically a multi-layer raster dataset with features used only for the segmentation stage (e.g., spectral bands, spectral indices, texture). The format of this data depends on the algorithm used for performing the segmentation. For example, SAGA GIS uses *.sgrid files, while GRASS uses a raster group (in a GRASS database) as input. Classification features are also typically a multi-layer raster dataset with features used for classification (e.g., spectral bands and indices, texture, elevation).

Alternatives – existing data sets: Existing, value-added data sets (forest maps) are available and should be considered when assessing indicator #1 and cross-checking your own maps. Most notably, the Global Forest Watch and the Global PALSAR-2/PALSAR/JERS-1 Forest/Non-Forest map. It facilitates – for example – tracking forest cover change globally since 2000 with 30m spatial resolution (Global Forest Watch) or since 2007 with 25 spatial resolutions (PALSAR-2/PALSAR/JERS-1 Forest/Non-Forest map). More details about existing data sets can be found in Annex 2.

4.3.7.1.2. Trajectory-based workflow ($\Delta rNBR$)

Running the above workflow to implement a trajectory-based workflow ($\Delta rNBR$) requires two basic data inputs (see Figure 4).

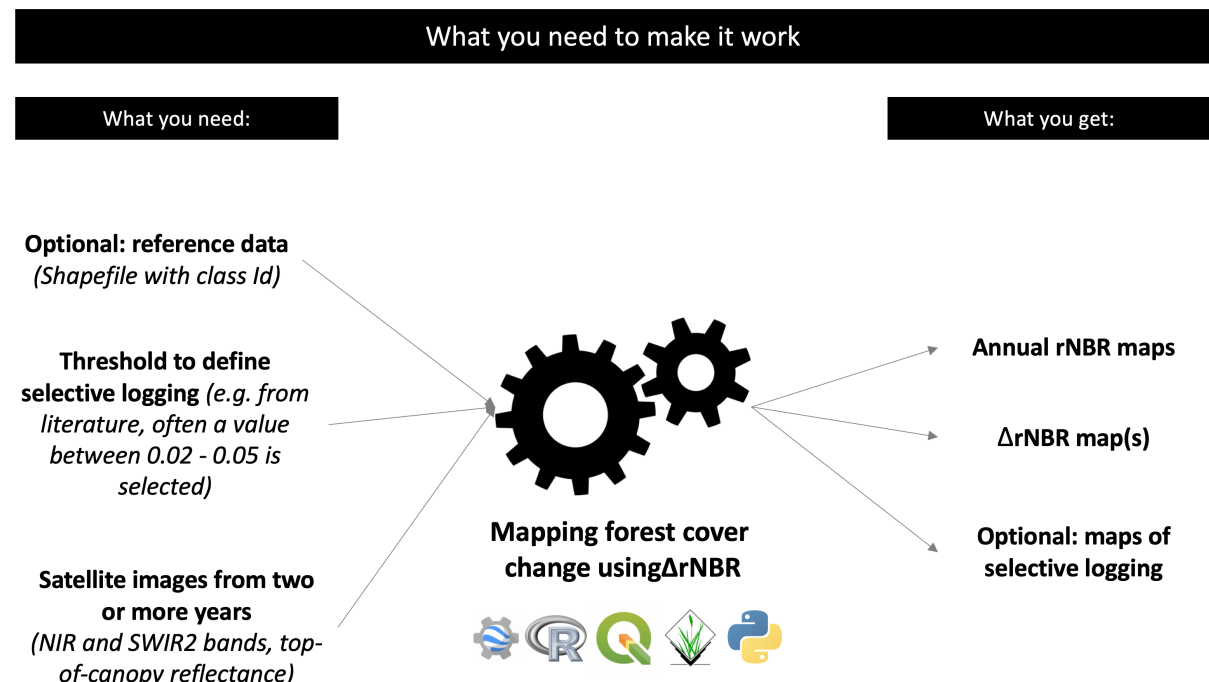


Figure 4: Overview of required data sets and information in NBR analysis.

Reference data (optional): The same requirements that apply to the reference data used in image classification (see above) apply here. As for that reference data, in-situ data can be substituted by VHR reference images. Without any reference data, proper thresholds for the NBR must be taken from the literature and the resulting, non-validated maps can only indicate forest loss.

Remote sensing data: Typically, a multi-layer raster dataset, recorded on several consecutive acquisition dates per period (time series) that can be acquired from open archives, such as ESA (Sentinel) or NASA (Landsat). The most commonly used file format is GeoTIFF. The Landsat satellites and the Sentinel-2A and Sentinel-2B satellites are described in more detail in Annex 1. These MR data are recommended for setting up trajectory-based approaches such as Δ rNBR mapping & monitoring. The spatial resolution of these sensors (10–30m) ultimately limits their applicability when detecting small-scale selective logging. For example, a previous study found that Landsat 8 mapped 36.9% more selective logging area compared to Sentinel-2 data, and that logging infrastructure was better detected from Sentinel-2 (43.2%) than Landsat 8 (35.5%) data, using a Δ NBR trajectory-based framework each time (Lima et al., 2019). However, another study found that moderate resolution images deliver reasonable results in a supervised image classification framework, for example the detection rate of logged pixels was approximately 90% (with roughly 20% commission and 8% omission error rates) (Hethcoat et al., 2019).

Alternatives – existing data sets: Not available, NBR needs to be calculated.

4.3.7.1.3. What limitations must be expected without in-situ data, and to what extent are other data sources suitable as substitutes for in-situ data?

Field validation is recommended but not mandatory. Without in-situ data, the interpretation of VHR images to acquire reference data is potentially limited but still possible. For example, users need context to correctly identify selective logging sites by relating them to phenomena in the area. Zenkevich et al. (2015) demonstrated how road proximity can be indicative of selective logging.

4.3.8. Cost benefit:

Good practice recommendation: Gather reference data, at best in-situ or from existing VHR sources (second choice), and acquire VHR images in at least two periods. Apply OBIA using machine learning algorithms such as RF to classify the VHR images and create annual forest vs non-forest cover maps. Assess and quantify land cover change, based on the annual maps. Evaluate the accuracy of the annual and change maps. Report accuracy metrics and calculate land cover area statistics corrected for accuracy and provide a second map showing a posteriori classification probabilities. It is important for remote sensing researchers to avoid assuming that high resolution images automatically imply high classification accuracies. They should be analysed using OBIA or Deep Learning methods (Hao et al., 2018).

Alternatives and trade-offs: Substitute in-situ data with reference data acquired from visual interpretation of Google Earth or other VHR images. Use and classify moderate spatial resolution images or apply the Δ rNBR method (both using Sentinel-2). Basically, the added value of this approach is merely that 10m Sentinel-2 data can be used, which enhances the level of detail compared to the Global Forest Watch as it is recently implemented (30m). Δ rNBR can be seen as a complementary approach to OBIA classification, but without reference data, Δ rNBR only delivers an indication of forest loss that still needs to be validated. When the focus lies on monitoring clearcutting, the Global Forest Watch is sufficient and accurate. Less processing is required if you directly use existing data

sets such as Global Forest Watch and the Global PALSAR-2/PALSAR/JERS-1 Forest/Non-Forest map. However, you will less likely identify small-scale deforestation such as selective logging.

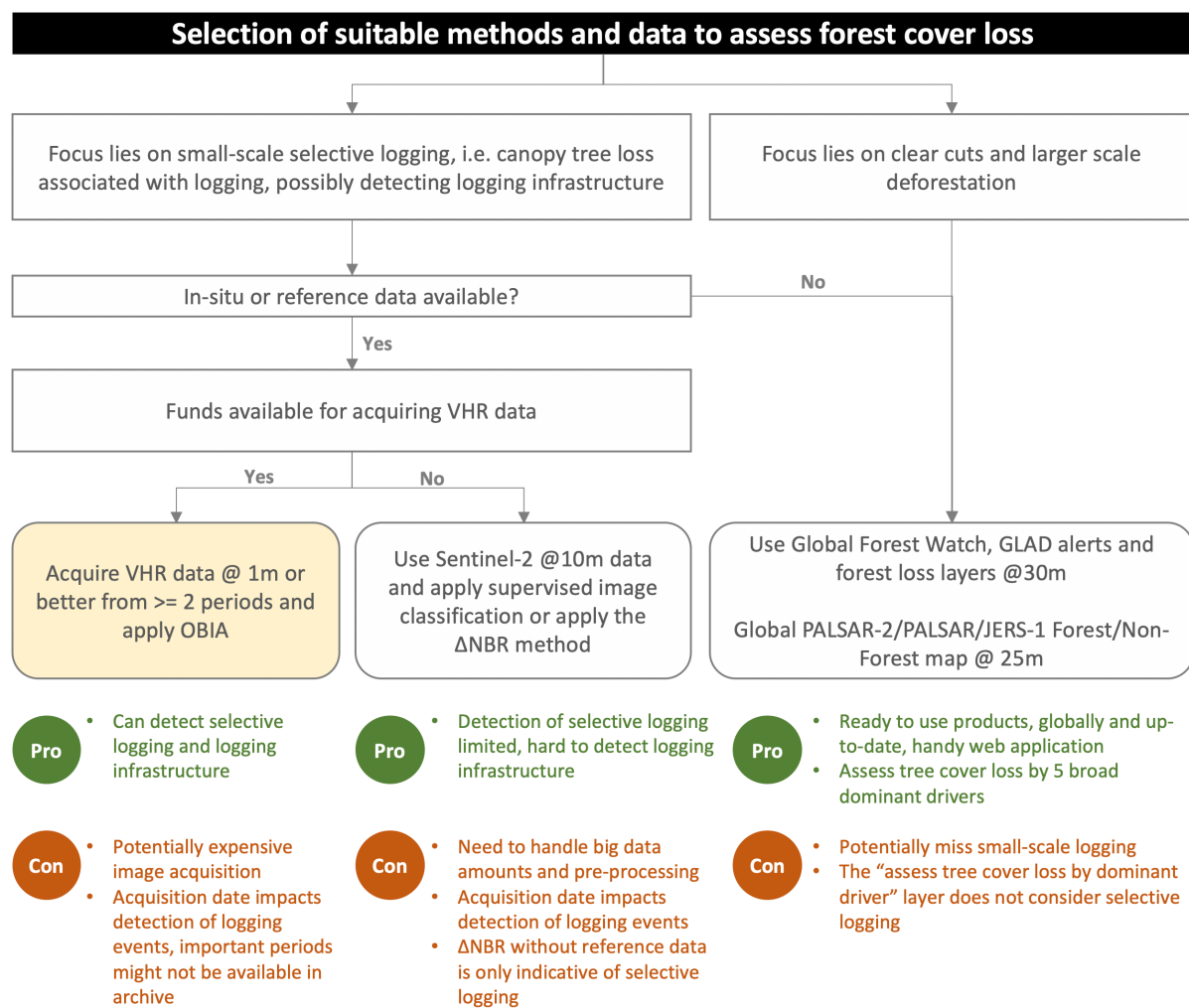


Figure 5: Guide for selecting proper imagery and methods for assessing forest cover change. The "gold standard" is highlighted in yellow colours. It provides the best results in terms of spatial detail.

5. Indicator #2 – forest fragmentation

5.1. Name and short description of the indicator

"Forest fragmentation" is defined as the spatial configuration of treed-vegetation, quantified by spatial indicators of forest patch fragmentation. It serves as a proxy for forest quality and forest/timber harvesting management.

5.2. Background and rationale behind indicator #2

Forest fragmentation refers to the amount and spatial configuration of treed-vegetation (Riitters et al., 2000) and is driven by both natural (e.g., fires, insects) and anthropogenic (e.g., harvest, logging) processes (Soverel et al., 2010). Deforestation not only reduces forest area but also changes the landscape configuration as a whole (Giles and Burgoyne, 1993).

Forest fragmentation, one of the major threats to biodiversity and forest conservation, is the process through which formerly large and continuous forest areas are converted to small, isolated patches. Reduction in sizes (areas) of remaining forest patches, increased isolation and loss of connectivity, and increased edge effects are the three main consequences of forest fragmentation. So landscape fragmentation metrics have been developed (McGarigal et al., 2015), some of which have the capacity to serve as spatial indicators for assessing the health of forest ecosystems and are commonly considered biodiversity indicators in national forest inventories. Forest fragmentation metrics are important for assessing whether critical components and functions of forests are being maintained over time.

Landscape fragmentation can be quantified through a suite of spatial pattern metrics that provide information about the amount and configuration of (forest) patches, distribution of patch sizes, and edge effects. These metrics enable landscape pattern comparisons at different locations and facilitate relative assessments of fragmentation change through time. The combined analysis of dense time series of forest maps and detailed forest change data allows for the tracking of forest fragmentation following disturbance events, providing useful information on the temporal evolution of spatial forest patterns. Given an adequate time period, it also provides information about the recovery of vegetation patterns to resemble pre-disturbance conditions.

Forest fragmentation and edge effects from deforestation and selective logging have been assessed in the Brazilian Amazon using remote sensing data (Broadbent et al., 2008). Previous studies used both moderate and VHR images to assess forest fragmentation in tropical regions (Tapia-Armijos et al., 2015; Taubert et al., 2018) or in temperate ecozones, such as Canadian forests (Hermosilla et al., 2019). Previous studies used Global Forest Watch data to assess deforestation and fragmentation, respectively (Vieilledent et al., 2018).

The choice of metrics to measure forest fragmentation for use as indicators of forest capacity to retain biodiversity is dictated both by the source data and by the range of biological effects being targeted. Summary statistics of landscape metrics are of little use for predicting responses of individual species without more detailed information about both species' requirements and environmental variation on the ground. However, to provide both an overview of forest status in relation to biodiversity and baselines to track changes that may affect forest biodiversity, simple statistical expressions of forest configuration can be useful. It is also important that the chosen metrics can be easily communicated and understood by the anticipated audience for the overview and monitoring, so

conceptually complex indices are generally less useful. The selection of metrics needs to reflect all three types of fragmentation effects:

- Area or patch size ("area");
- Interface with non-forest or edge effects ("edge");
- Isolation from or interconnection with other patches ("isolation").

5.3. Analysis approach and tools

5.3.1. Name of the approach

Assessment of forest fragmentation using forest fragmentation metrics (FFM).

5.3.2. The degree of processing required to achieve the desired product

FFM maps are computed based on existing forest maps (section 4).

5.3.3. Previous applications in the scientific context

Various studies assessed temporal changes in forest fragmentation through FFMs in tropical and temperate forests (Hermosilla et al., 2019; Tapia-Armijos et al., 2015; Taubert et al., 2018). Most of these studies used dedicated sets of FFMs that can be traced back to the original work of McGarigal et al. (2015), who developed open-source software called FRAGSTATS. FRAGSTATS computes several statistics for each patch and class (patch type) in the landscape and for the landscape as a whole. At the class and landscape level, some of the metrics quantify landscape composition, while others quantify landscape configuration.

The aforementioned studies focused mostly on a selection of just a few selected indices (see Table 6 and Table 7), which can be calculated for so-called "sampling units" using off-the-shelf software, such as FRAGSTATS. In previous studies, FFMs were computed on mostly 1×1km grids of landscape analysis units, i.e., the sampling area from which to calculate the metrics (Hermosilla et al., 2019; Tapia-Armijos et al., 2015). Forest fragmentation and edge effects accurately describe deforestation and selective logging, for example in the Brazilian Amazon (Broadbent et al., 2008).

Table 6: Overview of projects, scientific publications and most important findings.

Citation	Image source	Landscape analysis unit	Selected FFMs	Ecozone
(Hermosilla et al., 2019)	Landsat (30m)	1 × 1 grid cells	<ul style="list-style-type: none"> • Forest cover (proportion) • Number of forest patches • Mean forest patch size • Forest-non-forest joint count 	Temperate forests (Canada)
(Fynn and Campbell, 2019)	Landsat (30m) Sentinel-2(10m) NAIP (0.25m) UAV (0.03m)	The whole study area	<ul style="list-style-type: none"> • Forest patch density • Largest patch index • Edge density • Landscape shape index • Cohesion • Radius of gyration 	Temperate forests (USA)
(Tapia-Armijos et al., 2015)	B+W aerial (?) ASTER (15m)	The whole study area	<ul style="list-style-type: none"> • Number of forest patches • Total forest patch area • Mean forest patch area size • Largest patch index • Patch density • Mean proximity index • Total core area • Mean shape index 	Tropical forest (Ecuador)

			• Total edge length	
(Vieilledent et al., 2018)	Landsat (30m)	Moving window (51 x 51 Landsat pixels)	<ul style="list-style-type: none"> • Forest cover (proportion) • Distance to forest edge • Percentage of forest within the first 100m of the forest edge 	Tropical forest (Madagascar)

5.3.4. Brief technical and content description of a recommended workflow

Three groups of FFM (see Table 7) are recommended based on a review of the literature. The workflow to calculate these is as follows (see also Figure 6):

- Create (or acquire existing) two or more **binary forest (1) vs non-forest (0) maps** (section 4.3). If one wants to exclude the influence of a specific land cover type, e.g., water bodies, it should be classified as no-data in the input map.
- If applicable, **rescale the binary maps** if they have different spatial resolutions and use **nearest neighbour resampling**. For the sake of comparability, rescale the map with the higher spatial resolution to the same resolution as the lower resolution map.
- Define a **landscape analysis unit** – this step depends on the evaluative question. Landscape analysis units can be regular grids or hexagons, administrative units, or concession sites. The FFMs are calculated and summarised per landscape unit.
- Perform a fragmentation analysis and **calculate FFM key fragmentation metrics** for each landscape analysis unit and period, respectively.
- Assess **changes in annual fragmentation values (such as before vs after)**. Optionally: if several consecutive annual land cover maps are available, changes in annual fragmentation values could also be assessed for each metric using Theil-Sen non-parametric regression²⁸. In that case, provide a change map showing the difference in selected FFMs in the first and last year of the observation period.
- **Summarise statistics** of forest fragmentation metrics, for example by ecozone or administrative regions or project vs control sites, etc. (so called zonal statistics).

Table 7: Recommended set of forest fragmentation metrics and their definition. The names in the first column are taken from the R package 'SDMTools'.

Name	Group	Definition	Unit of the metric	Purpose
n.patches	Area	The number of patches of a particular patch type or in a class.	[Number of forest patches]	As the area of the landscape units does not vary, a larger number of forested patches indicates a more fragmented forest.
total.area	Area	The sum of the areas of all patches of the corresponding patch type.	[sqm]	Total area often does not have a great deal of interpretive value with regards to evaluating landscape patterns, but it is important because it defines the extent of the landscape. Moreover, total landscape area is used in the computations for many of the class and landscape metrics.
mean.patch.area	Area	The average area of patches.	[sqm]	Smaller mean sizes are indicative of more fragmentation.
prop.landscape	Area	The proportion of the total landscape represented by this class.	[0:1]	This metric is indicative of forest dominance, with higher values indicating more forest cover relative to non-forest cover classes.
total.edge	Edge	The total edge length of a particular patch type.	[metres]	Equals 0 when there is no class edge in the landscape; that is, when the entire landscape and

²⁸ Theil-Sen slopes are less sensitive to outliers than traditional linear regression and are therefore more commonly used in time series analyses.

				landscape border, if present, consist of the corresponding patch type, and the user specifies that none of the landscape boundary and background edge are to be treated as edges.
edge.density	Edge	The edge length on a per-unit area basis that facilitates comparison among landscapes of varying size.	[metres per hectare]	
mean.frac.dim.index	Isolation	The mean of the fractal dimension index.	None	A fractal dimension greater than 1 for a 2-dimensional patch indicates a departure from Euclidean geometry (i.e., an increase in shape complexity). FRAC approaches 1 for shapes with very simple perimeters such as squares, and approaches 2 for shapes with highly convoluted, plane-filling perimeters.
landscape.division.index	Isolation	Based on the cumulative patch area distribution and is interpreted as the probability that two randomly chosen pixels in the landscape are not situated in the same patch	None	Equals DIVISION = 0 if only one patch is present. Approaches DIVISION = 1 if all patches of class i are single cells.
patch.cohesion.index	Isolation	Measures the physical connectedness of the corresponding patch type.	None	COHESION equals 1 minus the sum of patch perimeter (in terms of number of cell surfaces) divided by the sum of patch perimeter times the square root of patch area (in terms of number of cells) for patches of the corresponding patch type, divided by 1 minus 1 over the square root of the total number of cells in the landscape, multiplied by 100 to convert to a percentage. Note, total landscape area (A) excludes any internal background present.

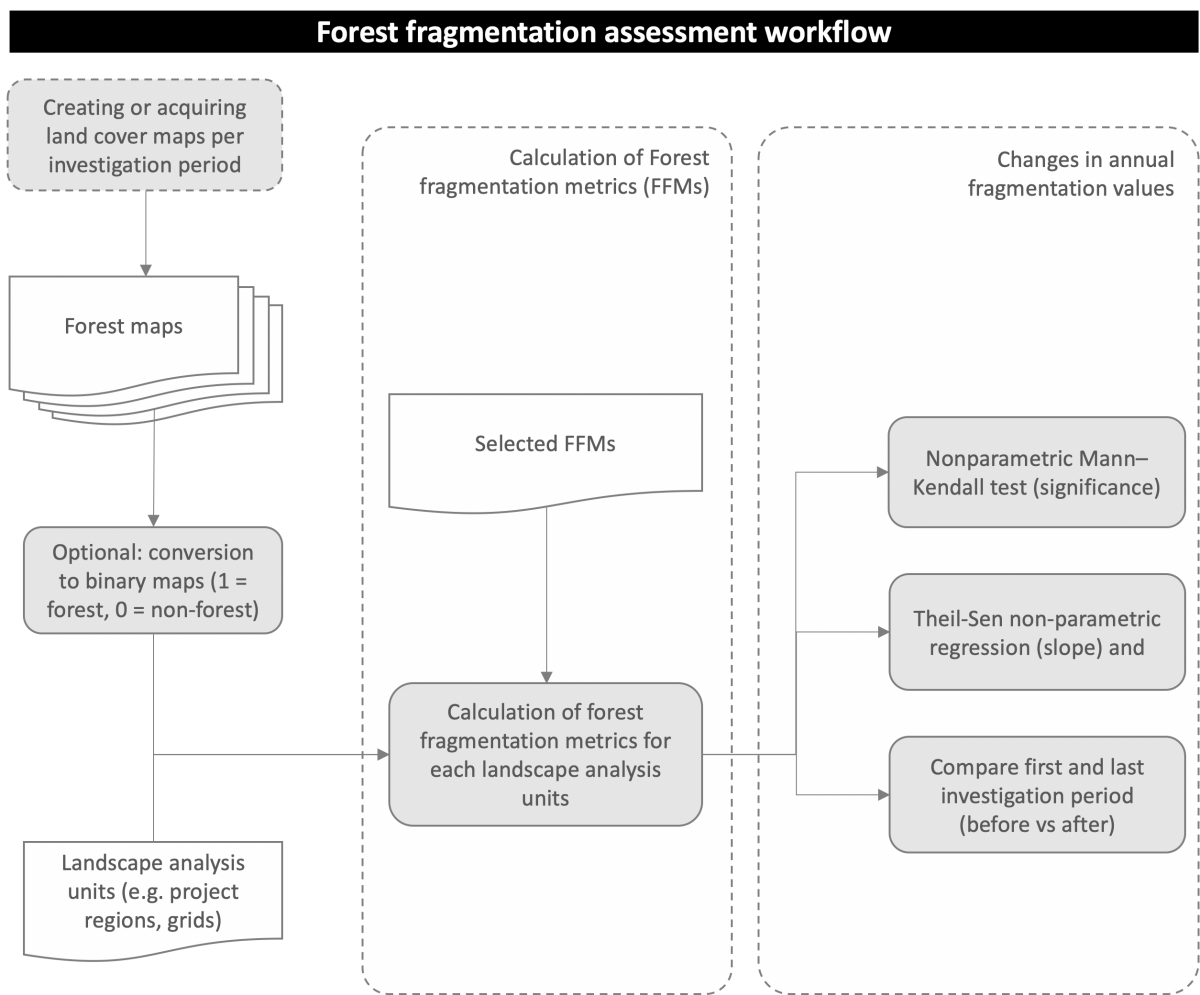


Figure 6: Flow chart and visualisation of the key processing steps used to derive forest fragmentation statistics from two periods.

Table 8: Available and recommended software packages to calculate forest fragmentation metrics.

Name	Description	Software	Reference	URL
FRAGSTATS (Spatial Pattern Analysis Program for Categorical Maps)	FRAGSTATS is a computer software program designed to compute a wide variety of landscape metrics for categorical map patterns. It is the most widely used software in this field and reimplemented in various other GIS and programming languages.	GUI	(McGarigal et al., 2015)	https://www.umass.edu/landeco/research/fragstats/fragstats.html
'landscapemetrics'	R-package that reimplements the most common metrics from FRAGSTATS	R	(Hesselbarth, 2019)	https://r-spatialecology.github.io/landscapemetrics/
'SDMTools'	R-package that reimplements the most common metrics from FRAGSTATS	R	(VanDerWal et al., 2019)	https://cran.r-project.org/web/packages/SDMTools/index.html
'r.forestfrag'	GRASS GIS module that calculates a forest fragmentation index, based on moving windows (kernels).	GRASS GIS		https://grass.osgeo.org/grass76/manuals/addons/r.forestfrag.html
'r.li'	Toolset for multiscale analysis of land	GRASS		https://grass.osgeo.org/grass74/manuals/r.li.html

Currently GRASS GIS version 7.6	scape structure that reimplements the most common metrics from FRAG-STATS	GIS	/		
LecoS (Landscape Ecology Statistics) Currently version 3.0.0	The QGIS Plugin LecoS is based on metrics taken from FRAG-STATS landscape ecology statistics	QGIS	(Jung, 2016)		

5.3.5. Required expertise

5.3.5.1. Further statistics?

Spatial aggregation of information requires some knowledge to assess statistics of central tendency. In addition, familiarity with the basics of landscape ecology is recommended as far as it is relevant for the calculation of landscape metrics (McGarigal et al., 2015).

5.3.5.2. Geodata processing and/or handling GIS?

A number of packages for using a GIS permit the analysis and characterisation of landscapes in terms of their patch composition, spatial relations and dynamics (Table 8). One such package, FRAGSTATS (McGarigal et al., 2015) is widely used for the description and analysis of landscape configuration. It offers a wide range of measures of varying complexity. It is necessary to handle at least a GUI-(graphical user interface) based software of FRAGSTATS version 4.2²⁹ or QGIS, which implements interfaces to FRAGSTAT functionality provided by R packages or GRASS. In addition, the QGIS Plugin 'LecoS' is based on metrics taken from FRAGSTATS.

5.3.5.3. Technical expertise in remote sensing?

No, because FFMs can be calculated based on existing maps.

5.3.5.4. Programming knowledge?

Not mandatory, the whole workflow can be implemented in QGIS (see 5.3.5.2). FRAGSTAT functionality is embedded in the R packages 'landscapemetrics' (Hesselbarth, 2019), the package 'SDMTools' (VanDerWal et al., 2019) or in the GRASS GIS module 'r.li'. R and GRASS GIS functionalities are embedded in QGIS.

5.3.6. How to validate the indicator maps?

In essence, the forest fragmentation metric maps cannot be validated directly. The validation is confined to the underlying forest maps, which are validated on their own (see chapter 4.3.6 or Annex 4).

5.3.7. Required input data

5.3.7.1. Suitable data sources for the approach

Existing, gridded land cover maps that entail spatial information about forest cover (section 4.3.7) is the input for forest fragmentation assessments. Land cover maps containing other land cover classes must be re-coded into binary maps (i.e., forest vs non-forest). These maps should have decent spatial

²⁹ The latest release is from 2015 and can be downloaded here: https://www.umass.edu/landeco/research/fragstats/downloads/fragstats_downloads.html#FRAGSTATS (last accessed 20 August 2019).

resolution (30m or better) that allows quantification of FFM relevant to the subject of investigation. Ideally, VHR images/maps are available. Regarding MR data, Flynn and Campbell (2019) found that "*Fragmentation metrics such as the number of patches or patch density, largest patch index, landscape shape index, edge density and radius of gyration showed similarities between Landsat and Sentinel Imagery compared with NAIP and UAV images*". This indicates that the Global Forest Watch (30m) could be a potentially suitable source for assessing FFM (instead of processing Sentinel-2 images). However, this study also indicates that there are major differences between FFMs calculated with MR vs VHR data.

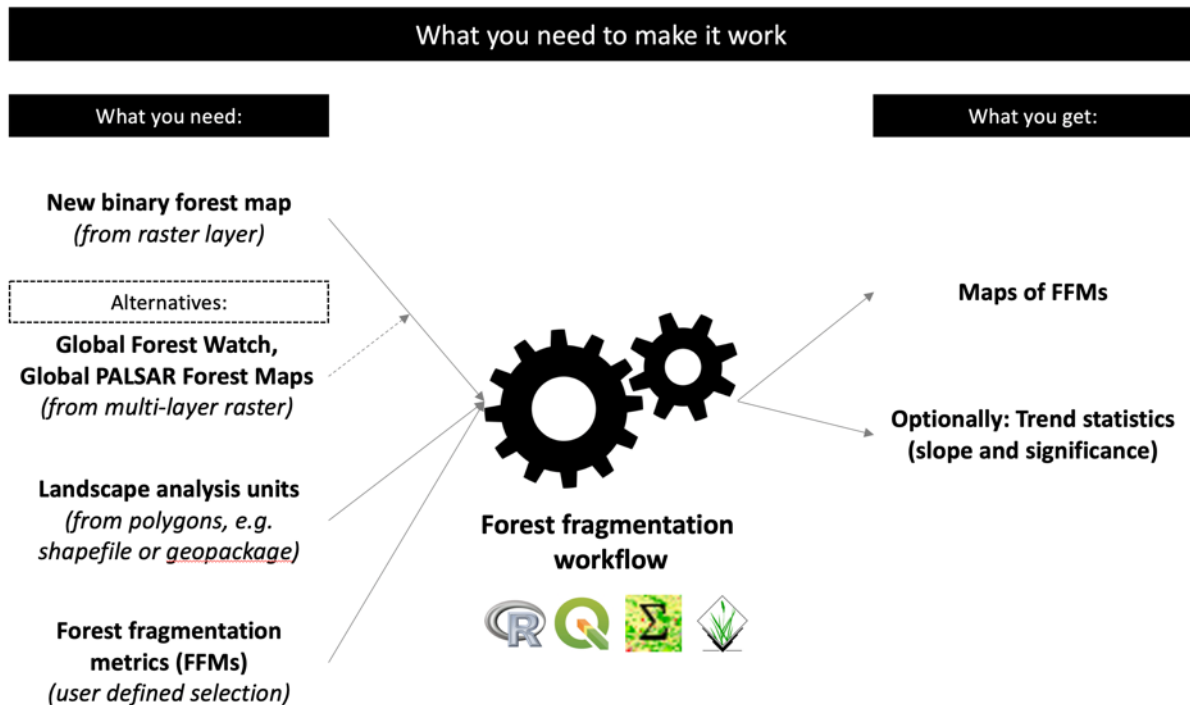


Figure 7: Overview of required data sets and information in forest fragmentation analysis.

5.3.7.2. What limitations must be expected without in-situ data, and to what extent are other data sources suitable as substitutes for in-situ data?

There are no limitations.

5.3.8. Cost benefit

Good practice recommendation: Acquire or create forest vs non-forest maps from VHR images in at least two periods and calculate a comprehensive set of FFMs (Table 7), based on these maps. This way, FFMs are likely to also reflect small-scale deforestation through selective logging.

Alternatives and trade-offs: The data available for performing a globally consistent evaluation of forest fragmentation are 30m resolution data provided by the Global Forest Watch. These can be downloaded and directly analysed in R or FRAGSTAT GUI, for example. This approach allows an assessment of FFMs at a large scale and at no cost. However, it comes at the expense of likely omitting small-scale forest fragmentation. Also consider the underlying forest definition for existing data sets,

which might deviate from the project requirement. Therefore, any fragmentation metric that is derived from these data will represent the distribution of forests only at this coarse scale, and indeed might be better said to represent the configuration of forested areas in the landscape than of individual patches of forest. Because of the problems associated with detecting small patches within very high or very low forest cover landscapes, fragmentation will be underestimated in areas of both very high and very low forest cover.

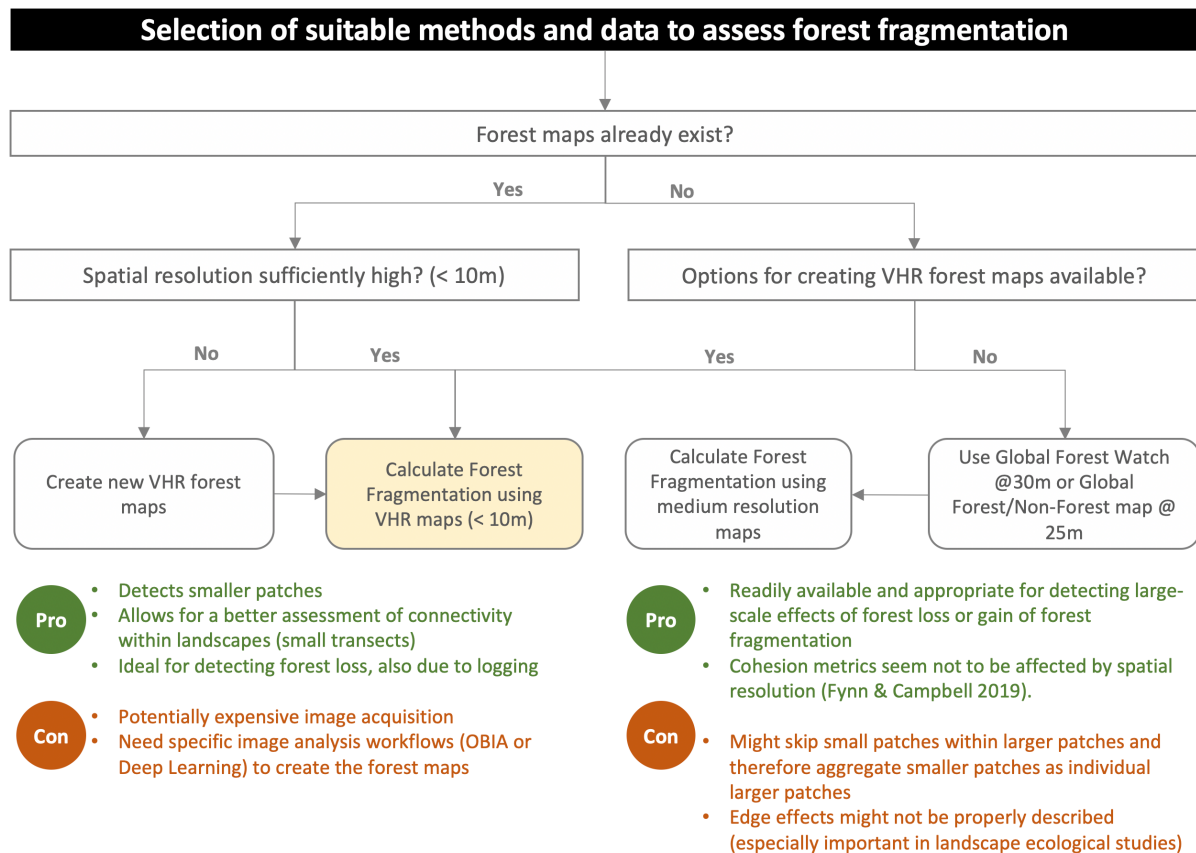


Figure 8: Guidance for selecting proper imagery and methods for assessing forest fragmentation. The "gold standard" is highlighted in yellow colours. It provides the best results in terms of spatial detail.

6. Indicator #3 – tree types

6.1. Name and short description of the indicator

"Tree types" are defined as broad categories of treed-vegetation (e.g. broad-leaved vs needle-leaved, natural vs plantations)³⁰.

6.2. Background and rationale behind indicator #3

Globally, up to 27% of forest loss has been attributed to permanent land use change for commodity production (Curtis et al., 2018). The expansion of industrial forest plantings is a critical driver of land cover land use changes. The main drivers of land cover change include expansion of agriculture and plantation estates, extraction of natural resources, infrastructure development, and small- and large-scale logging. Oil palm plantations are often blamed as the major cause of forest loss and deforestation in Indonesia and Malaysia. Deforestation, as well as other forms of land use change resulting from the development of new plantations, is also considered to be a large source of GHG emissions. Remote sensing-assisted classification of tree types is motivated by a wide variety of applications confronting the forest management and conservation sectors, such as resource inventories, biodiversity assessments or sustainable forest management.

6.3. Analysis approach and tools

6.3.1. Name of the approach

Supervised image classification for tree type mapping.

6.3.2. The degree of processing required to achieve the desired product

Readily available maps of tree types do not exist at the global level. Creating new maps requires acquisition of multitemporal images, i.e. several images per year, preprocessing these images including converting raw data to top-of-canopy reflectance and cloud removal, image compositing, calculating vegetation indices and applying machine learning algorithms in a pixel- or object-based workflow.

6.3.3. Previous applications in the scientific context

Tree types (and species) can be identified by classifying remote sensing data. Passive optical systems and especially hyperspectral systems generally showed high potential for classification of tree types and species. LiDAR data have proven to be suitable for regions with low numbers of species and might further increase their potential with new multispectral sensor systems (Axelsson et al., 2018). Previous studies reveal that the combination of multiple bands in the visible, NIR and SWIR ranges of the electromagnetic spectrum with a very high spatial resolution allows for tree type and even species classification at a single tree level. This is a promising alternative to the still relatively laborious and expensive acquisition of airborne data, although the latter is one efficient way to get a more detailed characterisation of canopies and background signals in single tree-based classification approaches in small study areas. The accuracy of forest type maps can be further enhanced when optical data is combined with radar data, called data fusion (Torbick et al., 2016).

An important step toward large-scale forest type mapping is making use of the advantages of harmonic and phenology features derived from dense image time series as compared with more con-

³⁰ This is not to be confused with tree species, which distinguishes different biological species.

ventional single-date and multi-date classification inputs (Liu et al., 2018; Ottosen et al., 2020; Pasquarella et al., 2018a; Persson et al., 2018). Applying multitemporal workflows is highly favoured because, even with two VHR images instead of one, classification accuracies can improve markedly. Poortinga et al. (2019) and Torbick et al. (2016) mapped plantations by using fusion of multitemporal Landsat-8, Sentinel 1 and 2 in forests in Southeast Asia, and decision tree algorithms. Their studies conclude that combining multi-sensor data from multispectral and SAR instruments (fusion) enhanced classification accuracy (see Table 9).

Table 9: Overview of projects, scientific publications and most important findings.

Citation	Image source	Region(s)	Method(s)	Selected land cover classes	Major findings
(Poortinga et al., 2019)	Landsat-8, Sentinel-2 and Sentinel-1	Myanmar	<ul style="list-style-type: none"> • Creation of image composites • Supervised image classification (decision tree) • Used GEE 	Cropland, forest, man-groves, palm oil, rubber, water, urban and built up	Good overall classification accuracy (84%) for the years 2017 and 2018. Used a posteriori classification probability maps.
(Torbick et al., 2016)	Landsat-8, PALSAR-2, Sentinel-1A	Myanmar and Indonesia	<ul style="list-style-type: none"> • Collected reference data from created image composites • Supervised image classification (decision tree) • Used GEE • Creation of image composites • Supervised image classification (decision tree) 	Agriculture, developed forest, plantation, water	Fusing all three sensors together provides the best overall classification performance. Overall classification accuracies were higher than 90%.
(Pasquarella et al., 2018b)	Landsat		<ul style="list-style-type: none"> • Combined existing Landsat time series algorithms to quantify both harmonic and phenological metrics in a new set of spectral-temporal features 		

6.3.4. Brief technical and content description of a recommended workflow

The complete workflow is similar to the workflow describe in section 4 and should be based on multitemporal, multi-source image classification. It applies the following steps in sequential fashion (see also Figure 9):

- **Imagery preprocessing** consists of removing clouds and shadows from optical data using the accompanying masks for the individual Sentinel and Landsat scenes.
- Conversion to top-of-canopy reflectance. Gaps in the images through clouds and shadows will be closed in the "image composites" step.
- Alternatively: Preprocessing of SAR images requires several consecutive steps. For medium resolution images, higher level products usually already exist, e.g. for Landsat 5/7/8 and Sentinel 1/2 (see Annex 1).
- Resampling all bands to 10m × 10m using nearest neighbour interpolation.
- **Calculating classification features:** for each image, compute a set of suitable vegetation indices (active sensors) or ratios (passive sensors).
- **Calculate multitemporal composites:** compositing refers to the process of combining spatially overlapping images into a single image based on an aggregation function. Multi-temporal images from the annual image collection can then be temporally composited with a maximum, minimum, and median value functions, or using percentiles, annually or separately for rainy and dry seasons, as an example.

- Calculate an integrated image stack that contains the composites from the previous step.
- Load train data (e.g. polygons).
- Calculate polygon statistics for classification features.
- Calibrate a Random Forest (RF) classifier.
- Return the evaluation scores, confusion matrices and trained classifiers.
- Apply the classifier to the entire integrated image stack and create a land cover map that contains the plantations.
- Repeat these steps for every period (i.e. different years).

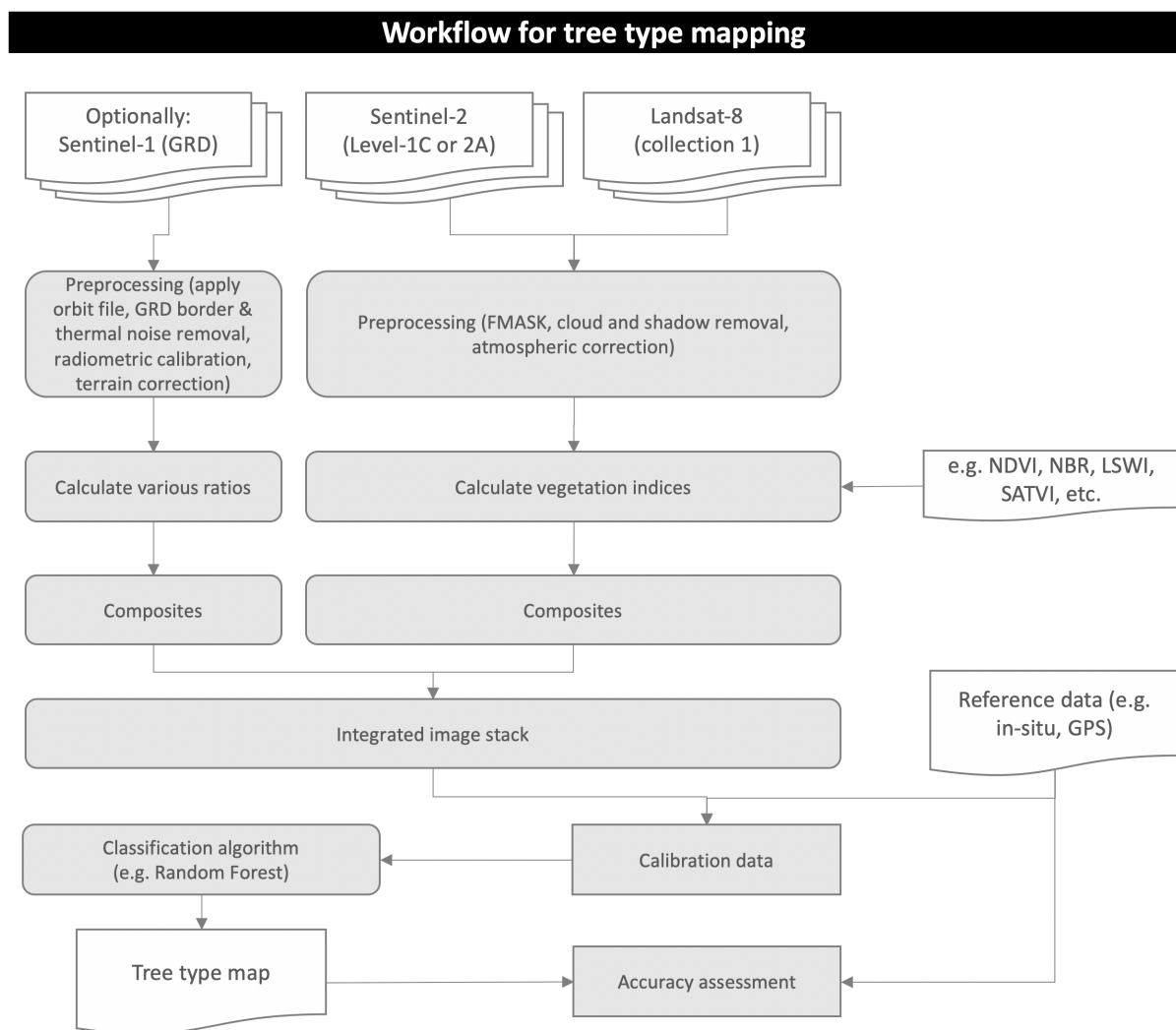


Figure 9: Flow chart and visualisation of the key processing steps used to derive tree type maps based on supervised image classification in one period. Note that object-based image analysis is not mandatory or even possible when using medium resolution satellite images.

6.3.5. Required expertise

6.3.5.1. Further statistics

No.

6.3.5.2. Geodata processing and/or handling GIS

The workflow can be implemented in QGIS using Orfeo Toolbox or the Semi-Automatic Classification Plugin (Congedo, 2016).

6.3.5.3. Technical expertise in remote sensing

Remote sensing expertise is required (time series analysis, image classification workflows, knowledge about machine learning).

6.3.5.4. Programming knowledge

If using a GUI is not an option, then programming knowledge (R, Python, GRASS GIS) is mandatory. The workflow can also be completely implemented in GEE, which has the advantage of access to the already preprocessed satellite data (here: Sentinel-1 and 2, Landsat-8 OLI) and huge computational capacities.

6.3.6. How to validate the indicator maps?

The result of this workflow is one or more thematic land cover maps(s), which can be validated using an accuracy assessment (see Annex 4 for more information). The good practices outlined by (Olofsson et al., 2014, 2013) should be considered to assess the map accuracy and to calculate error-corrected acreage estimates of different land cover types. The reference data can be used to adjust the area estimate as obtained from the map. There exist several guidelines that have a focus on the collection of reference data in the context of forestry. A summary is given in Annex 6.

6.3.7. Required input data

6.3.7.1. Suitable data sources for the approach

Reference data: As the particular focus is on investigating separability of plantations from natural forest, and given that cloud free-observations are available, reference data for plantations can potentially be collected by interpreting VHR images in Google Earth (see Figure 10). Digital tools such as CollectEarth provided by OpenForis³¹ support the collection of such reference data on-screen and are equipped to guide the user in (i) applying different reference data collection schemes (e.g. random or systematic), and (ii) the development of polygons for training and validation. The reference data that has the highest quality, however, still is the in-situ collected reference data. There exist several guidelines that have a focus on the collection of reference data in the context of forestry. A summary is given in Annex 6.

³¹ <http://www.openforis.org/tools/collect-earth.html> (last accessed: 25 September 2019).



Figure 10: Very high-resolution images in Google Earth showing the development of plantations in Cambodia. Left: 2010, Right: 2018.

Remote sensing data: Moderate resolution data such as those provided by Copernicus (Sentinel-1 and 2) or NASA (Landsat-8) can be used (see Annex 1). For mapping broad land cover categories. However, small plots and road side plantings are likely under-classified or mixed with forest or agriculture given the spatial resolution of the sensors. Plantations on high relief and complex topography requires effective SAR processing to handle viewing geometry (i.e., incidence angles, layover, foreshortening) and the availability of high resolution DEMs will be required in these cases. The fusion of SAR with optical data ultimately captures the suite of characteristics that make plantations (e.g. oil palm and rubber) unique (Torbick et al., 2016). Additional temporal information should further improve mapping. Thus, multitemporal analysis is recommended because a combination of active and passive sensor data provides a sufficiently dense spatio-temporal data series, even in regions with persistent cloud cover, to separate between different land cover and plantation types (Poortinga et al., 2019).

Alternatives – existing data sets: usually not available, but the Spatial Database of Planted Trees (SDPT Version 1.0) available via the Global Forest Watch (check the “Tree plantations” layer for the year 2015) or via the World Resources Institute (WRI)³² (Congedo, 2016) should be consulted (Annex 2).

6.3.7.2. What limitations must be expected without in-situ data, and to what extent are other data sources suitable as substitutes for in-situ data?

VHR data can substitute in-situ data if the particular focus is on investigating separability of plantations from natural forest, or between broad forest types (broad-leaved vs needle-leaved). Without in-situ data, certain cultivars (species, such as acacia, teak, eucalyptus, and bamboo) in plantations cannot be identified from VHR images.

³² <https://www.wri.org/publication/planted-trees> (last accessed last accessed: 25 November 2019).

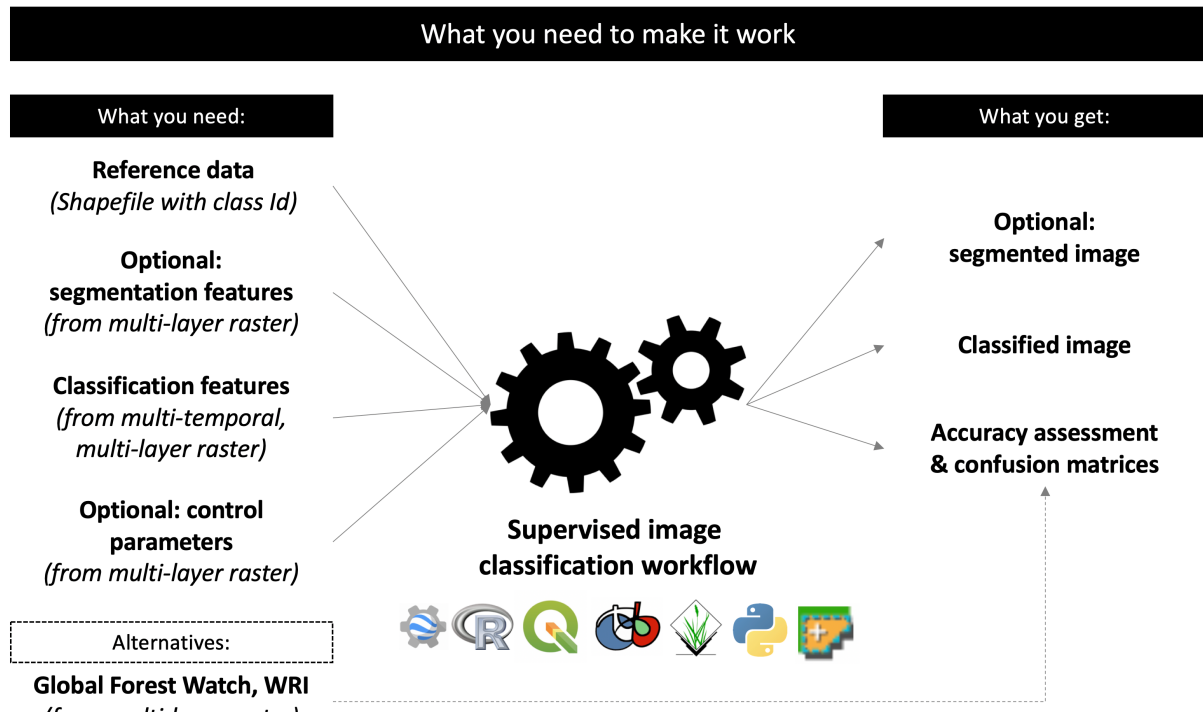


Figure 11: Overview of required data sets and information for creating forest type maps.

6.3.8. Cost benefit

Good practice recommendation: Gather reference data about tree types or plantations, at best in-situ or from existing VHR sources (second choice), and acquire multitemporal (i.e., several images per year) multi-source satellite images (i.e., multispectral and optical) in at least two periods. Apply machine learning algorithms such as RF to classify image composites and create annual land cover maps that entail information about tree types. Assess and quantify land cover change, based on the annual maps. Evaluate the accuracy of the annual and change maps. Report accuracy metrics and calculate land cover area statistics corrected for accuracy and provide a second map showing a posteriori classification probabilities.

Alternatives and trade-offs: use existing maps such as SDPT, but these are only available for some regions and certain years.

7. Indicator #4 – forest biomass

7.1. Name and short description of the indicator

"Forest biomass" is defined as above-ground biomass (AGB) of tree canopy and tree stem biomass including the forest floor, shrub layer, understorey, subcanopy and main canopy.

"Tree Stem Biomass" is defined as solid cubic metres (SCM) of tree stem biomass. This indicator is used to assess logging and economic factors of forestry.

Each of the methods focuses on the derivation of tree stem biomass that is economically exploited as timber wood through industrial logging. Although some of the RS-based methods perform better for the derivation of green forest biomass (indicator for carbon sequestration, forest inventory, biodiversity and habitat mapping).

7.2. Background and rationale behind indicator #4

Accurate measurement and mapping of biomass is a critical component of carbon stock quantification, climate change impact assessment, suitability and location of bio-energy processing plants, assessing fuel for forest fires, and assessing merchandisable timber. While above-ground biomass includes both live and dead plant material, most of the recent research effort on biomass estimation has focused on the 'live' component (live trees) due to the prominence of this component. Accurately estimating biomass is a prerequisite for better understanding the impacts of deforestation and environmental degradation on climate change as well as the economic benefits of forestry and agroforestry practices.

7.3. Analysis approach and tools

7.3.1. Name of the approach

- AGB biomass derivation based on
 - a. RS time-series metrics (TSM)
 - b. 3D modelling from stereo imagery (DSM) or airborne laser scanning (ALS)
 - c. SAR interferometry (InSAR) or Polarimetric SAR (PolSAR)
 - d. multisource SAR (SAR)
 - e. physical models
- SCM biomass derivation
 - a. 3D modelling from stereo imagery (DSM) or airborne laser scanning (ALS)
 - b. multisource SAR (SAR)

In certain cases the derivation of a Digital Surface Model (DSM) from stereo imagery can also be achieved using airborne flight missions (mostly from the topographical surveys of the respective state agency) or locally calibrated UAV/drone-based missions. Of course, the highest accuracy of tree stem biomass can be achieved through airborne or UAV-based laser scanning / LIDAR. However, in this review we do not discuss this approach as we assessed it as unfeasible due to its high operational and data processing costs.

7.3.2. The degree of processing required to achieve the desired product

Readily available maps of Forest AGB exist at global level, but not for tree stem biomass as this must be calibrated locally, and the derivation of the exact solid cubic metres only is only sufficiently reli-

ble when using VHR imagery, laser scanning or actual ground measurements. Creating new maps requires acquiring multitemporal images (i.e. several images per year), preprocessing these images (including converting raw data to top-of-canopy reflectance and cloud removal), image compositing, calculating vegetation indices, SAR image calibration and applying machine learning algorithms in a pixel- or object-based workflow.

7.3.3. Previous applications in the scientific context

Forest biomass can be estimated by associating pixel values from remote sensing data with in-situ data and thus calibrating a regression model to estimate new, unseen pixels to minimise model errors to the greatest extent possible. In general, regression summarises the statistical relationship between a dependent variable (canopy biomass in t/ha, m³/ha or kg/m², tree stem biomass in kg or m, tree height in m) and a series of independent (or explanatory) variables. The purpose of the analysis is to find the most optimum fit using a regression equation and to evaluate the goodness of fit through statistical metrics. For non-linear relationships, the regression equation becomes quadratic or of higher polynomial order when using parametric methods. For non-parametric methods (e.g. Random Forest or Gradient Boosting) the estimation is done based on decision trees.

Previous studies exploit a variety of methods based on optical satellite image analysis or active remote sensing from SAR imagery (interferometric analysis or polarimetric time series).

Table 10: Overview of projects, scientific publications and most important findings.

Citation	Image source	Region(s)	Method(s)	Selected dependent variable	Major findings
(Poortinga et al., 2019)	MODIS	Brazil	<ul style="list-style-type: none"> • Creation of multitemporal NDVI metrics • Bioclimatic variables • Linear regression 	Eucalyptus plantation biomass	<ul style="list-style-type: none"> • Good overall fit with RMSE of around 25m³/ha
(Torbick et al., 2016)	Landsat, ALOS PALSAR 2	China	<ul style="list-style-type: none"> • Collected reference data from in-situ campaigns • Combined SAR and optical variables • Supervised multivariate regression based on in-situ data (RF, ANN, SVM) 	Forest AGB in subtropical regions and stratified per forest type	<ul style="list-style-type: none"> • Best results with neural network regression • However, SAR and optical data alone cannot solve the problem • More variables needed (soil, climate data) • For biomass estimations > 120 MG/ha
(Pasquarella et al., 2018b)	SAR Sentinel-1, ALOS PALSAR 2, RADARSAT-2, TanDEM-X	Multiple	<ul style="list-style-type: none"> • Interferometric SAR from multiple wavelengths (X-band, C-band, L-band SAR) • Parametric and non-parametric regression • Backscatter, coherence 	<ul style="list-style-type: none"> • Above-ground carbon stock • AGB • Above-ground carbon density • Growing stock volume • Tree biomass 	<ul style="list-style-type: none"> • Estimating biomass in trunks, branches and foliage • Combination of multiple band wavelength for InSAR
(Maack et al. 2017)	SPOT-6/-7 Pleiades 1	Germany	<ul style="list-style-type: none"> • Stereo imaging • Derivation of digital surface model • Forest canopy height estimation • Comparison with LIDAR data estimates 	Forest canopy height	<ul style="list-style-type: none"> • Good alternative to LIDAR approach • Very high accuracy • Overestimation of low biomass areas
(Antropov et al. 2017)	ALOS PALSAR 2	Finland	<ul style="list-style-type: none"> • Polarimetric SAR time series • 3D DSM from TanDEM-X data • Canopy height derivation 	<ul style="list-style-type: none"> • AGB • Canopy height 	<ul style="list-style-type: none"> • RMSE = 24t/ha • Comparable to laser scanning data estimates
(Laurin et al. 2018)	Sentinel-1	Italy	<ul style="list-style-type: none"> • Polarisation bands and ratios • Multitemporal backscatter analysis 	<ul style="list-style-type: none"> • Tree stem biomass 	<ul style="list-style-type: none"> • RMSE = 46t/ha • R² = 0.7 • Regression of backscatter

			<ul style="list-style-type: none"> • Linear regression 		<ul style="list-style-type: none"> without interferometry • Possible mapping up to 400t/ha • Leaf presence in C-band data
(Pandit et al. 2019)	Sentinel-2	Nepal	<ul style="list-style-type: none"> • Texture metrics • Random Forest regression 	<ul style="list-style-type: none"> • AGB 	<ul style="list-style-type: none"> • RMSE = 5t/ha • Good fit
(Askar et al. 2019)	Sentinel-2	Indonesia	<ul style="list-style-type: none"> • Regression analysis of Vegetation Indices (NDVI, EVI, GNDVI) 	<ul style="list-style-type: none"> • AGB 	<ul style="list-style-type: none"> • Strong correlation • $R^2 = 0.81$

7.3.4. Brief technical and content description of a recommended workflow

We present four different and complete workflows, based on multitemporal, multi-source satellite image analysis from optical and active sensor platforms. Their primary focus is on spaceborne remote sensing data.

7.3.4.1. RS time series metrics

This approach is based on the derivation of optical or SAR image time series metrics capturing and describing the phenological development of forest biomass and growth patterns. It is described as follows:

- **Imagery preprocessing** consists of removing clouds and shadows from optical data using the accompanying masks for the individual Sentinel-2 and Landsat scenes.
- Conversion to top-of-canopy reflectance. Gaps in the images through clouds and shadows will be closed in “image composites” step.
- For medium resolution images, higher level products usually already exist, e.g. for Landsat 5/7/8 and Sentinel 1/2 (see Annex 1).
- Preprocessing of SAR images (preferably Sentinel-1 GRD data) requires several consecutive steps such as radiometric calibration, speckle filtering, terrain correction and flattening to derive the backscatter coefficient (e.g. sigma naught values per pixel).
- Resampling all bands to 10m × 10m using nearest neighbour interpolation.
- **Calculating explanatory features:** for each image, compute a set of suitable vegetation indices (active sensors) or ratios (passive sensors).
- **Calculate multitemporal metrics:** compositing refers to the process of combining spatially overlapping images into a single image based on an aggregation function. Multitemporal images from the annual image collection can then be temporally composited with a maximum, minimum, and median value function, or using percentiles, annually or separately for rainy and dry season, as an example.
- **Calculate an integrated image stack** that contains the composites from the previous step.
- **Load train data (e.g. polygons).**
- **Calculate polygon statistics** for explanatory features.
- **Calibrate** a Random Forest (RF) regressor.
- Return the evaluation scores and trained models.
- **Apply the regressor to the entire integrated image stack** and create a forest biomass map that contains the plantations.
- **Repeat** these steps for every period (i.e., different years).

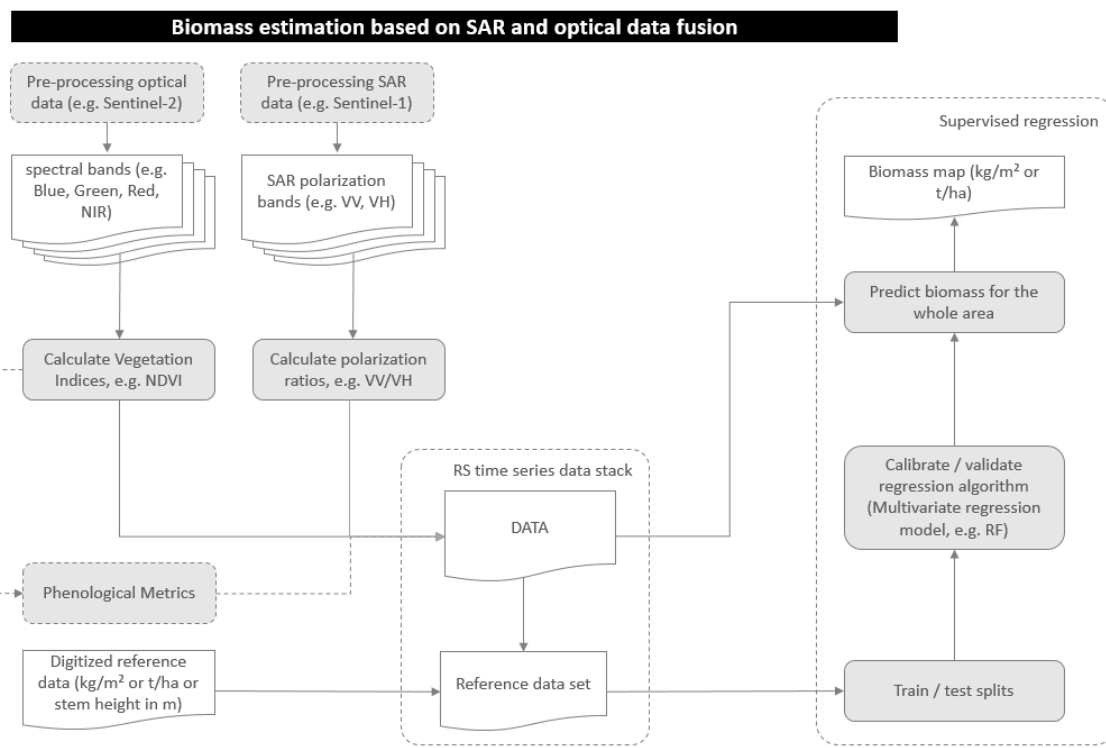


Figure 12: Flow chart for biomass estimation based on optical and SAR data fusion

7.3.4.2. 3D Modelling from stereo imagery

This approach is based on the derivation of a Digital Surface Model (DSM) from VHR stereo imagery from SPOT-6/-7, Pleiades 1a/1b or other source with stereo imaging capabilities.

- **Image acquisition:** cloud free, orthorectified, radiometrically calibrated and terrain corrected stereo or tri-stereo image pairs from Airbus
- Calculate interior and exterior orientation parameters
- Co-registration of image pairs
- Find tie-points and reference points for image pairs
- Extract point cloud data
- Calculate DSM with 5m x 5m resolution
- Resample DSM to 30m x 30m using bilinear interpolation.
- Subtract World DEM (SRTM or other) from DSM and derive normalized height model containing forest canopy heights (in metres)
- **Load in-situ data (e.g. polygons or GPS points with biomass data);**
- Convert canopy height (volume) in forest biomass through linear regression
- Return the evaluation scores and trained models;
- **Repeat** these steps for every period (i.e., different years).

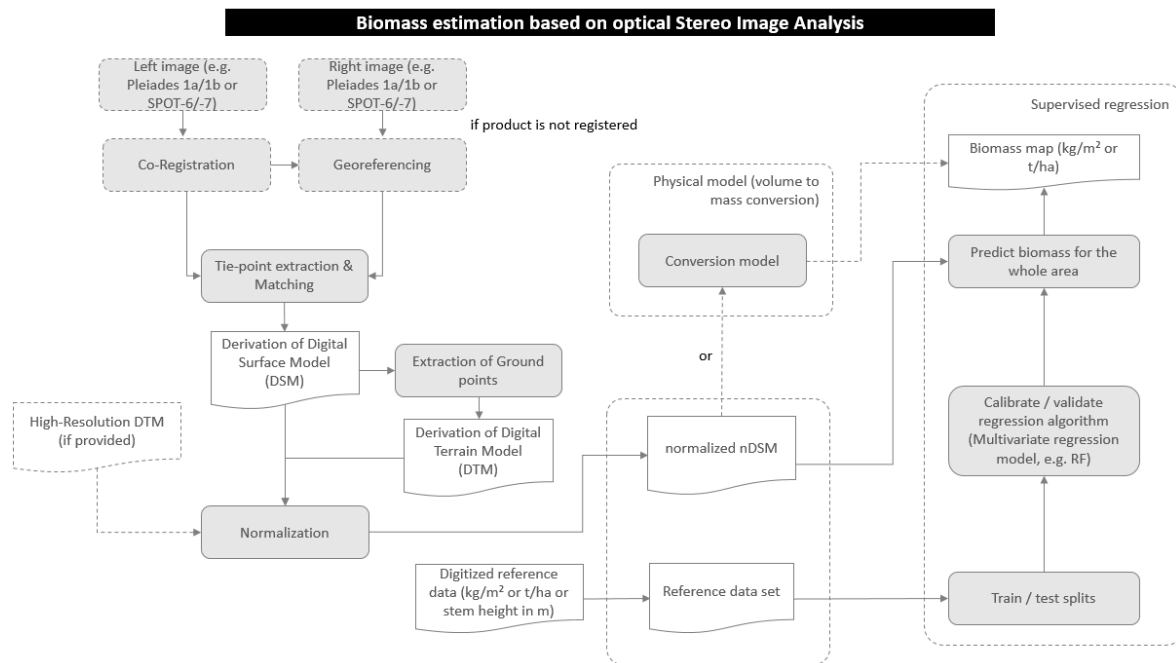


Figure 13: Flow chart for biomass estimation based on optical stereo image analysis

An alternative, but very costly approach is given through Airborne Laserscanning (ALS), either from UAV or airborne platforms. The advantage of ALS over other methods is the capability of direct measurements and a relatively high observation point density. The laser scanner emits signals which are returned at a) the canopy (first return), b) stems, branches and leaves in the understory (intermediate return) and c) the ground (last return). The computation of these vertical metrics allows the derivation of forestry biomass indicators such as:

- diameter-at-breast height
- canopy and stem height
- stem volume
- age
- crown ratio
- stem, bark and total mass

A standard framework is described as following:

- **Data acquisition:** high density point cloud data (8-100 points per sqm), with 3-dimensional coordinates
- Point cloud processing in software such as LAS Tools, QGIS/GRASS or ArcMAP (3D-Analyst)
- Removal and filtering of outlier data points (noise, systematic error points)
- Extraction of the different return signal categories (canopy, understory, ground points)
- Calculate DSM with 1 x 1m resolution
- Calculate DEM with 1 x 1m resolution based on ground signal points and interpolate if needed (e.g. spatial interpolation methods such as Inverse Distance Weighting or Kriging)
- Subtract DEM from DSM and derive normalized height model containing canopy or stem heights (in metres)
- Use additional optical imagery (or derived vegetation indices) to compute the spatial extent of green canopy if needed and calculate the total canopy biomass (e.g. estimation of carbon sequestration applications) based on the derived vertical metrics from the ALS data

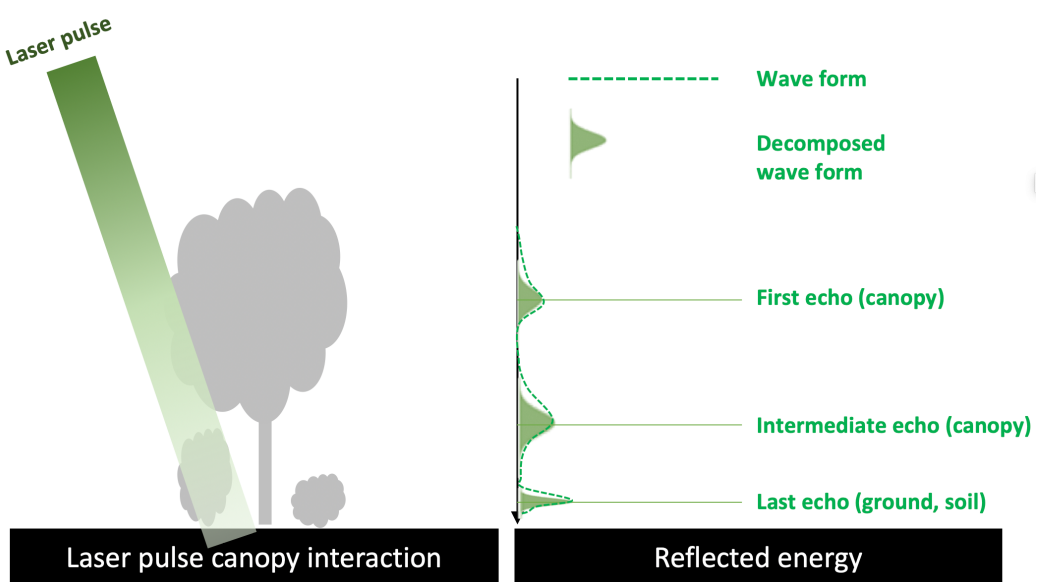


Figure 14: A schematic depiction of the laser pulse and response within forest canopies (from: adapted from Leiterer et al. 2015¹)

ALS approach is the most accurate, but financially and computationally (some datasets may have > 50 million points in a single point cloud) expensive approach, with the data costs reaching starting from 120€ per sqkm (including manhours, expenses and costs for data processing such as image stitching and bundle adjustment) whereas satellite borne systems are capable to capture a much larger area at once (usually image swath widths are greater than 20x20km).

7.3.4.3. SAR Interferometry (InSAR)

This approach is based on interferometric SAR image analysis, preferably from free Sentinel-1 SLC (Single Look Complex) data.

- **Sentinel-1 image preprocessing:** orbit file application and correction, radiometric calibration, speckle filtering, terrain correction, co-registration of SAR image pairs
- Derive interferogram
- Deburst and calculate coherence
- Topographic phase removal
- Phase filtering
- **DSM derivation**
- Subtract World DEM (SRTM or other) from derived DSM and derive normalized height model containing forest canopy heights (in metres)
- **Load in-situ data (e.g. polygons or GPS points with biomass data);**
- Convert canopy height (volume) in forest biomass through linear regression
- Return the evaluation scores and trained models;
- **Repeat** these steps for every period (i.e., different years).

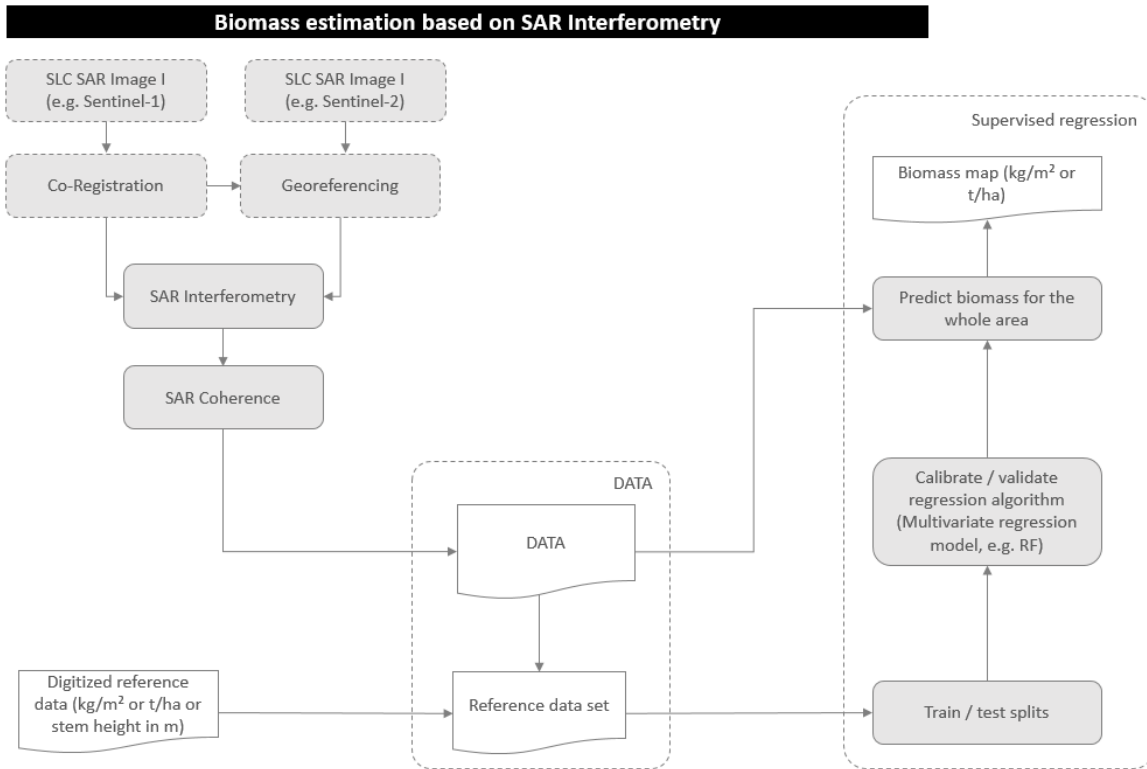


Figure 15: Flow chart for biomass estimation based on SAR Interferometry

7.3.4.4. Multisource SAR

This approach is based on the differential application of multisource SAR data with different wavelengths: shorter wavelength X-band data (from TerraSAR-X platform) is reflected directly at the canopy or vegetation surfaces whereas longer wavelength L-Band data (ALOS PALSAR 2) is able to penetrate plant leaf matter and to bounce off at tree stems or thicker branches. The returning signal is also mixed with volumetric scattering depending on the tree type and look angle.

- **Sentinel-1 image preprocessing:** orbit file application and correction, radiometric calibration, speckle filtering, terrain correction, co-registration of SAR image pairs
- Derive interferogram
- Deburst and calculate coherence
- Topographic phase removal
- Phase filtering
- **DSM derivation**
- Subtract World DEM (SRTM or other) from derived DSM and derive normalized height model containing forest canopy heights (in metres)
- **Load in-situ data (e.g. polygons or GPS points with biomass data);**
- Convert canopy height (volume) in forest biomass through linear regression
- Return the evaluation scores and trained models;
- **Repeat** these steps for every period (i.e., different years).

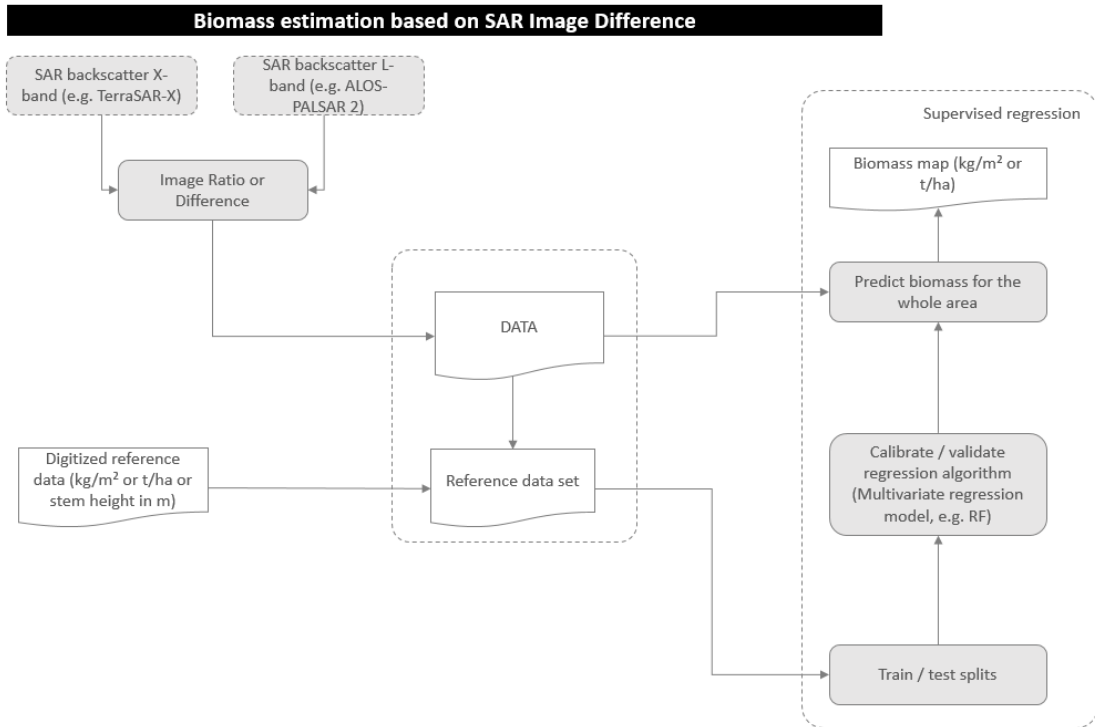


Figure 16: Flow chart for biomass estimation based on SAR data analysis with different signal wavelengths

Additionally, polarimetric information from the different polarisation bands (vertical and horizontal) can be deployed to distinguish horizontal (forest canopy and green biomass based on analysis of the volumetric scattering of the SAR signal) and vertical biomass components.

So-called Quadpol polarisation, which is found in sensor systems such as TerraSAR-X, contains a cross-combination of the possible polarisations of the electromagnetic wave in vertical-vertical (VV), vertical-horizontal (VH), horizontal-vertical (VH) and horizontal-horizontal (HH) bands. Sentinel-1 contains only Dualpol polarimetry in VV and VH, making it more difficult to capture horizontal scattering effects.

7.3.5. Required expertise

7.3.5.1. Further statistics

Yes.

7.3.5.2. Geodata processing and/or handling GIS

The basic linear regression workflow can be implemented in ArcGIS using the Spatial Statistics Toolbox (proprietary) or Weka 3 (open source machine learning toolbox, <https://www.cs.waikato.ac.nz/ml/weka/>). The 3D modelling workflow can be implemented in QGIS and OrfeoToolbox by using the stereo framework (https://docs.qgis.org/2.6/de/docs/user_manual/processing_algs/otb/stereo/stereoframework.html). However, advanced non-linear multivariate regression should be performed via machine learning toolkits such as scikit-learn or R.

7.3.5.3. Technical expertise in remote sensing

Remote sensing expertise is required (time series analysis, image classification workflows, knowledge about machine learning).

7.3.5.4. Programming knowledge

When using a GUI is not an option, then programming knowledge (R, Python, GRASS GIS) is mandatory. The workflow can also be completely implemented in GEE, which has the advantage of access to the already preprocessed satellite data (here: Sentinel-1 and 2, Landsat-8 OLI) and huge computational capacities.

7.3.6. How to validate the indicator maps?

The result of this workflow is one or more forest biomass map(s). There exist several guidelines that have a focus on the collection of reference data in the context of forestry, including biomass estimation and validation of such maps. A summary is given in Annex 6.

7.3.7. Required input data

7.3.7.1. Suitable data sources for the approach

Reference data:

As the particular focus is on the extraction of tree stem biomass, a biophysical parameter, ground truth data from in-situ observations is crucial for the calibration and validation of empirical and physical models. Image interpretation can only lead to the extraction of categorical data without in-situ data collection, such as the qualitative categorisation (e.g. low, medium or high biomass) of tree stem biomass from forest density interpretation in Google Earth imagery or through vegetation indices from Copernicus data.



Figure 17: Very high-resolution images in Google Earth showing the development of plantations in Cambodia. Left: 2010, Right: 2018.

Remote sensing data: Moderate resolution data such as those provided by Copernicus (Sentinel-1 and 2) or NASA (Landsat-8) can be used (see Annex 1) for the extraction of biomass through multivariate regression and machine learning. However, small plots and roadside plantings are likely under-classified or mixed with forest or agriculture given the spatial resolution of the sensors. Plantations on high relief and complex topography require effective SAR processing to handle viewing geometry (i.e., incidence angles, layover, foreshortening) and the availability of high resolution DEMs will be required in these cases. The fusion of SAR with optical data ultimately captures the suite of charac-

teristics that make plantations (e.g. oil palm and rubber) unique (Torbick et al., 2016). Additional temporal information should further improve the derivation of forest biomass.

For the exact derivation of tree heights from 3D modelling, VHR stereo imagery can be used from the SPOT-6/-7 and Pleiades 1a/1b platforms. However, VHR stereo imagery is not free and significant costs should be considered (ranging between EUR 12 and EUR 30 per sqkm). Moreover, the processing of VHR data requires a high-performance computing environment and Big Data handling capabilities (a Sentinel-2 granule with 100x100km swath has a file size of approx. 1GB whereas the same swath with VHR data is 100 times the size).

The third method is based on mono-temporal analysis and requires SAR data with different wavelengths and frequencies such as the image difference between X-band (TerraSAR-X) and L-band (ALOS PALSAR 2) sensors.

The fourth method is based on SAR interferometry and requires SLC (Single Look Complex) data from Sentinel-1 or other (proprietary) SAR data sources (TerraSAR-X, ALOS PALSAR, etc).

Alternatives – existing data sets: available datasets are mostly related to AGB such as

- Above-ground live wood biomass density (Global Forest Watch)
- Global forest biomass map (GEOCARBON, biomasar.org)
- European map of living forest above-ground biomass (EU Open Data Portal)
- Global 1-degree maps of forest area, carbon stocks, and biomass, 1950-2010 (ORNL DAAC)
- MODIS Net & Gross Primary Products in 500m spatial resolution (USDAAC, NASA)
- IIASA's Global Forest Database
- Tropical Africa and Southeast Asia 1980 and 2000 Forest Biomass Maps
- Mexico Forest Biomass Map (250m) and many more national forest biomass mapping projects (Zhang et al, 2019: A Review of Regional and Global Gridded Forest Biomass Datasets).

7.3.7.2. What limitations must be expected without in-situ data, and to what extent are other data sources suitable as substitutes for in-situ data?

As forest biomass is a biophysical parameter, it cannot be derived from uncalibrated remote sensing data. However, proxy estimates can evaluate the change of biomass density through simple vegetation index (NDVI, NDWI) image difference change detection. When using stereo imagery for 3D modelling, forest and single tree heights can be extracted directly from the Digital Surface Models (DSM) without in-situ data. However, a validation of the derived results cannot be performed as well, and the quality of the derived map and model cannot be assessed. An overview of different product sources is given in Annex 2.

7.3.8. Cost benefit

Good practice recommendation: Gather reference data about tree stem biomass, either per forest plot or GPS coordinates of captured in-situ data. Apply machine learning algorithms such as RF to estimate biomass from image composites and create annual forest biomass maps with per-pixel biomass estimates. Assess and quantify forest biomass change, based on the annual maps. Evaluate the accuracy of the annual and change maps. Report accuracy metrics and calculate forest biomass statistics corrected for accuracy and provide a second map showing per-pixel R² (coefficient of determination) or RMSE (round mean square error) scores.

Alternatives and trade-offs: Estimate tree heights (canopy height) from 3D model based on stereo imagery analysis. However, data costs may be prohibitive.

8. Indicator #5 – individual tree crowns

8.1. Name and short description of the indicator

"Individual tree crowns" are defined as the top part of the tree, which features branches that grow out from the main trunk and support the various leaves used for photosynthesis.

8.2. Background and rationale behind indicator #5

The detection of individual tree crowns (ITC) with automated algorithms is its own field of research. In previous studies, single tree delineation was either performed manually or with automated algorithms that were often based on earlier studies (Zhen et al., 2016). One suggestion to increase applicability is to use manually delineated crowns in the training stage followed by applying the trained algorithm to crown objects automatically delineated from airborne laser scanning (ALS), also referred to as Light Detection and Ranging or LiDAR data. LiDAR data was found to be advantageous for single tree delineation as it is less affected by occlusions and shading than passive optical data (Dalponte et al., 2014).

In recent years ALS has thus become an operational tool for producing forest inventory data with wall-to-wall coverage over large areas by combining the ALS data with conventional measurements from field sample plots (White et al., 2013; Zhang et al., 2015). Basically, two methods for analysing the ALS data can be distinguished: area-based approaches (ABA) and the ITC approach, sometimes also referred to as individual tree detection (ITD). In the ABA, ALS raw data are aggregated on the inventory plot level by describing them according to height and canopy density metrics. These metrics can subsequently be used as independent variables in regression models. In the ABA, forest stand attributes are estimated for a grid cell (typically 20–30m on a side), based on metrics that summarise the distribution of the point cloud within the cell.

Likewise, in the ITC approach, either canopy height models (CHM) or the ALS raw data point clouds are segmented into (single) tree crowns. However, this method depends on the accuracy of tree identification and is prone to errors that result from over- or under-segmentation of tree crowns. Tree properties can subsequently be estimated using the segment properties, such as segment area or ALS-derived height metrics as explanatory variables. This method is more intuitive than ABA since the response variable refers to the single tree, which is in fact the smallest unit on which forest management is carried out. In addition, ITC provides the tree coordinates.

8.3. Analysis approach and tools

8.3.1. Name of the approach

Individual tree crown (ITC) detection and classification.

8.3.2. The degree of processing required to achieve the desired product

The mapping approach encompasses an analysis chain which consists of preprocessing LiDAR (and optionally VHR images), followed by an image segmentation and classification procedure.

8.3.3. Previous applications in the scientific context

Dalponte et al. (2014) found that ITC delineated on hyperspectral and ALS data provided different classification results. It has been shown that ITC delineation on CHM derived from ALS data provided

a higher tree detection rate than that on hyperspectral bands, and an even better detection rate than manual digitisation. Weinstein et al. (2019) used deep learning (DL) to classify RGB aerial images in an attempt to work without ALS. They found that, compared to LiDAR methods, DL and RGB images achieved very good results but they postulated that combining LiDAR and RGB is likely to further increase accuracy.

The most widely applied active data source for ITC in the last decade is discrete return ALS data (Zhen et al., 2016). Three-dimensional ALS data with high spatial resolution facilitate derivation of a large number of statistical features (e.g., tree height, quartile heights, crown base height) that are difficult to generate from spectral imagery. Breidenbach et al. (2010) enhanced ITC based on the fusion of ALS and RGB-NIR aerial imagery and then applied the ITC results to predict species-specific volume. However, most of these integrated studies used active data sources (ALS) for crown delineation and then applied multispectral imagery, e.g., to perform species classification (Zhen et al., 2016). Based on the literature review it can be said that ALS data offer the greatest added value for ITC detection and mapping. A good overview on forestry applications of ALS is given by Maltamo et al. (2014). Jakubowski et al. (2013) compare different approaches to delineate ITCs.

Table 11: Overview of projects, scientific publications and most important findings.

Citation	Image source	Region(s)	Method(s)	Reference data	Major findings
(Dalponte et al., 2014)	• Airborne hyperspectral and ALS	Norway	• Manual delineation (hyperspectral data) • Automatic from hyperspectral and ALS (Poisson forest stand model applied by Ene et al. (2012))	• Field data from 23 circular plots, diameter at breast height, tree coordinates, tree species	• ALB was more accurate in identifying ITCs
(Weinstein et al., 2019)	• Airborne RGB images	California, USA	• Deep Learning	• Reference trees by visual interpretation of airborne RGB Images and additional data from LiDAR-based maps • Used for training the DL	• Compared to LIDAR methods, DL and RGB images achieve very good results • Combining LiDAR and RGB likely to increase accuracy
(Mohan et al., 2017)	• UAV-derived point clouds from RGB images	Wyoming, USA	• Local maxima algorithm (implemented in the rLiDAR package in R)	• Reference trees by visual interpretation of airborne RGB images • Used for validation	• Derived tree counts with acceptable accuracy (F score > 0.80)
(Breidenbach et al., 2010)	• ALS • Aerial optical images	Norway	• Segmentation (local maxima using canopy surface model) and subsequent classification (RF)	• Field data (GPS): tree species, diameter at breast height, tree height • Used for training and validation	• Errors of type i) resulted in 6% of the measured trees in the field inventory being located outside of any crown segment
(Tochon et al., 2015)	• Airborne hyperspectral data and ALS	Hawaii and Panama	• Segmentation (binary partition tree)	• Manually digitized ITCs from hyperspectral data • Used for validation	• Correctly segmented up to 68% of tree crowns
(Zhang et al., 2015)	• Airborne hyperspectral data and ALS	Dallas, USA	• DTM, vegetation LiDAR points via NDVI from hyperspectral canopy surface point extraction (local maximum method), donut expanding and sliding method (segmentation)	• Diameter at breast height, tree coordinates, tree species, health condition	• The tree climbing algorithm described above may work for trees with a single well-defined apex, such as most conifers, for trees with multiple tops or a concave crown shape, commission errors may occur

8.3.4. Brief technical and content description of a recommended workflow

A recommended workflow to create maps of ITCs uses a combination of ALS and optical VHR data, and consists of several consecutive steps (Figure 19):

- **Acquire and process ALS data (drone or aerial) and VHR images** (drone, aerial, or satellite) for the entire area of interest (wall-to-wall coverage).
- **Acquire tree-level measures (reference data)** from sampled ground plots and summarise to the plot level, alternatively from existing VHR data via digitisation of reference ITCs.
- Create three basic products from the ALS point data (see Figure 18):
 - LiDAR data filtering is one important first step to separate ground from above-ground laser points returns. Ground points are then used to build a digital terrain model (DTM)³³, which will assist with the elimination of local terrain impact on tree metric estimation.
 - The point cloud is processed to generate an accurate DEM from the classified ground returns and a DSM from the non-ground first returns.
 - Finally, a canopy height model (CHM) is generated by subtracting the DEM from the DSM;
- Apply a **segmentation** technique to extract ITCs, e.g. using local minima/maxima methods or mean shift segmentation.
- For each segment, derive **metrics** (response & predictors) from the input data (e.g. mean band values or textures from optical VHR data; x,y,z and CHM from ALS).
- Perform a **classification** to create a final map of ITCs (separate tree from non-tree segments). If you have reference data about tree species, you would then classify the segments into individual species at this point of the workflow.
- Use reference data (at best in-situ, including GPS positions of individual tree trunks, diameter at breast height, and tree height) to **validate** the final map.

Three Important Lidar Data Products: CHM, DEM, DSM

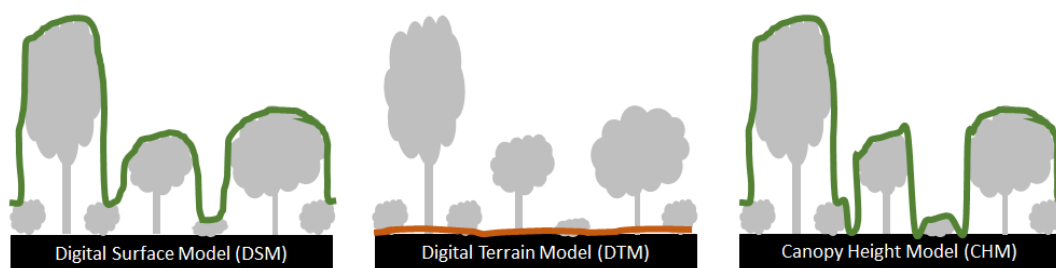


Figure 18: Three Important Lidar Data Products: DSM, DTM, CHM.

Table 12: Freely available software and tools suitable for calculating indicator #5 "Single tree crowns".

Name	Purpose	Most important functions	Link
R	xxx	• Raster processing: R package	https://cran.r-project.org

³³ Please note that in some countries, a DTM is actually synonymous with a DEM. This means that a DTM is simply an elevation surface representing the bare earth referenced to a common vertical datum. For further details: <https://pubs.usgs.gov/tm/11b4/pdf/tm11-84.pdf> (last accessed: 25 November 2019).

		'rLiDAR' • Raster processing: R package 'lidR'	http://project.org/web/packages/lidR/readme/README.html https://github.com/gisma/uavRst/wiki/Building-a-Canopy-Height-Model-(CHM)-using-lidR
GRASS		Geomorphons to detect ITCs r.geomorphon	http://grasswiki.osgeo.org/wiki/LIDAR https://grasswiki.osgeo.org/wiki/Lidar_Analysis_of_Vegetation_Structure https://grass.osgeo.org/grass76/manuals/addons/r.geomorphon.html
liblas			https://liblas.org/
QGIS		LASTools	http://www.cs.unc.edu/~isenburg/lastools/ https://docs.qgis.org/2.14/de/docs/user_manual/processing_algs/LidarTools/lastools.html
Python		laspy	https://laspy.readthedocs.io/en/latest/

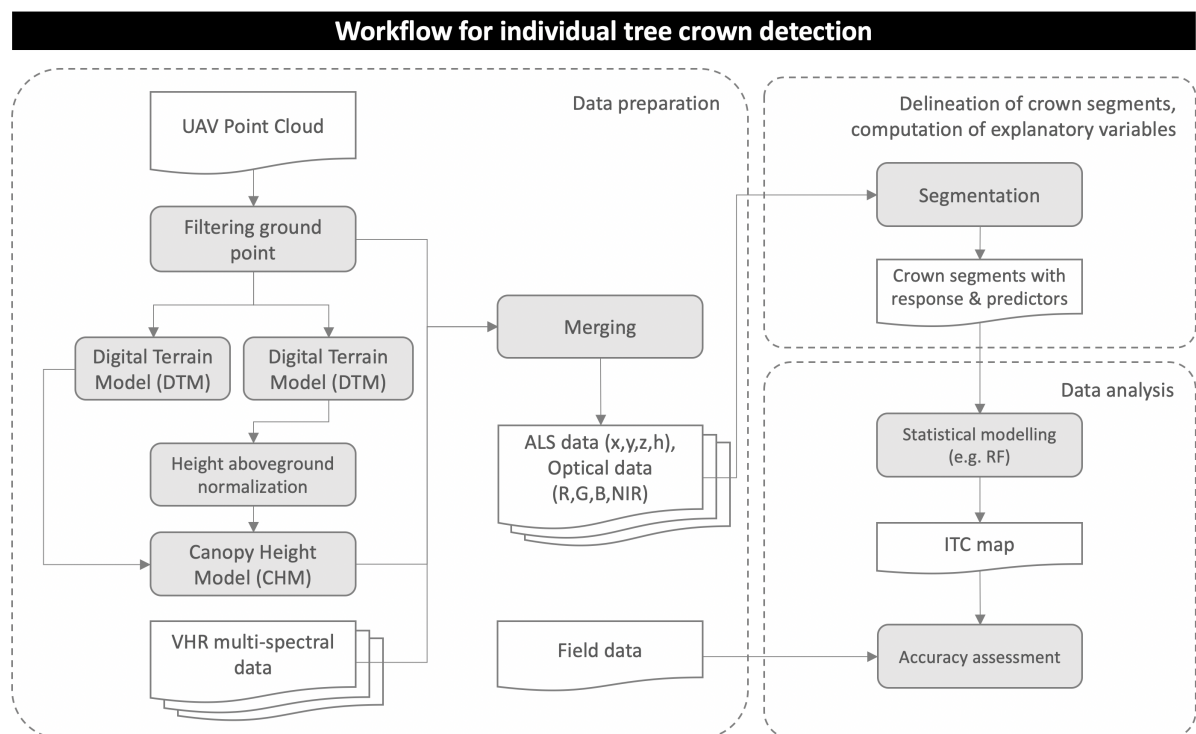


Figure 19: Flow chart and visualisation of the key processing steps used to derive individual tree crown maps.

8.3.5. Required expertise

8.3.5.1. Further statistics?

No.

8.3.5.2. Geodata processing and/or handling GIS?

Yes, preprocessing and analysis of LiDAR data.

8.3.5.3. Technical expertise in remote sensing?

Advanced knowledge is required to preprocess and handle LiDAR processing and segmentation techniques. Image classification and machine learning are optional.

8.3.5.4. Programming knowledge?

Not mandatory but recommended. The complete workflow could be realized in QGIS using the LASTools Plug-In³⁴. Otherwise, packages for processing of both LiDAR and optical VHR data exist in R, GRASS, and Python (see Table 12).

8.3.6. How to validate the indicator maps?

Assessing a segmentation quality is a challenging task in general, since it requires the definition of meaningful evaluation criteria, and those criteria are often to be defined with respect to a given goal and available ground truth data. Most criteria found in the literature ask for a reference segmentation to be used. An ITC could be described in the corresponding segmentation by one of the following four different states: detected, over-segmented, under-segmented, or missed. The segmentation accuracy could be evaluated by using the percentage of ITCs which were classified as correctly detected regarding the total number of ITCs tested. It is very unlikely that an automatically delineated crown exactly matches a manually delineated one. This inaccuracy between the two regions, which can be evaluated by the number of mis-segmented pixels, also depends on the size of the region manually delineated. Also, an ITC could be composed of one segment or several segments. In practice, every segment that shares at least 50% of its pixels with the ITC could be considered an element of the ITC.

In addition, an accuracy assessment can inform the user about the quality of the map regarding the separation of forest vs non-forest (Annex 4). In addition, there exist several guidelines that have a focus on the collection of reference data in the context of forestry. A summary is given in Annex 6.

8.3.7. Required input data

8.3.7.1. Suitable data sources for the approach

Reference data: Can be extracted from VHR optical or LiDAR images by visual interpretation and digitisation in a GIS. It contains the delineation of ITCs and can be stored in ESRI Shapefile or Geopackage format.

Remote sensing data: Previous studies suggest that VHR LiDAR (drone or airborne) is the ideal input dataset for the ITC segmentation and classification workflow (see Annex 1). VHR optical imagery (visible and NIR bands) complement this and can – in an integrated fashion with LiDAR – even enhance the accuracy of ITC detection. It can further be used to connect this workflow with tree species classification.

³⁴ LASTools can also be used from the ARCGIS toolbox.

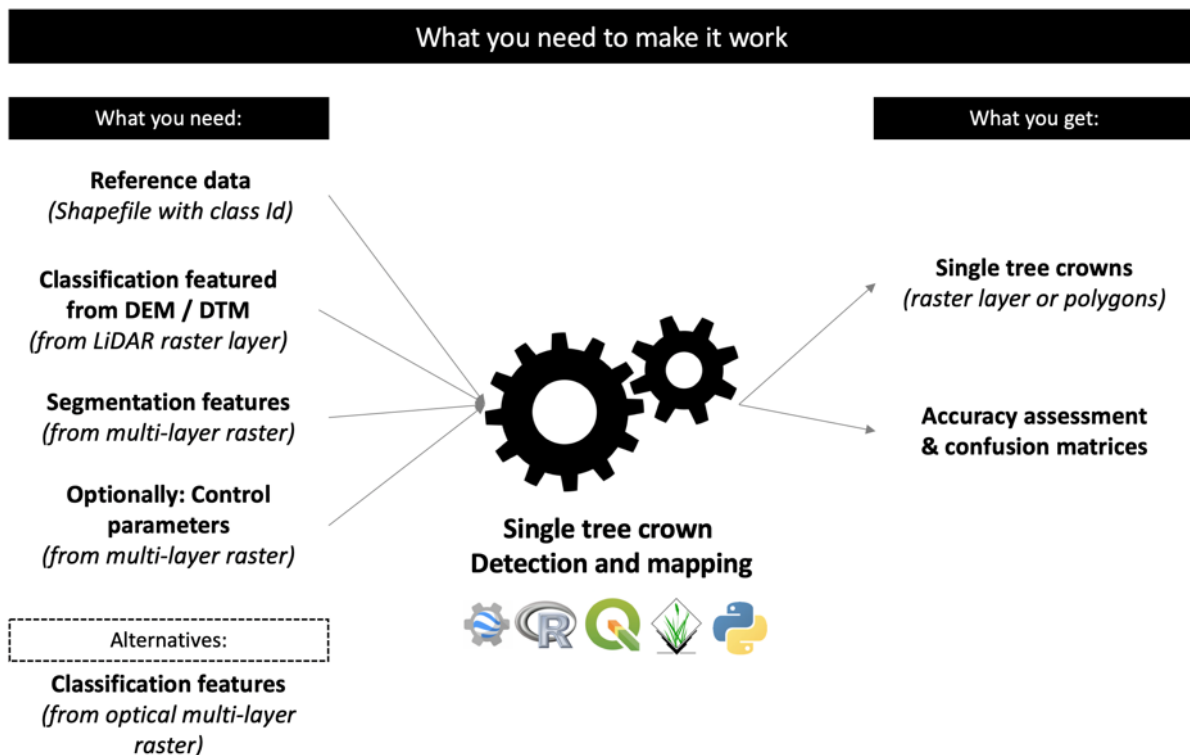


Figure 20: Overview of required data sets and information for creating single tree crown maps.

8.3.7.2. What limitations must be expected without in-situ data, and to what extent are other data sources suitable as substitutes for in-situ data?

Highest confidence can only be gained by validating the accuracy of ITC maps using ground-sampled reference data, such as GPS-located information about forest trunks. Without any reference data, ITC can still be extracted from the image segmentation of LiDAR, but the maps remain unvalidated. Without in-situ data, reference data collected from VHR image sources might be incomplete or erroneous (e.g. not possible to unequivocally delineate individual trees in dense forest stands). Still, manually delineated ITCs from VHR is a viable alternative to in-situ data. It should be noted, however, that a previous study (Dalponte et al., 2014) found that automatic segmentation of hyperspectral data was more accurate in identifying ITCs than manual digitisation from the same data source.

8.3.8. Cost benefit

Good practice recommendation: Acquire a LiDAR data set (ALS or drone), then use programming or QGIS to create (i) DEM, (ii) DSM, and from these two (iii) a CHM. Then apply a segmentation technique such as local maxima to create tree crown objects (ITCs). Use optical VHR data in addition (i) to improve the accuracy of the ITC detection and (ii) to validate the results.

Alternatives and trade-offs: Alternative to LiDAR, optical VHR images can only be analysed through segmentation and/or DL techniques. However, these require a solid reference dataset, either in-situ or from the VHR images themselves. Without LiDAR or optical VHR, the maps are likely to contain groups of trees, rather than ITCs, due to the coarser resolution of the MR data.

9. Indicator #6 – soil erosion

9.1. Name and short description of the indicator

Deforestation-induced erosion (especially gully erosion, i.e. removal of soil along drainage lines by surface water runoff).

9.2. Background and rationale behind indicator #6

Soil erosion is a major problem around the world because of its effects on soil productivity, nutrient loss, siltation in water bodies, and degradation of water quality. The logging and clearcutting of rain forests are some of the leading causes of soil erosion worldwide, but also natural events such as fire contribute to this and are not restricted to the tropics. Agriculture is another major cause of deforestation and erosion. The loss of trees, which anchor the soil with their roots, causes widespread erosion throughout the tropics. Initially, this triggers so-called gully erosion, i.e. removal of soil along drainage lines by surface water runoff. The most important consequences concern changes in soil responsiveness to the water action and the subsequent increase in sediment transport and erosion. Deforestation, logging or post-fire soil loss can increase in the first year by several orders of magnitude compared to the pre-event erosion period.

The rate of increase for soil loss after forest clearing is astonishing; a study in Ivory Coast (Cote d'Ivoire) found that forested slope areas lost 0.03 tons of soil per year per hectare; cultivated slopes annually lost 90 tons per hectare, while bare slopes lost 138 tons per hectare (Unesco, 1978). Soil erosion models have been used to assist the mapping of soil erosion quantity and soil erosion risk. One of the most commonly used soil erosion models is the Universal Soil Loss Equation (USLE) and its family of models: Revised Universal Soil Loss Equation (RUSLE), Revised Universal Soil Loss Equation version 2 (RUSLE2), and Modified Universal Soil Loss Equation (MUSLE). While its implementation is relatively straightforward, compared to other modelling approaches, one drawback of (R)USLE is that it cannot account for soil losses due to ephemeral gullies, which is a relevant phenomenon in initial stages of erosion after deforestation. This can lead to under-prediction of soil loss estimates (Benavidez et al., 2018).

Mapping gullies in many areas is difficult because of the presence of dense canopy (esp. forests), which precludes identification through aerial photogrammetry and other remote sensing methods. Moreover, the wide spatial extent of some gullies makes their identification and characterisation through field surveys a very large and expensive proposition. One cheaper and more expeditious way to detect gullies can be achieved in terms of morphological characteristics. Since DEMs provide the most important source of quantitative morphometry, they are a popular choice for mapping gullies (Eeckhaut et al., 2011; Francipane et al., 2018). Different procedures have been developed to operate based on these high-resolution DEM data, (i) pixel-based and (ii) OBIA. The identification of areas with high potential for gully channel development is often performed using geomorphometric features such as slope or spatially derived stream power estimates from second-order topographic indices, such as the Compound Topographic Index (CTI). Previous studies suggest that DEMs in this context should be derived from LiDAR data (ALS or drone). Others recommended that delineation of ephemeral gullies, by using tools such as the Compound Topographic Index (CTI) developed by (Thorne et al., 1985), combined with (R)USLE could improve the identification of vulnerable areas within a watershed.

9.3. Analysis approach and tools

9.3.1. Name of the approach

Two approaches are of interest, (i) mapping soil (gully) erosion using OBIA and LiDAR derivates, and (ii) modelling the soil erosion quantity and/or risk (see Table 13).

Table 13: Summary of two approaches and the rationale behind selecting one of them.

Name	Gully erosion mapping using ALS and other VHR data	Soil erosion modelling
Description	<ul style="list-style-type: none"> Segmentation and classification of VHR images 	<ul style="list-style-type: none"> Estimate the quantity of eroded soil using modelling
Suitable data	<ul style="list-style-type: none"> DEM or DTMs from VHR data from ALS (usually 1–2m) 	<ul style="list-style-type: none"> Common equations of soil erosion models such as (R)USLE require various input data sets
Preference	<ul style="list-style-type: none"> Focus is gully erosion mapping, possibly below canopy Funds for VHR image acquisition available 	<ul style="list-style-type: none"> Only apply if modelling the quantity of eroded soil or (changes in) soil erosion risk is in the foreground
Strengths	<ul style="list-style-type: none"> Previous studies demonstrated that this workflow can produce accurate maps of gully erosion features 	<ul style="list-style-type: none"> (R)USLE is relatively straightforward to implement and delivers reasonably accurate estimates of soil erosion quantity
Limitations	<ul style="list-style-type: none"> Mostly costly data (LiDAR from ALS or drones) Optical VHR data can be used as an alternative if LiDAR data is not available 	<ul style="list-style-type: none"> Requires acquisition or creation of various data sets

9.3.2. The degree of processing required to achieve the desired product

The mapping approach encompasses an analysis chain which consists of preprocessing LiDAR (and optionally VHR images), calculation of LiDAR derivates, followed by an image segmentation and classification procedure. The modelling workflow encompasses the analysis of various auxiliary data (e.g. soil maps, precipitation, DEMs) sets that contribute to the equations of models.

9.3.3. Previous applications in the scientific context

Eeckhaut et al. (2011) demonstrated how mapping landslides can be accomplished under dense vegetation cover using OBIA. They applied image segmentation to LiDAR derivatives from DTMs and found that circa 70% of the landslides of an expert-based inventory were also included in the OBIA-based map. Similarly, Francipane et al. (2018) applied OBIA to 1m resolution LiDAR-based DEMs, from which they calculated various morphometric indexes (e.g. slope gradient and curvature). Similar studies can be found from Tedesco et al., who combined ALS with optical VHR data. The latter was used in the image segmentation instead of the LiDAR derivatives. These were instead used in a decision tree to delineate gully erosion. Frankl et al. (2019) combined an assessment of the impact of forest cover change from 1938–2016 in Ethiopia on gully network expansion. Shruthi et al. (2015) applied OBIA to Ikonos-2 and GeoEye-1 data for mapping gully erosion. The study determined that the rule set developed for gully feature extraction is more sensitive to the spatial resolution of the imagery used than the quality or resolution of the digital terrain model and its derivatives. Xu et al. (2019) calculated several features, such as VI from Landsat-8 OLI images and slope from ASTER DEM, and calculated a PCA from these. Finally, they applied thresholds to indicate the occurrence of gully erosion. Although they report an overall accuracy close to 90%, it should be noted that, similar to the NBR method used to identify selective logging, such approaches might be useful to indicate the locations of soil erosion when VHR data is not available.

Modelling soil erosion using (R)USLE has been reported in previous studies (Andreoli, 2018; Duarte et al., 2016). At present, many mathematical models categorised as empirical, conceptual, physically-based or process-oriented are available to estimate soil erosion at different spatial and temporal scales. The choice of which model is applicable, however, primarily remains linked to a matter of data

availability rather than what type of information has to be obtained. Scaling in space and time remains a great challenge for the new mechanistic models. As a result, old fashion grey-type models such as USLE and the Revised USLE (RUSLE) are still by far the most widely applied soil erosion prediction models globally. At the current state of the art, process-based physical models are not yet mature enough and input data availability is a continuing source of concern for large-scale scale applications, simple physically plausible empirical methods for predicting soil erosion such as RUSLE can provide reasonably accurate estimates for most practical purposes.

9.3.4. Brief technical and content description of a recommended workflow

9.3.4.1. Mapping soil (gully) erosion using OBIA and LiDAR derivates

This workflow consists of the following consecutive steps (Figure 21):

- Acquire **LiDAR** data (wall-to-wall) and optionally optical or hyperspectral VHR data.
- Acquire **reference data** about gullies or manually digitise gullies from VHR data.
- Calculate a **DEM or DTM** from LiDAR.
- Based on this, calculate a set of **geomorphometric features** such as slope gradient, TPI, flow accumulation, curvatures, etc.
- Apply **segmentation** (as described in section 4.3.4, for example) to the calculated features and apply rules to determine which features belong to gullies (e.g. $TPI < 1.5$) – this requires some trial and error. You should have some reference data to calibrate your method. Note that rules developed in one place might not necessarily work in another place.
- With sufficient reference data, automate this process by applying an **OBIA classification workflow (supervised image classification)**.

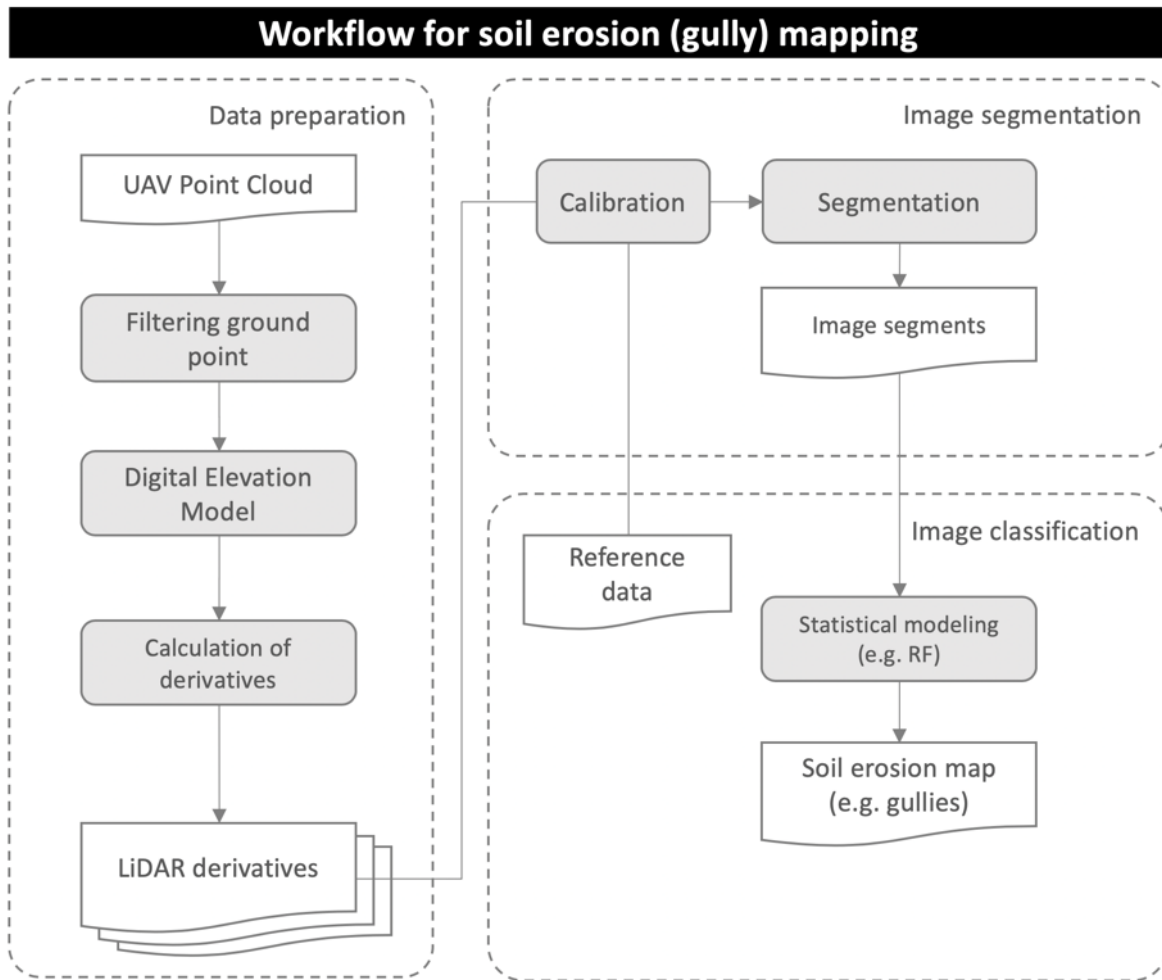


Figure 21: Flow chart and visualisation of the key processing steps used to derive gully erosion maps.

9.3.4.2. Modelling the soil erosion quantity and/or risk

The workflow to quantify soil erosion requires processing different data sources. The RUSLE model, initially used to quantify soil losses over agricultural parcels, provides estimates of sediment displacement within each cell (or pixel) of the model due to hydric processes (rainfall and surface runoff). The six parameters of the RUSLE model are directly derived or estimated from the following data: rainfall R factor; digital elevation model (DEM) LS factor; land use and land cover databases K, C and P factors. The principal equation for the RUSLE model family is below:

$$A = R \times K \times LS \times C \times P$$

where A is mean annual soil loss (metric tons per hectare per year), R is the rainfall and runoff factor or rainfall erosivity factor (megajoule millimetres per hectare per hour per year), K1 is the soil erodibility factor (metric ton hours per mega-joules per millimetre), L is the slope length factor (unitless), S is the slope steepness factor (unitless), C is the cover and management factor (unitless), and P is the support practice factor (unitless). Although the application of the (R)USLE seems to be a simple linear equation at first glance, this review addresses the complex equations that go into calculating its sub-factors, such as rainfall erosivity, which requires gridded precipitation data.

This workflow consists of the following consecutive steps (Figure 22):

- Acquire a **DEM**, **soil map**, **landcover map**, and **rainfall map** using existing data (Table 15).
- Calculate R-, K, LS-, C-, and P factor maps from these data.
- Apply principal equation for the RUSLE model.

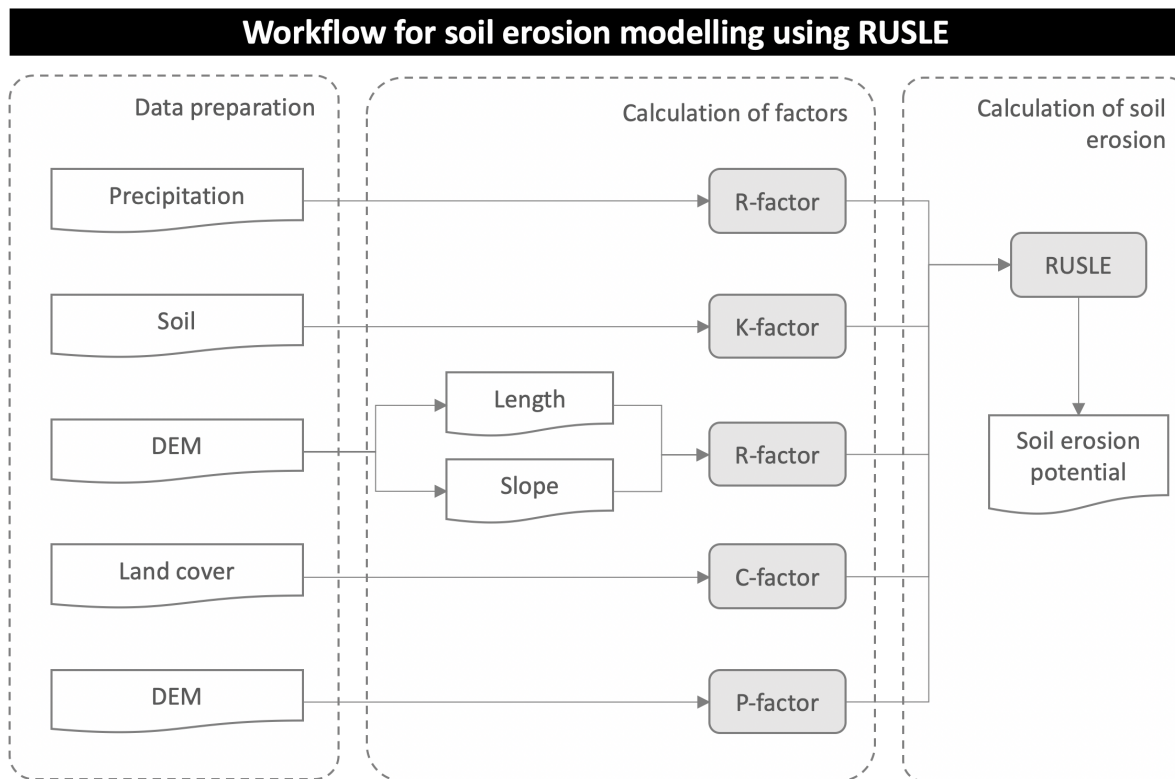


Figure 22: Flow chart and visualisation of the key processing steps used to model soil erosion using RUSLE.

Table 14: Freely available software and tools suitable for calculating indicator #6 "soil erosion". For LiDAR processing (e.g. creation of DEM), please refer to Table 12.

Name	Function	Purpose	Link
GRASS	r.neighbors r.slope.aspect r.fill.dir	Derive topographic position index (TPI), slope, and flow accumulation features (geomorphometric) that can be used in image classification to map gullies	http://grasswiki.osgeo.org/wiki/LIDAR https://grasswiki.osgeo.org/wiki/Lidar_Analysis_of_Vegetation_Structure https://grass.osgeo.org/grass76/manuals/addons/r.geomorphon.html
QGIS		Application of RUSLE to estimate soil erosion in QGIS (Book chapter / tutorial)	(Andreoli, 2018; Duarte et al., 2016)

9.3.5. Required expertise

9.3.5.1. Further statistics

Solid understanding of soil erosion processes is required if soil erosion modelling is applied.

9.3.5.2. Geodata processing and/or handling GIS

Preprocessing and analysis of LiDAR data.

9.3.5.3. Technical expertise in remote sensing

Advanced knowledge is required to handle LiDAR processing, image segmentation and classification techniques (machine learning).

9.3.5.4. Programming knowledge

Not mandatory but recommended. The complete workflow could be realized in QGIS using the LASTools Plug-In (LiDAR processing) and Orfeo toolbox (image segmentation and classification). Otherwise, packages for processing of both ALS and VHR data exist in R, GRASS and Python. RUSLE is implemented as a QGIS plugin and could be used without programming (Andreoli, 2018).

9.3.6. How to validate the indicator maps?

For validity and reliability of the results based on classification of soil erosion maps, accuracy assessment has to be performed for each class (Annex 4). Landslide inventory maps obtained through visual inspection of LiDAR derivative maps and field surveys can be used to calibrate the segmentation and also to validate the resulting indicator map. Validating the soil erosion rates produced by the (R)USLE is difficult because of the lack of easily obtainable observational soil erosion records, especially in data-scarce environments.

Of the (R)USLE applications reviewed by Benavidez et al. (2018), ~30 % presented explicit comparisons between their modelled soil loss from (R)USLE and observed soil loss, modelled soil loss from (R)USLE and other models (one study), and soil loss from multiple models and observed soil loss (one study).

9.3.7. Required input data

9.3.7.1. Suitable data sources for the approach

9.3.7.1.1. Mapping soil (gully) erosion using OBIA and LiDAR derivates

Reference data: Can be extracted from VHR optical or LiDAR images by visual interpretation and digitisation in a GIS. It contains the delineation of gullies and can be stored in ESRI Shapefile or Geopackage format. For the modelling,

Remote sensing data: LiDAR (ALS or drones) can be used to identify geomorphometric features associated with gullies. See section 8.3.7 for a description of LiDAR. Optical VHR data can complement the workflow to improve the classification accuracy (see Annex 1). In principle, optical VHR data can also substitute the LiDAR data.

Remote sensing images that were found to deliver accurate soil erosion maps, including gully erosion, have sub-metre spatial resolution and are from LiDAR systems. See Annex 3 for characteristics about LiDAR systems.

Alternatives – existing data sets: Soil erosion maps suitable for project evaluation do not exist at the desired spatial level of detail.

9.3.7.1.2. Soil erosion modelling and risk assessment

Reference data: Values for calculating the parameter factors (Table 15) can be found in the literature (Benavidez et al., 2018).

Remote sensing data: The rainfall erosivity factor (R) can be derived from gridded precipitation data, such as CHIRPS or TRMM. The use of DEMs, ideally from LiDAR, alternatively from ASTER, to calculate the upslope contributing area and the resulting LS factor allows researchers to account for more topographically complex landscapes. The relatively coarse globally available DEMs ($\sim 30\text{m}$ at best) are less suited to field and sub-catchment scale studies where it may be important to capture effects of micro-topography. Benavidez et al. (2018) gives an overview of previously published LS factors worldwide. For the cover and management factor (C), existing land cover maps such as the Climate Change Initiative (CCI) Land Cover Data Set can be used (see Annex 2).

Alternatives – existing data sets: Soil erosion maps suitable for project evaluation do not exist at the desired spatial level of detail.

Table 15: Potentially useful data sources for deriving six parameters of the (R)USLE model.

Param- eter	Unit	Description	Data sets
R	Rainfall erosivity factor ($\text{MJ}\cdot\text{mm}\cdot\text{ha}^{-1}\cdot\text{h}^{-1}\cdot\text{year}^{-1}$)	Monthly average accumulated rainfall	CHIRPS ³⁵ , TRMM
K	Soil erodibility factor ($\text{Mg}\cdot\text{h}\cdot\text{MJ}^{-1}\cdot\text{mm}^{-1}$)	Susceptibility to soil erosion, transportability of sediments and amount and rate of runoff	Soil maps, e.g. soilgrids project ³⁶ , literature values (Benavidez et al., 2018)
LS ³⁷	Slope length factor and slope steepness factor (unitless)	L and S factors represent the effect of topography on the soil erosion rate	DTMs/DEM ^s e.g. ASTER GDEM (30m) ³⁸
C	Cover and management factor (unitless)	C factor reflects surface cover and cover management impacts on soil erosion. Defined as the ratio of soil loss from a field with particular cover and management to that of a field under "clean-tilled continuous fallow"	Land use / land cover maps such as CCI vegetation indices, literature values (Benavidez et al., 2018)
P	Conservation supporting practices factor (unitless)	Expression of the effects of agricultural management practices	Literature values , e.g. (Benavidez et al., 2018)

Training data is used for parametrisation of the segmentation (e.g. manually digitised gullies) and for the subsequent classification of objects into thematic classes (such as “gully erosion”). Without reference data, the segmentation parameters and quality must be assessed visually. Without DEMs or DTMs from LiDAR, reference data can be obtained by visual interpretation of VHR images. Google Earth can be an alternative source, but very small initial gully erosion features, especially under canopy, are likely not detectable in optical data. The gully erosion mapping workflow can in principle be implemented even without any training data, which can be realised by applying expert rules (e.g. certain thresholds applied to the steepness or curvature in the terrain can be defined as “gully erosion”).

9.3.7.2. What limitations must be expected without in-situ data, and to what extent are other data sources suitable as substitutes for in-situ data?

Mapping gully erosion can confuse actual gully erosion with bare soil (remains indicative). Soil erosion quantity requires very extensive field work for model calibration.

³⁵ <https://www.chc.ucsb.edu/data/chirps> (last accessed 28 November 2019).

³⁶ <https://www.isric.org/explore/soilgrids> (last accessed 28 November 2019).

³⁷ Reference value of K-factor can – for example - be obtained from the ‘Soil Erodibility in Europe High Resolution dataset’ (Panagos et al. 2014) provided by the JRC’s European Soil Data Centre (ESDAC): <https://www.tandfonline.com/doi/full/10.1080/19475705.2019.1578271> (last accessed 12 September 2020).

³⁸ www.inspaceystems.or.jp/ersdac/GDEM/E/4.html (last accessed 28 November 2019).

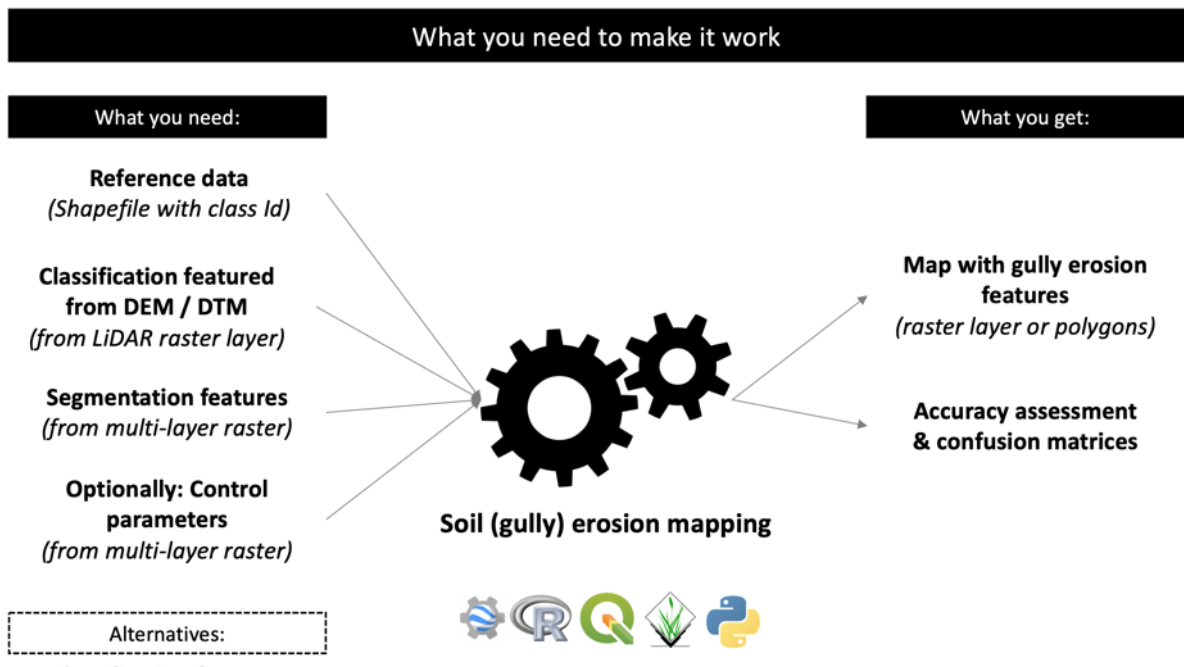


Figure 23: Overview of required data sets and information for creating soil erosion (gully) maps.

9.3.8. Cost benefit

Good practice recommendation: Acquire LiDAR data (aerial or drone) and calculate DEMs or DTMs. Calculate geomorphometric features like slope or curvature and apply segmentation techniques, followed by rules applied to each object to identify the gully erosion (e.g. apply thresholds to slopes). Apply supervised image classification instead of manual rules if you have reference data. Without LiDAR, use VHR optical data and supervised image classification. Use (R)USLE modelling to estimate the actual amount of soil eroded, if of interest.

Alternatives and trade-offs: Calculate VIs from VHR, perform a PCA, and based on this, perform either unsupervised image classification, manually assign clusters to the “gully erosion” class or perform a visual inspection of the images.

In general, since the (R)USLE does not account for all the complex interactions associated with soil erosion, its predicted soil erosion rates should be taken as best estimates rather than absolute values. The (R)USLE is a good first attempt at identifying vulnerable areas and estimating soil loss for a landscape at the baseline scenario due to the model's relative simplicity and few data requirements.

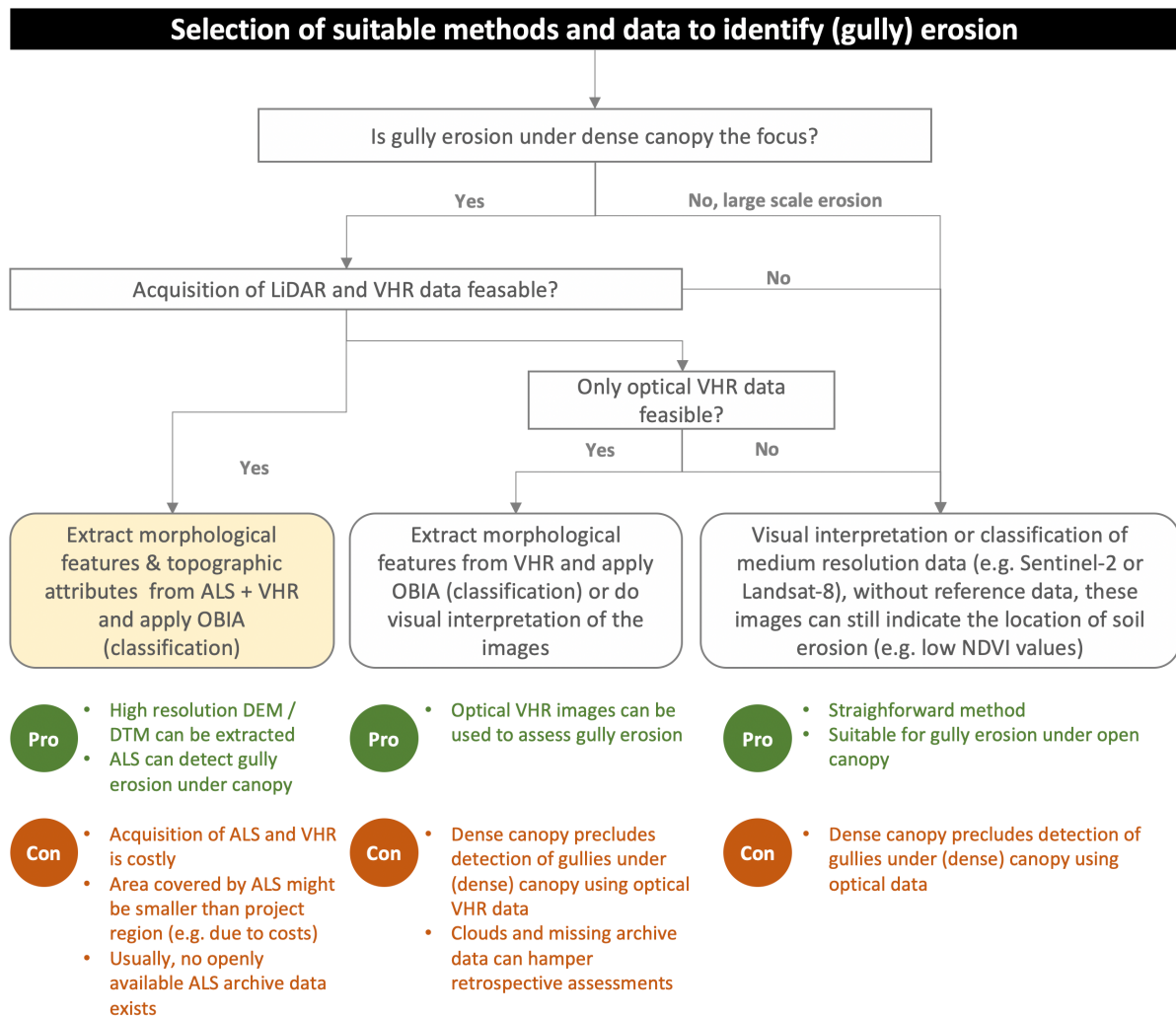


Figure 24: Guidance for selecting proper imagery and methods for assessing soil erosion (especially gully erosion). The "gold standard" is highlighted in yellow colours. It provides the best results in terms of spatial and thematic detail.

10. Indicator #7 – afforestation and reforestation

10.1. Name and short description of the indicator

"Afforestation and reforestation" This indicator is defined as an establishment of a forest cover in a location where the forests have been cleared in the recent past, usually to repurpose the land for activities like agriculture, mining, or others.

The remote sensing-based indicator describes one specific aspect of afforestation/reforestation, namely the success rate in terms of number or percentage of surviving seedlings in a certain area (e.g. within a tree planting area).

The assessment takes place within a relatively short period after the initial planting, i.e. 2–5 years, which means that a fully-grown forest stand has not necessarily been established. Hence, this indicator requires a different method than forest cover mapping (section 4), because it focuses on evaluating the growth status of tree seedlings in relatively early stages.

10.2. Background and rationale behind indicator #7

The Intergovernmental Panel for Climate Change (IPCC) defines reforestation as an establishment of a forest cover in a location where the forests have been cleared in the recent past, usually to repurpose the land for activities like agriculture or mining.

Afforestation stands for the establishment of forests where previously there have been none, or where forests have been missing for a long time. It should be noted that some areas are afforested even if they have not been known to sustain forests at any time in recent history. However, this practice remains controversial because it inevitably leads to the destruction of an original non-forest ecosystem (e.g. natural grassland).

So, both reforestation and afforestation represent a conversion of non-forested areas into new forests. The only difference is the length of time that has passed since the area has been deforested. The IPCC views these processes as activities directed by human action. Other definitions may include natural forest cover regeneration or establishment as well.

Project evaluators frequently express their requirement to assess the success of afforestation/reforestation projects. This indicator focuses on assessing and quantifying the survival rate of planted trees. It does not address the issue of planting trees in the right places, i.e. the choice of species according to – for example – environmental conditions (targeting)³⁹.

³⁹ A separate section on this topic is planned for the near future.

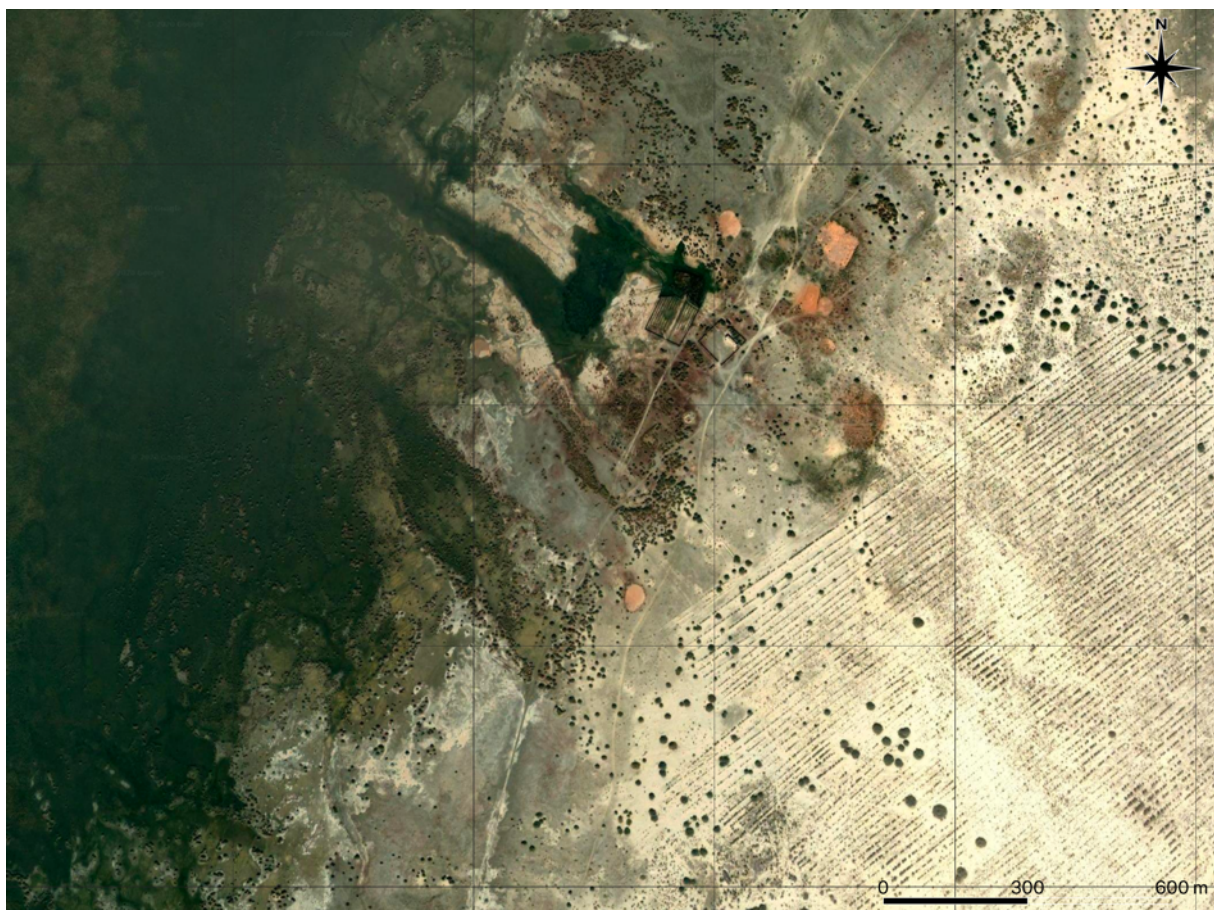


Figure 25: Afforestation planting seen in a very high-resolution satellite image in the Aralkum desert, Central Asia. Source: Google Earth.

10.3. Analysis approach and tools

10.4. Name of the approach

There are two potential ways to monitor afforestation/reforestation: (i) acquiring and analysing commercial VHR remote sensing images provides the highest level of detail because in principle, individual seedlings can be monitored. This makes it possible to actually quantify the number of surviving seedlings ("success rate"); (ii) analysing multitemporal, freely available satellite data allows proxying vegetation growth and can be an alternative to the former approach. Table 16 provides guidance for users when making a choice between these two approaches.

Table 16: Summary of two approaches and the rationale behind selecting one of them.

Name	Computation of afforestation/reforestation success rates using very high resolution (VHR) data	Vegetation growth monitoring using medium resolution (MR) data
Description	<ul style="list-style-type: none"> Classification or visual interpretation of VHR images in at least one period (year), e.g. 2–5 years after the initial planting (depending on the evaluation requirement) 	<ul style="list-style-type: none"> Assessment of change in canopy cover and vegetation growth based on vegetation indices from satellite images
Suitable data	<ul style="list-style-type: none"> VHR data (<10m), recommended: < 1m for highest detail 	<ul style="list-style-type: none"> Moderate spatial resolution data ($\geq 10m$)
Preference	<ul style="list-style-type: none"> Focus is on quantifying success rates; single tree seedlings need to be monitored Funds for VHR image acquisition are available 	<ul style="list-style-type: none"> Very high-resolution data (<10m) is neither available nor affordable Focus lies on proxying vegetation growth in afforestation/reforestation sites
Strengths	<ul style="list-style-type: none"> Facilitates quantification of success rates 	<ul style="list-style-type: none"> Facilitates assessment of changes in vegetation cover

	<ul style="list-style-type: none"> Better suited for assessments of seedling status just a few years after the plantings 	<ul style="list-style-type: none"> that are characteristic of vegetation regrowth Assessment of large-scale afforestation using freely available data (Sentinel, Landsat) Due to the availability of images in the archive and repeated global data acquisition plans of MR satellites, monitoring is feasible without data costs Potentially better suited for longer term monitoring
Limitations	<ul style="list-style-type: none"> Mostly costly data Analysis impacted by the choice of image acquisition timing, which in turn can be limited by cloud cover Often only limited archive data available, because VHR satellite sensors are not equipped/tasked for global coverage (compared to Landsat or Sentinel) Need to parameterise image segmentation, at best based on reference polygons, or visual inspection or VHR images required 	<ul style="list-style-type: none"> Detection of seedlings likely limited due to the spatial resolution of the sensors (mixed pixels) Need to process large data amounts because the method is based on multitemporal images, can potentially limit the use of Desktop PCs and might require cloud computing solutions Understorey vegetation can mix with the vegetation signals that stem from seedlings

10.5. The degree of processing required to achieve the desired product

The desired product consists of thematic maps showing a quantification of success rate (e.g. percentage of surviving tree seedlings) and change maps, i.e. maps containing information about where changes occur in vegetation cover. It requires analysis of raw or already preprocessed satellite data using machine learning analysis, visual interpretation of images (i.e. quantifying success rates), or statistical analysis such as change detection (i.e. monitoring vegetation growth).

10.6. Previous applications in the scientific context

Previous studies found a strong correlation between afforestation/reforestation and remote sensing data (Akike and Samanta, 2016; Gerlein-Safdi et al., 2020; Liu et al., 2019). Ideally, remote sensing images with a sufficiently high spatial resolution (e.g. <1m) are available to allow counting of individual seedlings and assessment of their status after a certain period, e.g. 2–5 years after the initial planting (Panque-Gálvez et al., 2014). Based on such imagery, individual tree seedlings can be identified and the surviving trees be counted (Figure 25 and Figure 26).

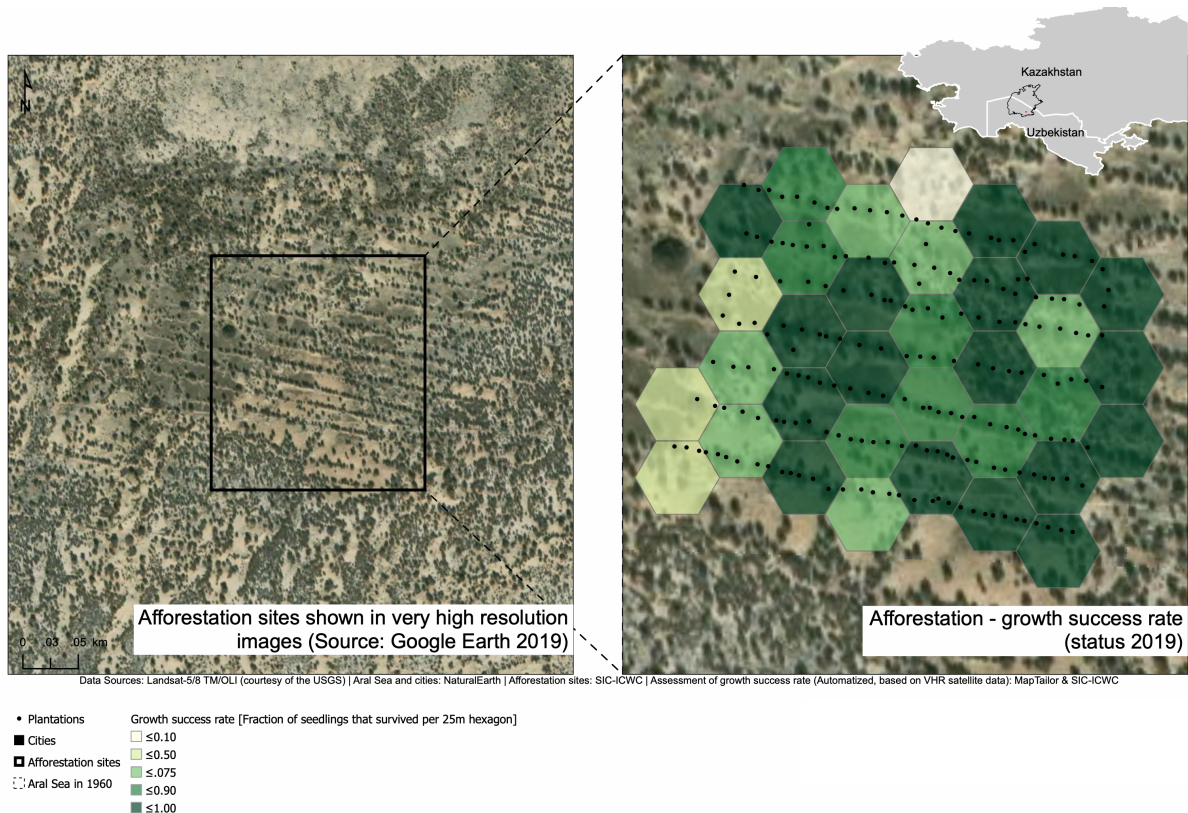


Figure 26: Left: Afforestation planting seen in a very high-resolution satellite image. Right: Assessment of afforestation success rate. Source: Google Earth, Analysis: MapTailor Geospatial Consulting GbR.

Optical satellite data such as Landsat-8 or Sentinel-2 are suitable for tracking changes in forest vegetation cover in different biomes of the world (Demina et al., 2018; Shen et al., 2019). Demina et al. (2018) combined in-situ field measurements and UAV data to classify satellite images according to the two classes of ‘restored’ or ‘not restored’. Based on this, they tracked reforestation as exemplified in the Severodvinsk and Onezhsk forestry districts of the Arkhangelsk region of Russia’s Arctic zone. The “tasseled cap” multi-channel satellite image transformation method is employed as a tool for detecting a reduction in forest cover and analysing reforestation, based on Sentinel-2.

Paneque-Gálvez et al. (2014) provide a review of the existing literature regarding environmental applications of drones, including forest monitoring, and drew first-hand experience flying small drones to map and monitor tropical forests and training people to operate them.

Gerlein-Safdi et al. (2020) used solar-induced chlorophyll fluorescence (SIF) from the Global Ozone Monitoring Experiment (GOME-2) satellite to examine vegetation water content and photosynthetic activity, respectively, and to compare the trends in vegetation water and photosynthetic signals with the official reforestation statistics provided by the government. While indicators of vegetation growth such as SIF or biomass (see section 7) are more challenging to extract from remote sensing data, simple vegetation indices such as NDVI can be directly computed from the images and used as a proxy for vegetation cover and growth. Leeuwen (2008) examined satellite-based time-series vegetation greenness data (NDVI) and phenological measurements to monitor and quantify vegetation recovery after wildfire disturbances. The advantage of this approach is that, in principle, it runs without in-situ data. Without having high resolution images (e.g. due to financial constraints in the project, cloud cover or non-availability of images in the archive) freely available satellite images can be used as an alternative to track vegetation growth. At the moment, freely available imagery provides a spatial resolution of 10m (Sentinel-2) or 30m (Landsat-8), at best.

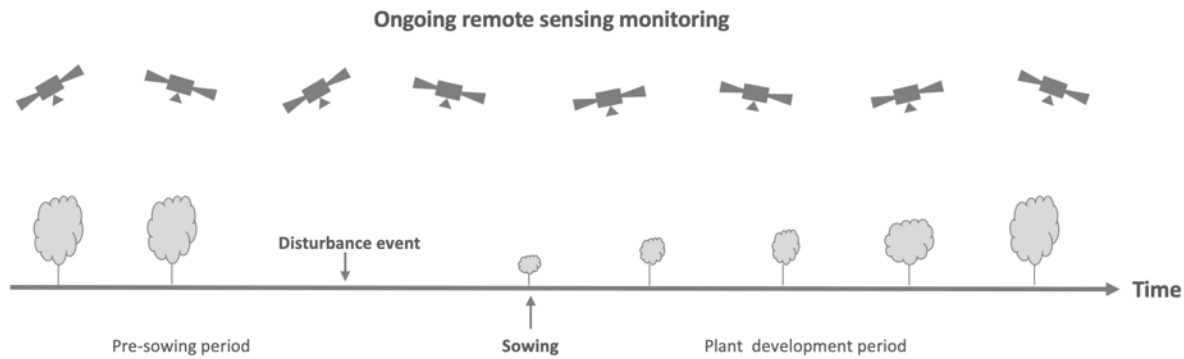


Figure 27: Schematic overview of remote sensing-based monitoring of vegetation growth.

10.6.1.1. Quantifying the success rates

Quantifying the success rate requires an assessment of remote sensing images that have a very high spatial resolution (see Annex 1) and that is sufficient for identifying individual seedlings or tree crowns. This method is better equipped to assess afforestation/reforestation within only a few years after the initial planting took place. Some issues should be considered before acquiring the VHR images:

- First, they should fit the peak vegetation time period when seedlings are clearly visible. The use of a single image off-season leads to an underestimation of the number of seedlings and makes it difficult to assess their status (e.g. surviving or dead), if selected improperly.
- Second, the spatial resolution should be high enough for discerning single seedlings or tree crowns, especially when quantifying success rates by counting surviving seedlings is in the foreground.
- Third, in addition to multispectral bands in the visible part of the electromagnetic spectrum, imagery should include the near-infrared (NIR) band, which facilitates detection of changes in tree seedling cover more accurately.

A recommendable workflow consists of the following consecutive steps (Figure 28):

- Acquire VHR (satellite, aerial or drone) data (wall-to-wall) from the whole study area (e.g. planting locations) after the initial planting has begun (e.g. 2–5 years after planting).
- Optional: Create spatial information about the locations of individual seedlings using on-screen digitisation of VHR images or use existing GPS points.
- Apply OBIA (see section 4) or visual inspection of the VHR images to identify surviving vs potentially dead seedlings.
- Summarise the number or percentage of the detected surviving seedlings per area unit (e.g., a regular grid of a certain cell size, or per planting area), which gives the success rate (number of surviving vs dead seedlings).

Afforestation / reforestation assessment workflow using high resolution imagery

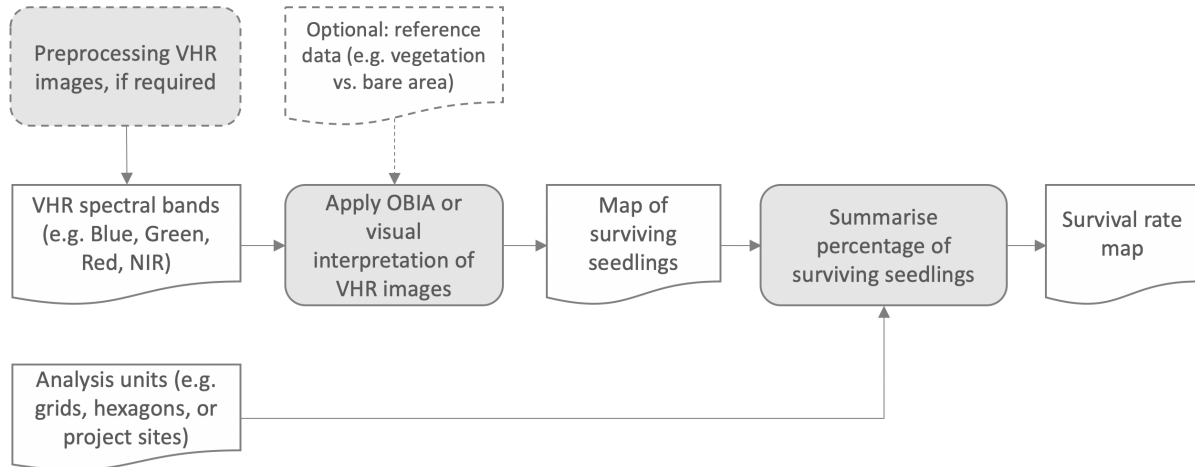


Figure 28: Detailed flow chart and visualisation of the key processing steps used to assess the survival rate of seedlings in afforestation/reforestation locations.

10.6.1.2. Vegetation growth monitoring (as a proxy for afforestation success)

Monitoring changes in the vegetation cover without VHR data or calibration of an OBIA is a potential alternative, for example, in cases where VHR data cannot be acquired due to financial constraints. A recommendable workflow consists of the following consecutive steps (Figure 29):

- **Imagery preprocessing** consists of the acquisition of top-of-canopy (TOC) reflectance Landsat⁴⁰ and/or better Sentinel-2⁴¹ satellite images in all years after the initial planting. Images should be selected to cover on-leave season.
- **Masking** clouds and cloud shadows (e.g. using the CFMask⁴² layers provided for Landsat images, or the cloud masks provided for Sentinel-2⁴³).
- **Calculation of the NDVI (or variants such as red edge NDVI, NDRE)** for each cloud-free TOC image according to this formula:

$$NDVI = \frac{NIR - RED}{NIR + RED}$$

or

$$NDRE = \frac{NIR - RE}{NIR + RE}$$

⁴⁰ The USGS Landsat 8 Surface Reflectance Tier 2 dataset is the atmospherically corrected surface reflectance from the Landsat 8 OLI/TIRS sensors. These images contain 5 visible and near-infrared (VNIR) bands and 2 short-wave infrared (SWIR) bands processed to orthorectified surface reflectance, and two thermal infrared (TIR) bands processed to orthorectified brightness temperature. These data have been atmospherically corrected using LaSRC and includes a cloud, shadow, water and snow mask produced using CFMASK, as well as a per-pixel saturation mask. For more information refer to: https://www.usgs.gov/land-resources/nli/landsat/landsat-collection-2#qt-science_support_page_related_con=1#qt-science_support_page_related_con (last accessed 19 August 2019).

⁴¹ The Level-2A product provides top-of-canopy (TOC) reflectance images, using the Sen2Cor processor and derived from the associated Level-1C products. Each Level-2A product is composed of 100x100km² tiles in cartographic geometry (UTM/WGS84 projection). Level-2A products have been systematically generated at the ground segment over Europe since March 2018, and the production was extended to global in December 2018. Level-2A generation can also be performed by the user through the Sentinel-2 Toolbox using the associated Level-1C product as input. For more information refer to: https://earth.esa.int/web/sentinel/user-guides/sentinel-2-msi/product-types/level_2a (last accessed 19 August 2019).

⁴² <https://www.usgs.gov/land-resources/nli/landsat/cfmak-algorithm> (last accessed 19 November 2019).

⁴³ <https://sentinel.esa.int/web/sentinel/technical-guides/sentinel-2-msi/level-1c/cloud-masks> (last accessed 19 November 2019).

where NIR is the near infrared band (Landsat-8: band 5, Sentinel-2: band 8), RED the red band (Landsat-8: band 4, Sentinel-2: band 4)⁴⁴ and RE the red edge (Sentinel-2: band 8A).

- **Assess annual VI values and changes of the VI over the years.** An increase of the VI can be indicative of successful seedling growth within a planting area. A decrease can be indicative of planting failure, but can also indicate changing hydrological or meteorological conditions (e.g. drought).

A variant of this workflow can be coupling spectral unmixing and change analysis for monitoring of long-term vegetation dynamics (Hasan et al., 2019). Instead of VI such as NDVI or NDRE, satellite images are converted into fractional cover maps, e.g. photosynthetic vegetation, non-photosynthetic / wood, bare substrates / soils. -> Species or cover fractions, but in situ data is needed. However, the method requires "libraries" of spectral end-members for each relevant surface cover type. Such libraries describe the multi-spectral signature of pure constituent materials (called endmembers). They can be derived from a (potentially very large) online spectral library or created by in-situ measurements and used for unmixing purposes.

Afforestation / reforestation assessment workflow using medium resolution imagery

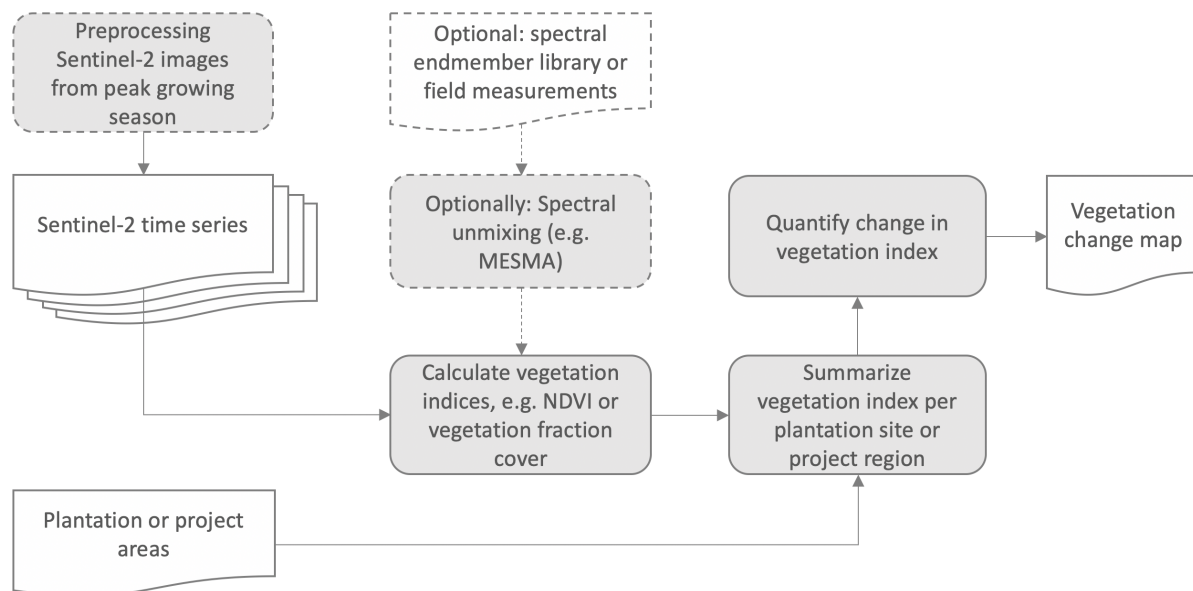


Figure 29: Detailed flow chart and visualisation of the key processing steps used to assess changes in vegetation cover in afforestation/reforestation locations.

⁴⁴ In order to have the same analysis scale, the spatial resolution of all input data should be rescaled to have the same size, e.g. 10m of Sentinel-2 NIR bands.

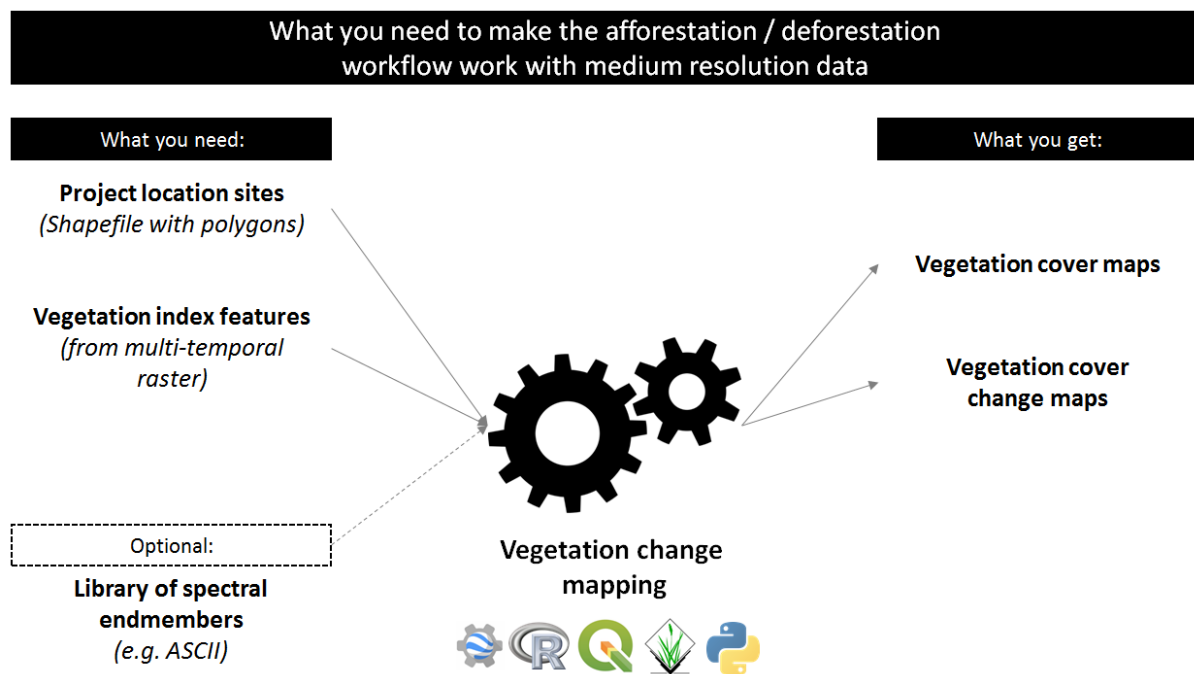


Figure 30: Overview of required data sets and information for creating vegetation change maps.

10.6.2. Required expertise

10.6.2.1. Further statistics?

Spatial aggregation (such as the number of surviving seedlings per project region) of information requires some knowledge to assess and understand statistics of central tendency.

10.6.2.2. Geodata processing and/or handling GIS?

Knowing how to use at least a GUI- (graphical user interface) based GIS like QGIS⁴⁵ is mandatory. For fast geodata processing, it is advisable to work in GEE⁴⁶ or DIAS⁴⁷, which requires JavaScript programming⁴⁸, or other statistical programming languages with raster processing capabilities, such as R⁴⁹ or Python⁵⁰.

10.6.2.3. Technical expertise in remote sensing?

Basic understanding of remote sensing image analysis is mandatory for both workflows, such as image preprocessing and optionally supervised image classification (OBIA). A valid alternative is visual interpretation of VHR images and on-screen digitisation in GIS, which still requires a solid understanding of image interpretation and at least basic GIS experience.

10.6.2.4. Programming knowledge?

⁴⁵ <https://www.qgis.org/en/site/> (last accessed 19 August 2019).

⁴⁶ <https://earthengine.google.com/> (last accessed 12 September 2020).

⁴⁷ <https://www.copernicus.eu/en/access-data/dias> last accessed 12 September 2020.

⁴⁸ <https://developers.google.com/earth-engine/tutorials> (last accessed 19 August 2019).

⁴⁹ <https://www.r-project.org/> (last accessed 19 August 2019).

⁵⁰ <https://www.python.org/> (last accessed 19 August 2019).

Statistical programming languages with raster processing capabilities, such as R⁵¹ or Python⁵². Both methods, quantifying success rates or monitoring vegetation growth, can also be implemented without programming in QGIS (using GRASS GIS and Orfeo Toolbox). In some instances, it might be possible to visually inspect VHR satellite images provided by Google Earth or Microsoft Bing for a first visual assessment.

10.6.3. How to validate the indicator maps

The workflows create maps of vegetation cover change or success rates, respectively, which could be evaluated through comparison with in-situ data. Having GPS-located data about the status of seedlings (surviving or dead) including photographic documentation would facilitate validation of the estimated success rates and/or the detected locations of seedlings. Annex 4 provides details about the accuracy assessment. In addition, there exist several guidelines that have a focus on the collection of reference data in the context of forestry. A summary is given in Annex 6.

10.6.4. Required input data

10.6.4.1. Suitable data sources for the approach

10.6.4.1.1. Quantifying the success rates

Running the workflow to quantify success rates requires a few basic data inputs (see also Figure 31).

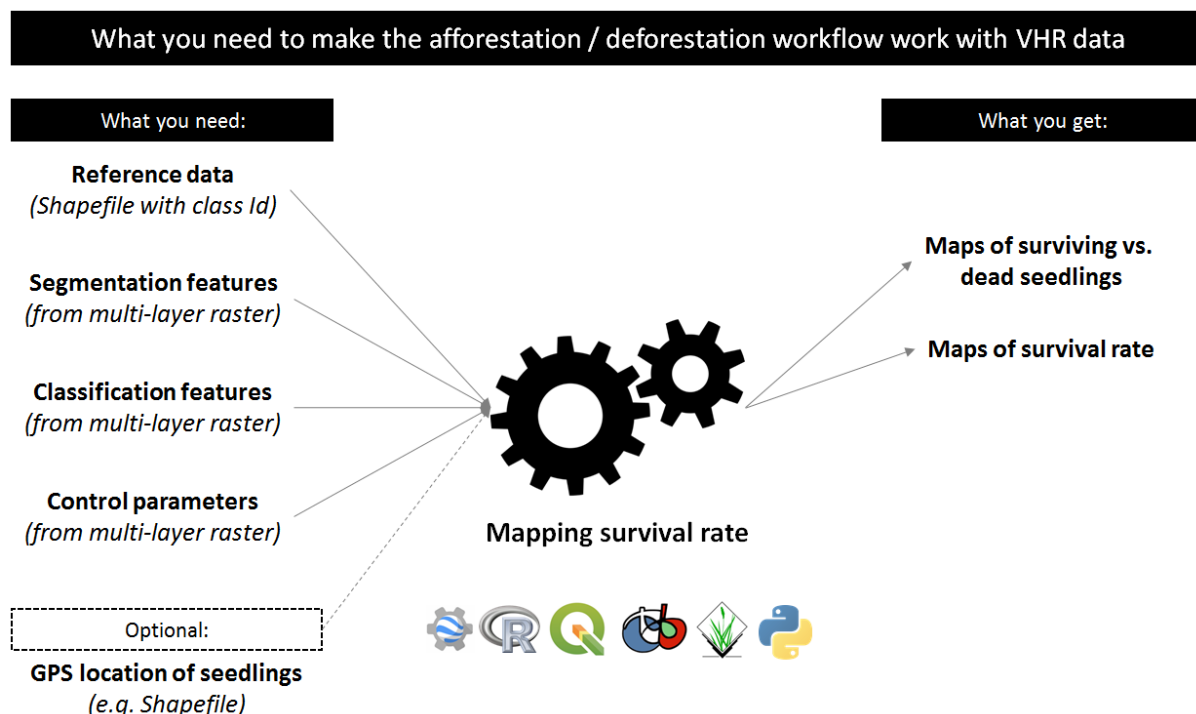


Figure 31: Overview of required data sets and information for creating survival rate maps.

⁵¹ <https://www.r-project.org/> (last accessed 19 August 2019).

⁵² <https://www.python.org/> (last accessed 19 August 2019).

Reference data: Entails in-situ collected or hand-digitised locations of seedlings (or planting rows), delineated using VHR images, Google Earth, or after field visits to the site. If attributing the status of the planting is in the focus of the assessment, this training data set should contain information about the status of the seedlings (e.g. surviving or dead). Typically, reference data is provided in shapefile or GeoPackage format. Without such reference data, the indicator maps cannot be validated.

Remote sensing data: Typically, a multi-layer raster dataset, recorded on one acquisition date, i.e. 2–5 years after the initial planting. For quantifying success rates, VHR data needs to be acquired from a commercial provider, be it from satellite images, aerial flights or drones (see Annex 1). Acquiring data with a spatial resolution (pixel size) better than 1m in order to unambiguously identify individual seedlings is recommended. The most commonly used file format is GeoTIFF.

10.6.4.1.2. Vegetation growth monitoring

Running the workflow to monitor vegetation growth with (freely available) moderate resolution satellite images requires two basic data inputs (see Figure 32).

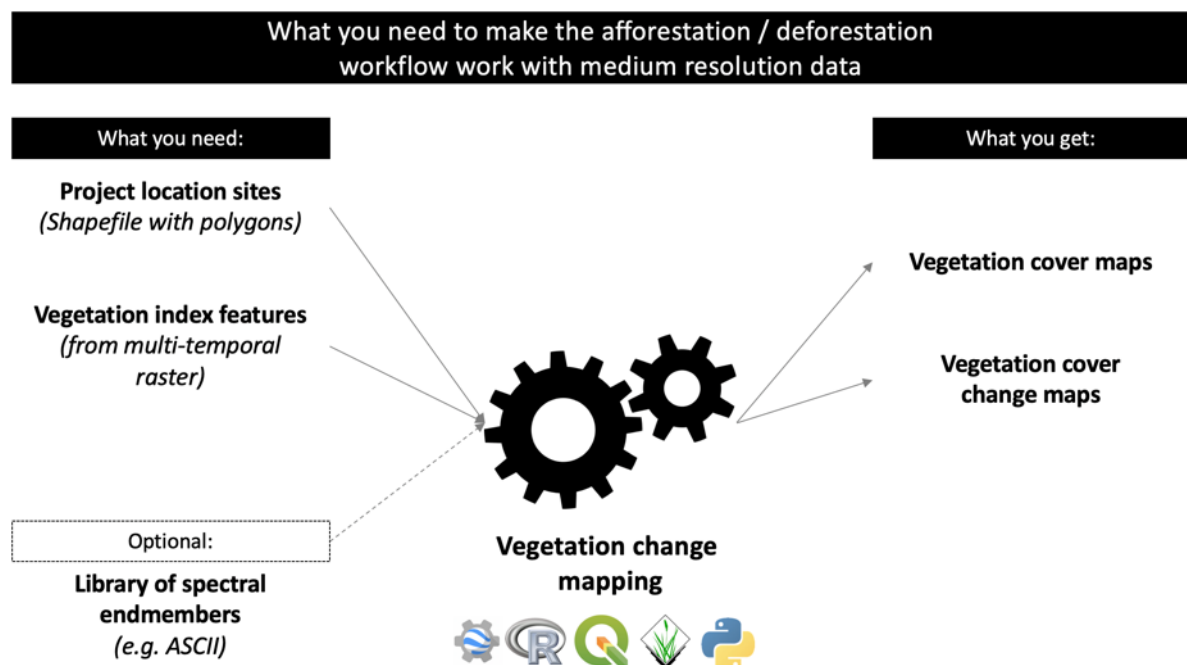


Figure 32: Overview of required data sets and information in NBR analysis.

Reference data (optional): Strictly speaking, reference data is not required but recommended. It would be of the same type as for the former workflow.

Remote sensing data: Typically, a multi-layer raster dataset, recorded in consecutive years (time series) after the initial planting (e.g. in every year including and after the year of the initial planting). This data set can be acquired from open archives, such as ESA (Sentinel) or NASA (Landsat). The most commonly used file format is GeoTIFF. Top-of-canopy (TOC) satellite images and vegetation indices are provided free of charge by, for example, Google Earth Engine⁵³ or USGS EROS Archive⁵⁴. Use Sen-

⁵³ https://developers.google.com/earth-engine/datasets/catalog/COPERNICUS_S2_SR or https://developers.google.com/earth-engine/datasets/catalog/LANDSAT_LC08_C01_T1_SR (last accessed 17 September 2020).

⁵⁴ https://www.usgs.gov/core-science-systems/nli/landsat/landsat-data-access?qt-science_support_page_related_con=0#qt-science_support_page_related_con (last accessed 17 September 2020).

tinel-2 MSI: MultiSpectral Instrument, Level-2A or USGS Landsat 8 Surface Reflectance Tier 1. The Landsat satellites and the Sentinel-2A and Sentinel-2B satellites are described in more detail in Annex 1.

10.6.5. What limitations must be expected without in-situ data, and to what extent are other data sources suitable as substitutes for in-situ data?

Field validation is recommended but not mandatory. Without in-situ data, the indicator maps cannot be validated. Within the workflow for assessing success rates with VHR data, calibration data for the OBIA method could be substituted by collecting calibration data on-screen through the interpretation of the VHR data itself. Users might need to bring in some knowledge on spatial context, for example, to correctly identify seedlings in regular planting rows.

Having accurate delineations (e.g. ESRI Shapefile or Geopackage polygons) of the afforestation sites is recommended. These should ideally only contain the afforested/reforested land.

10.6.6. Cost benefit

Good practice recommendation: Gather reference data, at best in-situ or at least from existing VHR sources (second choice), and acquire VHR images in at least one period after the initial planting (e.g. 2–5 years, depending on the evaluative requirement).

Apply OBIA using machine learning algorithms such as RF to classify the VHR images and create a map that distinguishes surviving vs dead seedlings, or substitute the OBIA by visual interpretation of the imagery to manually identify seedlings.

Quantify the survival rate, e.g. number of surviving seedlings in relation to all seedlings within a reference unit (such as regular grids, hexagon or planting areas). If in-situ data exists, evaluate the accuracy of the maps.

Check pricing of VHR images in Annex 1. The availability of VHR images in the image archive might be limited. New VHR image acquisitions can be tasked, but tasking VHR systems is more expensive, compared to VHR archive images.

Take into account that, for visual analysis of afforestation, a coarser spatial resolution might lead to underestimation of growth success because of the mixed pixel problem: seedlings/trees with a diameter below a certain threshold might not be identifiable by the interpreter and/or be falsely assigned as "unsuccessfully grown", although in reality there might be small trees present.

Drones might yield even more accurate results than satellites but operating them is more expensive because they have to be flown on specific trajectories over smaller swaths of land. Also note that growth success does not equal biomass. Please refer to section 7 for more details on indicators that relate to biomass.

Alternatives and trade-offs: Use moderate spatial resolution images, such as Sentinel-2, calculate vegetation indices (VI) and track changes in VI values over time to proxy vegetation growth. Consider the effect of changes in the hydrological (ground water) and/or meteorological conditions to understand the impact of factors like droughts on the vegetation growth, for example.

This workflow requires less processing and no reference data. However, it does not quantify success rates; rather, it serves as a proxy for vegetation growth. The pixel size of freely available satellite images (10m at best) limits the detectability of individual seedlings and the mixed pixel phenomena

can have an impact on the analysis. For example, surrounding vegetation cover or undergrowth such as grasses or herbs can influence the vegetation signal, so that ultimately no direct shot can be taken on the growth of the seedlings. The biome in which the analysis is taking place must be considered, e.g. did the planting take place on bare ground? Is there understorey or other vegetation such as grasslands etc. that can impact the analysis?

Another variant is applying the method to identify individual tree crowns (section 8). However, this requires obtaining LiDAR data.

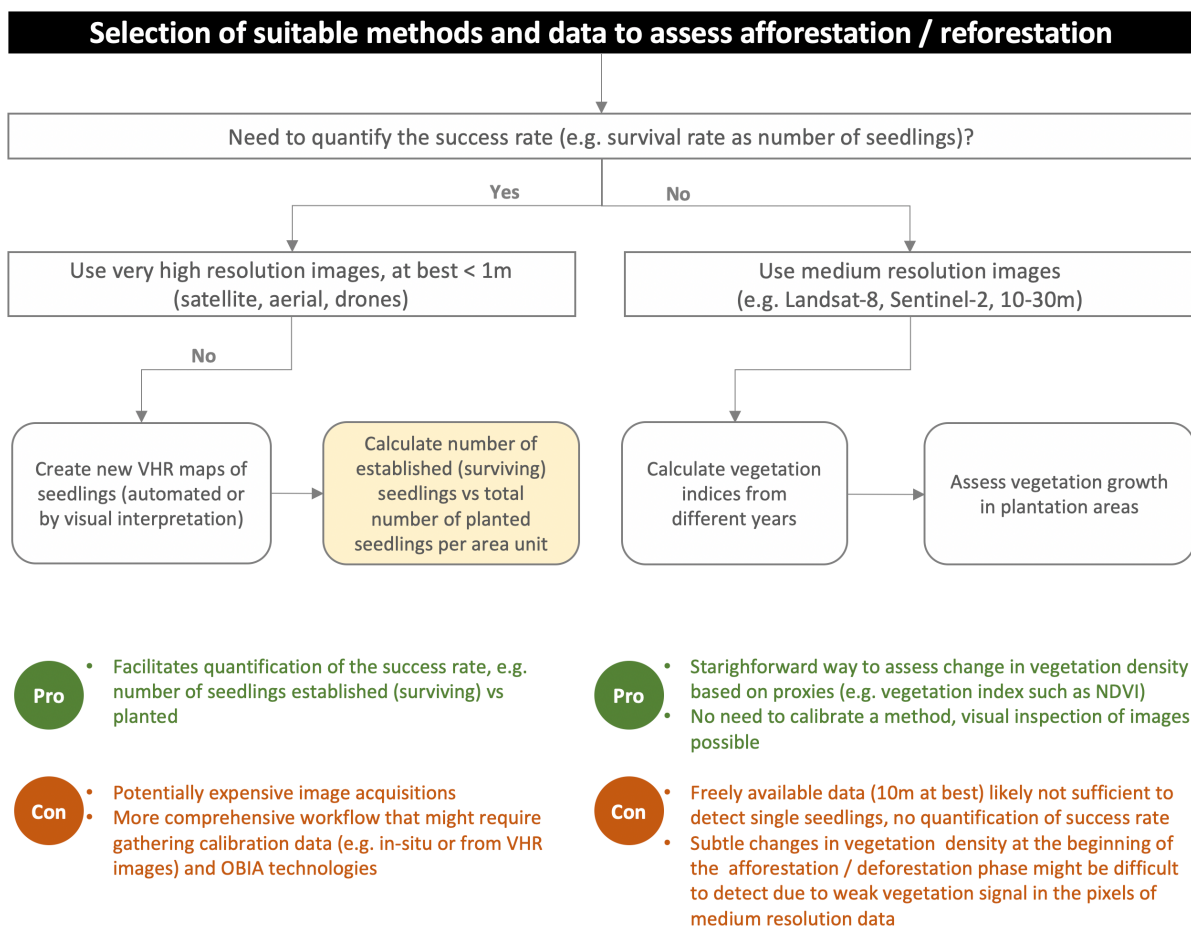


Figure 33: Guidance for selecting proper imagery and methods for assessing afforestation/reforestation success. The "gold standard" is highlighted in yellow colours. It provides the best results in terms of spatial and thematic detail.

Recommendation: Consider using auxiliary data in addition to any of the two above-mentioned workflows in order to relate the observed success rates or vegetation cover changes with – for example – ecological conditions. Table 17 lists some potential data sets and how they could be used to enhance understanding of the impact of environmental and other conditions on afforestation/reforestation success or failure.

Table 17: Examples of freely available geodata that can be used to understand the impact of environmental and other conditions on afforestation/reforestation success or failure.

Parameter	Source	Description
-----------	--------	-------------

Soil properties	ISRIC ⁵⁵	A system for digital soil mapping based on global compilation of soil profile data and environmental layers. Understand impact of soil properties on ecosystem productivity or soil erosion.
Elevation	National digital elevation models or SRTM ⁵⁶ /ASTER ⁵⁷ elevation models	Understand impact of elevation (slope, aspect) such as susceptibility to soil erosion, transportability of sediments and amount and rate of runoff, sunshine duration, etc.
Rivers	OSM ⁵⁸ or Hydrosheds project ⁵⁹	Distance to rivers might be indicative of water supply
Roads	OSM	Distance to roads might be indicative of accessibility to the afforestation/reforestation sites and options for regular ground checks or management
Precipitation	Local weather stations or CHIRPS ⁶⁰	Understand impact of precipitation on afforestation/reforestation success or failure
Temperature	Local weather stations or ECMWF ERA-5 ⁶¹	Understand impact of temperature on afforestation/reforestation success or failure

⁵⁵ <https://soilgrids.org/> (last accessed 17 September 2020)

⁵⁶ <http://srtm.csi.cgiar.org/> (last accessed 17 September 2020)

⁵⁷ <https://asterweb.jpl.nasa.gov/gdem.asp> (last accessed 17 September 2020)

⁵⁸ <https://www.openstreetmap.org/> (last accessed 17 September 2020)

⁵⁹ <https://www.hydrosheds.org/> (last accessed 17 September 2020)

⁶⁰ <https://www.chc.ucsb.edu/data/chirps> (last accessed 17 September 2020)

⁶¹ <https://www.ecmwf.int/en/forecasts/datasets/reanalysis-datasets/era5> (last accessed 17 September 2020)

11. Indicator #8 – Assessment of vegetation cover change and land degradation

11.1. Name and short description of the indicator

"Vegetation cover change / land degradation" – This indicator is defined as an establishment or a loss in vegetation cover and can be used to specifically map degraded land, defined as the continuous reduction or loss of the productivity of the land due to a combination of natural and anthropogenic causes.

11.2. Background and rationale behind indicator #8

Remote sensing can be used for monitoring land degradation to improve the tracking and monitoring of the achievement of the sustainable development goal (SDG) 15.3.1 indicator ("proportion of land that is degraded over a total land area"). The SDG 15.3.1 indicator has three LDN sub-indicators: land cover, land productivity, and soil organic carbon. Here, indicator #8 and the proposed method for assessing it is largely in line with the SDG sub-indicator "Land Productivity" and commonly proposed methods for its computation. The major difference is that here, the use of high-resolution satellite data (Sentinel-2, Landsat-5/7/8) is encouraged to map vegetation change and degradation at the local scale (see Figure 34).

In the context of project planning, it can be used to identify locations that experienced a loss in vegetation cover and land degradation, e.g. due to overgrazing or otherwise overused resources. These "hot spots" of vegetation loss /degradation might become the priority areas, where project measures are to be implemented first.

The assessment considers long-term time series of satellite images, that stretch over many years or even decades – the availability of freely available archive data, such as Landsat, which goes back in the 1980s, is a suitable asset for the analysis of vegetation change and land degradation over such a long time period.

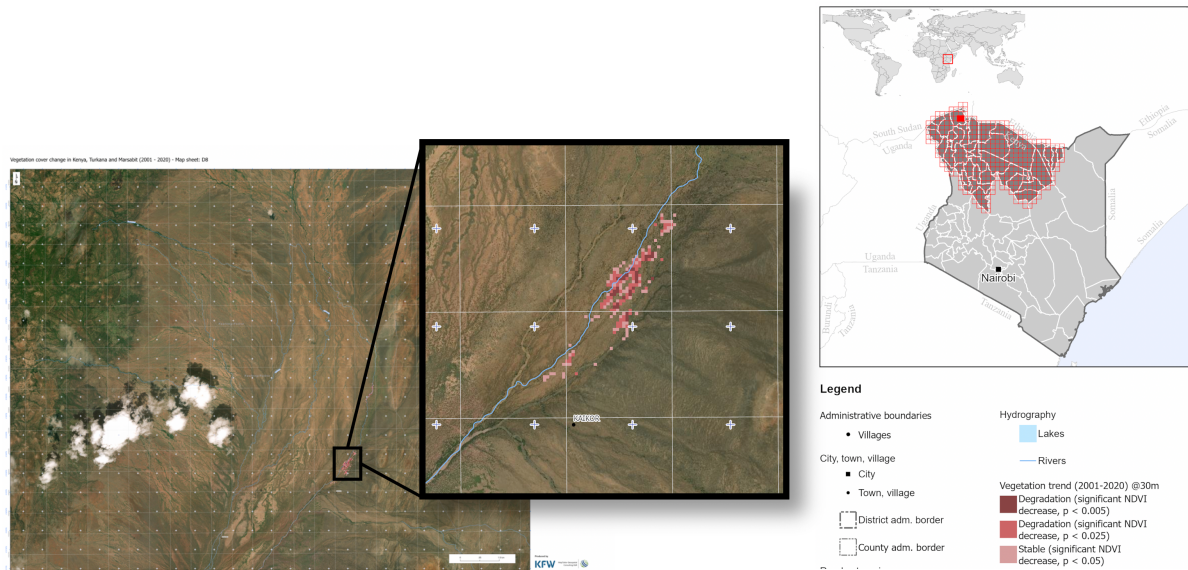


Figure 34: Example of a map showing the trend in vegetation cover in Kenya the period 1997-2020.

11.3. Analysis approach and tools

11.4. Name of the approach

The approach for mapping changes in land productivity (aka SDG 15.3.1.) or vegetation cover change / land degradation (aka Indicator #8), respectively, is based on linear trend analysis of time series of annual vegetation indices (like NDVI) from satellite images (see Figure 35) against time. Indicator #8 measures the trajectory of change in land productivity over time. It is calculated at the pixel level using linear regression. Degradation of vegetation cover is expected to result in a statistically-significant negative slope in the NDVI-time regression.

Finally, a Mann-Kendall non-parametric significance test is applied (Kendall, 1938), considering only significant changes (slope values), such as those that show a pre-defined p-value (e.g. ≤ 0.05). The rank-based, non-parametric Mann-Kendall test is suitable in this context as it makes none of the assumptions about the normal distribution or serial correlation. The Kendall's correlation coefficient (τ), ranges from -1 to +1 and measures the degree to which an observed trend is consistently in/decreasing. A value of +1 indicates a trend that continuously increases and never decreases and a value of -1, vice versa. A value of 0 indicates no consistent trend. The null hypothesis that the samples are randomly ordered was tested two-sided and rejected if τ was significantly different from zero ($\alpha=0.1$).

Positive significant trends in NDVI would indicate potential improvement in land condition, and negative significant trends potential degradation. Positive and negative changes in NDVI indicate increasing and decreasing productivity associated with vegetation recovery and degradation, respectively.

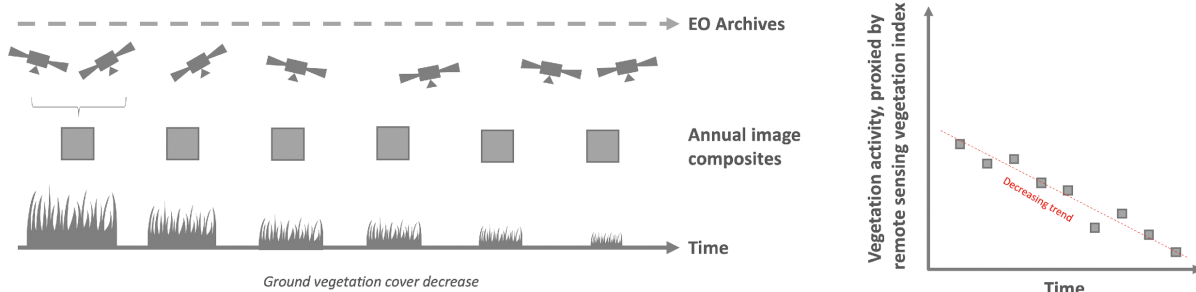


Figure 35: Idealized and very simplified scheme of the vegetation cover trend assessment. Annual satellite image composites are used to calculate annual vegetation indices, which proxy biomass. The temporal change (trend) of these vegetation index values is used to identify regions with positive or negative vegetation index trends. Source: MapTailor GbR.

11.5. The degree of processing required to achieve the desired product

The desired product consists of maps showing (i) positive or negative trend slopes and (ii) and assessment of the statistical significance (p-values) of the observed linear trend slopes. It requires analysis of raw or already preprocessed satellite data using statistical methods (trend assessment), and the combination of the two outcomes (slopes, trend significance) to create the final maps as shown in Figure 34.

11.6. Previous applications in the scientific context

Following the terminology used in the context of the SDG 15.3.1., land productivity can be defined as the biological productive capacity of the land. Land productivity is the biological productive capacity of land. The net primary productivity (NPP) is the net amount of carbon assimilated after photosyn-

thesis and autotrophic respiration over a given period of time and is typically represented in units such as kg/ha/yr. NPP can be estimated from satellite remote sensing derived indicators. NPP is a variable time consuming and costly to estimate on ground, thus, instead some "surrogates" of NPP can be retrieved from remote sensing, such vegetation indices (VI)⁶², for example the NDVI, which is a normalized ratio of the red and near-infrared portions of the electromagnetic spectrum (Rouse et al., 1974). A gradual loss of vegetation productivity and cover over time is often used as a proxy of land degradation when remote sensing is used for its assessment. Land productivity can then be measured by the NDVI, which expresses the vigor and vitality of green vegetation and can be used as a substitute indicator for active cropland with a higher vegetation productivity than barren or fallow land (Jones and Vaughan, 2010).

Because of its ease of use and relationship to many ecosystem parameters, NDVI has seen widespread use in rangeland ecosystem studies, e.g. biomass production (Reeves et al., 2005, 2001), grazing impacts and management, dry land degradation, or vegetation dynamics and phenology. NDVI is computed by taking the ratio of red and near infrared (NIR) bands from a remotely-sensed images:

$$NDVI = \frac{p_{NIR} - p_{Red}}{p_{NIR} + p_{Red}}$$

where p denotes electromagnetic radiation. Healthy vegetation (chlorophyll) reflects more near-infrared (NIR) and green light compared to other wavelengths. But it absorbs more red and blue light. The result of this formula generates a value between -1 and +1. If you have low reflectance (or low values) in the red channel and high reflectance in the NIR channel, this will yield a high NDVI value. And vice versa. Overall, NDVI is an established and standardized way to measure vegetation health. NDVI values indicate healthier or denser vegetation, whilst low NDVI indicates less or no vegetation cover.

Previous studies demonstrate the usefulness of long-term NDVI trend analysis to map land degradation (Fensholt et al., 2013; Higginbottom and Symeonakis, 2014; Röder et al., 2008) and it became one of the corner stones for assessing the SDG 15.3.1 sub-indicator on land productivity (Higginbottom and Symeonakis, 2014).

11.6.1.1. Mapping trends in vegetation cover using satellite-based vegetation index

Mapping trends in the vegetation cover to identify land requires an assessment of multi-temporal remote sensing images from many consecutive years, that have a high spatial resolution of 10-30m (see Annex 1). This is sufficient to identify – for example – degraded land at the local level (such as in the proximity of water ponds where overgrazing might cause a loss in vegetation cover and hence land productivity). A recommendable workflow consists of the following consecutive steps (Figure 36):

- **Imagery preprocessing** consists of the acquisition of top-of-canopy (TOC) reflectance Landsat⁶³ and/or Sentinel-2⁶⁴ satellite images at best in each year during the observation period

⁶² For example, the Normalized Difference Vegetation Index (NDVI), the Soil-Adjusted Vegetation Index (SAVI) or the Enhanced Vegetation Index (EVI).

⁶³ The USGS Landsat 8 Surface Reflectance Tier 2 dataset is the atmospherically corrected surface reflectance from the Landsat 8 OLI/TIRS sensors. These images contain 5 visible and near-infrared (VNIR) bands and 2 short-wave infrared (SWIR) bands processed to orthorectify surface reflectance, and two thermal infrared (TIR) bands processed to orthorectify brightness temperature. These data have been atmospherically corrected using LaSRC; this includes a cloud, shadow, water and snow mask produced using CFMASK, as well as a per-pixel saturation mask. For more information refer to: https://www.usgs.gov/land-resources/nli/landsat/landsat-collection-2?qt-science_support_page_related_con=1#qt-science_support_page_related_con (last accessed 19 August 2019).

⁶⁴ The Level-2A product provides Top Of Canopy (TOC) reflectance images, using the Sen2Cor processor and derived from the associated Level-1C products. Each Level-2A product is composed of 100x100km² tiles in cartographic geometry (UTM/WGS84 projection). Level-2A products are systematically generated at the ground segment over Europe since March 2018, and the production was extended to global in December 2018. Level-2A generation can also be performed by the user using the Sentinel-2

(e.g. 10-15 consecutive years). Images should be selected (i) to cover on-leaf seasons and – if known – periods of suspected or known vegetation peak.

- **Masking** clouds and cloud shadows (e.g. using the CFMask⁶⁵ layers provided for Landsat images, or the cloud masks provided for Sentinel-2⁶⁶).
- **Optionally: Masking of areas that are not of interest** (this requires either an existing land cover map, or other data sets)
- **Calculation of the NDVI index** for each cloud-free TOA image according to this formula:

$$NDVI = \frac{NIR - RED}{NIR + RED}$$

where NIR is the near infrared band (Landsat-8: band 5, Sentinel-2: band 8), and RED the shortwave red band (Landsat-8: band 4, Sentinel-2: band 4)⁶⁷.

- **Create annual aggregates** of NDVI values, e.g. by selecting the maximum numerical NDVI value per pixel per year.
- **Compute a linear trend** through the annual NDVI composites (i.e. NDVI against time), which results in a map showing trend slopes
- **Assess the trend significance** by applying the Mann-Kendal test, this results in a second map showing the trend significance (p-values)
- **The per-pixel slope of the regression, and the associated p-value are the primary analysis outputs. Combine these two outputs** to create a more meaningful, final map, for example with the following categories (the following categories are just a proposal):
 - Significant Degradation (sign. NDVI decrease, p<0.01)
 - Degradation (sign. NDVI decrease, p<0.05)
 - Stable (sign. NDVI decrease, p<0.1)
 - Stable (sign. NDVI increase, p<0.1)
 - Improvement (sign. NDVI increase, p<0.05)
 - Significant Improvement (sign. NDVI increase, p<0.01)

A variant of this workflow is considering the effect of precipitation on the observed trend. Water can change over time, and can have an impact on the amount of vegetation biomass produced every year. When annual integrals of NDVI are used, it is important to interpret the trend maps described above by looking at historical precipitation information as well, e.g. by assessing precipitating anomalies or trends. This is to avoid taking the observed productivity trends as human caused land degradation, while the in fact might be caused by regional patterns of changes in water availability. A commonly used method to consider precipitation explicitly is based on the so-called RESTREND (Ibrahim et al., 2015; Wessels et al., 2007). The aforementioned workflow is then adjusted and uses linear regression models to predict NDVI for a given rainfall amount, concisely, it applies ordinary least-squares (OLS) regressions between the NDVI residuals versus time. Trends in the difference between the predicted NDVI and the observed NDVI (i.e. "residuals") are then interpreted as possibly non-climatically related productivity change:

- **Calculate annual NDVI composites** as described above, using Sentinel-2/Landsat5/7/8 data
- Compute annual precipitation sum (of the growing period)

Toolbox using the associated Level-1C product as input. For more information refer to: <https://earth.esa.int/web/sentinel/user-guides/sentinel-2-msi/product-types/level-2a> (last accessed 19 August 2019).

⁶⁵ <https://www.usgs.gov/land-resources/nli/landsat/cfmask-algorithm> (last accessed 19 November 2019).

⁶⁶ <https://sentinel.esa.int/web/sentinel/technical-guides/sentinel-2-msi/level-1c/cloud-masks> (last accessed 19 November 2019).

⁶⁷ In order to have the same analysis scale, the spatial resolution of all input data should be rescaled to have the same size, e.g. 10m of Sentinel-2 NIR bands.

- Apply pixel-wise ordinary least square (OLS) regression models of NDVI against rainfall. The OLS minimizes the sum of the squared residuals and it is widely used in environmental studies. The method measures the linear relationship between a dependent (y) and independent variables (χ), and it is represented by the equation:

$$y = \alpha + \beta\chi + \varepsilon$$

where y is the dependent variable (NDVI), χ the independent variable i.e., rainfall, α the intercept, which represents the value of y when χ is 0 (measured in units of the y variable), and β is the slope of the relationship between the χ and y variables, and it measured the rate of change of y per unit change of χ . ε is the error term:

- **Calculate the residual difference** between the observed NDVI and the predicted NDVI from the linear model. This is called RESTREND residuals.
- Do another linear regression of the RESTREND residuals against time. Trends in these residuals are interpreted as changes in vegetation productivity that might be independent of rainfall.
- Apply the **Mann-Kendal non-parametric test**.
- **Combine the slope and significance maps** to create a more meaningful, final map, using the same map legend as proposed before (or adjust it to your own needs).

Please note that the RESTREND method has some limitations, e.g. a previous study found that a simulated land degradation intensity $\geq 20\%$ caused the otherwise strong relationship between NDVI and rainfall to break down, making the RESTREND an unreliable indicator of land degradation (Wessels et al., 2012). That study recommends that the results of such analyses will vary between different environments and should therefore be tested across regions (Wessels et al., 2012) and another study even suggest taking into account and including other factors such as soil moisture index datasets in the analysis (Ibrahim et al., 2015).

Workflow to assess trends in vegetation cover / land productivity

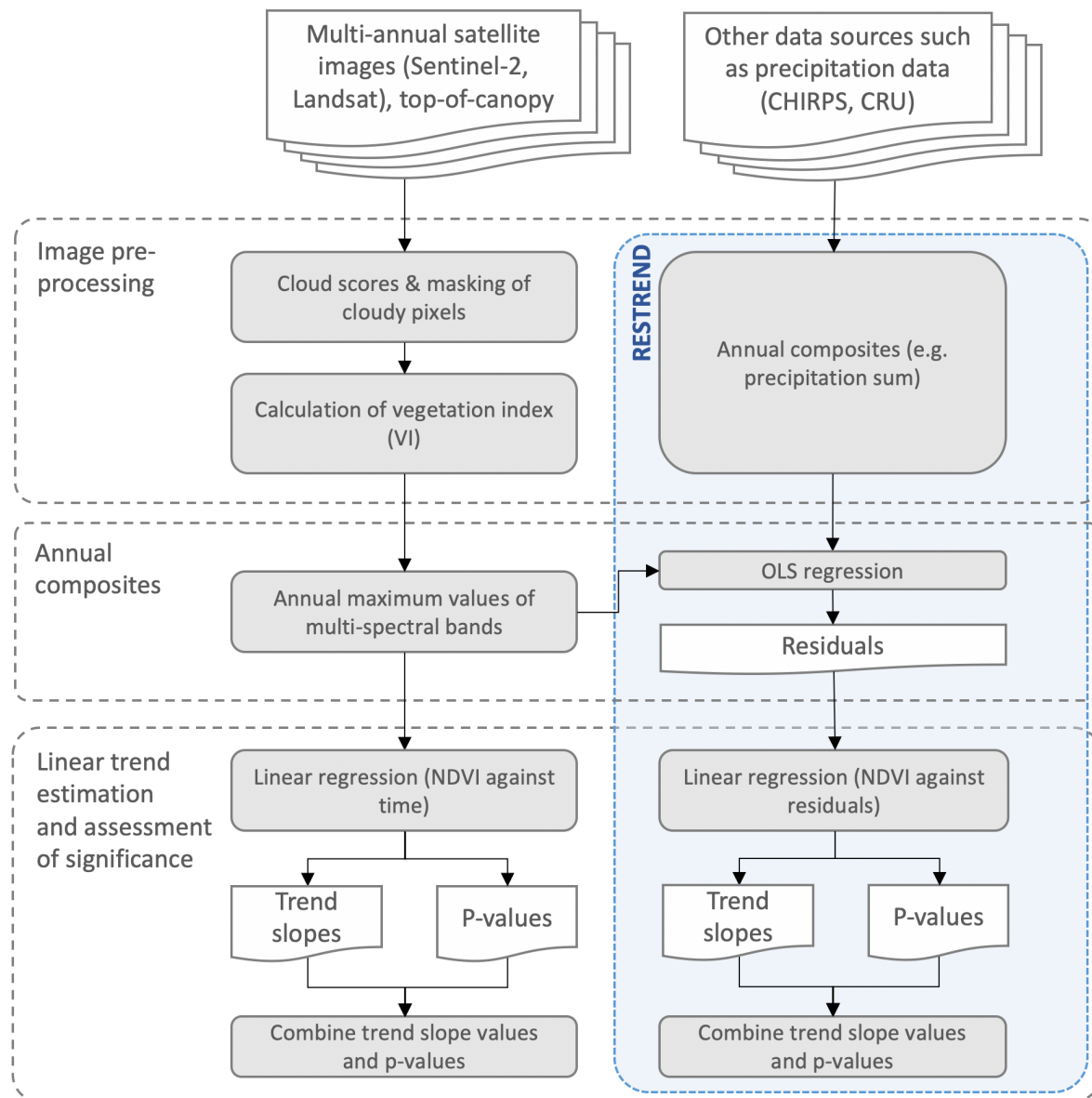


Figure 36: Detailed flow chart and visualisation of the key processing steps used to assess changes in vegetation cover / land productivity (left: linear trend of vegetation index against time, right: linear trend of residuals against time).

11.6.2. Required expertise

11.6.2.1. Further statistics?

Regression techniques, e.g., linear trend estimation, tests of significance such as Mann-Kendall non-parametric tests. In order to apply the RESTREND analysis, some criteria must be met and should be tested, such as normality of residuals resulting from the linear regression (Shapiro-Wilk test), or homoscedasticity, i.e., the variance of the residuals should be constant throughout time (e.g. Breusch-Pagan). If one or more of this or other test fail, then this finding should be communicated in the maps (e.g. by flagging pixels as "as noncompliant").

11.6.2.2. Geodata processing and/or handling GIS?

Some degree of programming experience is required to use workflows such as those provided by the mapme.vegetation R Package⁶⁸, which provides functionality to assess indicator #8. For fast geodata processing, it is advisable to work on a server or to alternatively use GEE⁶⁹ or DIAS⁷⁰, which requires JavaScript programming⁷¹, or other statistical programming languages with raster processing capabilities, such as R⁷² or Python⁷³.

11.6.2.3. Technical expertise in remote sensing?

Basic understanding of remote sensing image analysis is mandatory, such as image preprocessing and statistical analysis.

11.6.2.4. Programming knowledge?

Statistical programming languages with raster processing capabilities, such as R⁷⁴ or Python⁷⁵, or implementing the workflow in GEE.

11.6.3. How to validate the indicator maps?

The workflow creates a map showing different categories of vegetation change, which could be evaluated through comparison with in-situ data. Having GPS-located data about the status of land productivity, including field based NPP estimations, long-term field validation, at best with photographic documentation would facilitate validation of the observed vegetation trends and any statement about land degradation that will be made based on the observed trends. Existing guidelines should be consulted for more details on field observations on land degradation and vegetation loss (Stocking and Murnaghan, 2013)⁷⁶.

11.6.4. Required input data

11.6.4.1. Suitable data sources for the approach

Running the above workflows to implement a vegetation cover / land productivity trend requires various basic data inputs (see also Figure 37).

⁶⁸ <https://github.com/mapme-initiative/mapme.vegetation> (last accessed 5 September 2021).

⁶⁹ <https://earthengine.google.com/> (last accessed 12 September 2020).

⁷⁰ <https://www.copernicus.eu/en/access-data/dias> last accessed 12 September 2020).

⁷¹ <https://developers.google.com/earth-engine/tutorials> (last accessed 19 August 2019).

⁷² <https://www.r-project.org/> (last accessed 19 August 2019).

⁷³ <https://www.python.org/> (last accessed 19 August 2019).

⁷⁴ <https://www.r-project.org/> (last accessed 19 August 2019).

⁷⁵ <https://www.python.org/> (last accessed 19 August 2019).

⁷⁶ <https://archive.unu.edu/env/plec/l-degrade/index-toc.html> and <https://www.taylorfrancis.com/books/mono/10.4324/9781849776219/handbook-field-assessment-land-degradation-michael-stockling-niamh-murnaghan> (last access 5 September 2021)

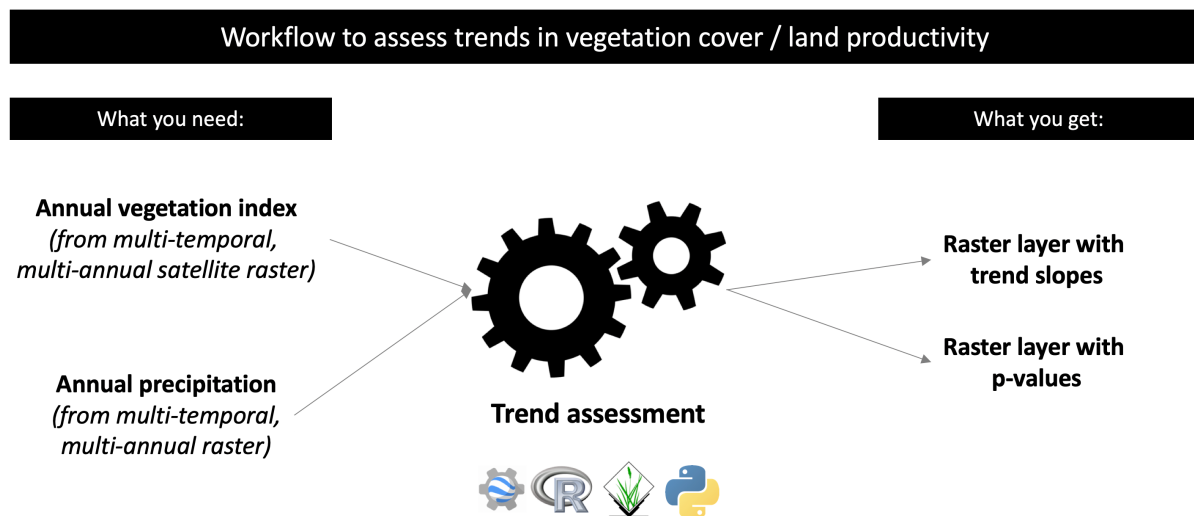


Figure 37: Overview of required data sets and information in vegetation trend analysis.

Reference data: The workflow can be used without in-situ reference data. Yet, it is desirable to have additional ground reference, such as long-term field observations of vegetation cover change, soil erosion, or similar to validate the trend maps and to be able to attribute the observed trends in the maps with land degradation.

Remote sensing data: This is typically a multi-layer raster dataset recorded on several consecutive acquisition dates per annual growing period and for several, consecutive observation years, i.e. multi-temporal imagery from freely available satellite systems such as Sentinel-1, Sentinel-2 and Landsat-8 (see Annex 1). The data format is usually GeoTiff.

In addition to the satellite EO, the application of the RESTREND method requires additional data sets of precipitation. One example is the data set Climate Hazards Group InfraRed Precipitation with Station Data (CHIRPS⁷⁷). CHIRPS data is a 30+ year quasi-global rainfall dataset (Funk et al., 2015). CHIRPS data incorporates satellite imagery with in-situ station data to create gridded rainfall time series for trend analysis and seasonal drought monitoring. Some other studies used rainfall data from the Climate Research Unit (CRU) of the University of East Anglia. The CRU data is a monthly gridded rainfall estimate based on monthly observational data, which is calculated from daily or sub-daily data by National Meteorological Services and other external agencies. The data consists of total monthly rainfall in millimetres calculated on a 0.5° grid and are based on an archive of monthly averages of daily maximum and minimum temperatures and rainfall provided by thousands of weather stations distributed across the world.

Alternatives – existing data sets: Existing maps that show vegetation trends / trends in land productivity at the local level usually only exist in the context of studies or projects. Some global maps do exist, yet, these are based on different methodology and do not necessarily capture the dynamics of vegetation that is of relevance for the project. An overview of some existing global maps of degraded lands is given in a review study (Gibbs and Salmon, 2015). According to this review, it should also be considered that from a methodology pin t of view, there are different definitions (workflows) that create "degrader land maps": The major approaches used to quantify degraded lands can be grouped

⁷⁷ <https://www.chc.ucsb.edu/data/chirps> (last access 15 August 2021).

into four broad categories: (i) expert opinion, (ii) satellite-derived net primary productivity, (iii) bio-physical models, and (iv) mapping abandoned cropland. Hence, in most cases, a new calculation of such maps, if they are providing relevant information to the project, is likely required in order to match the specific requirement of the project.

11.6.5. Cost-benefit:

It is a method that can be implemented without in-situ data and using freely available satellite images, hence, it is a relatively cost-efficient approach. It can be used to identify hot-spots of land degradation, which might be useful in project planning.

12. Indicator #9 – Cropland / crop type mapping

12.1. Name and short description of the indicator

"Crop type" – Defined as an indicator for mapping cultivated areas, i.e. plowed and sown, and for subsequently estimating cropland and/or crop type acreage.

12.2. Background and rational for indicator #9

Timely and accurate knowledge about the geospatial distribution of cropland and crop types at regional to continental scales is crucial for monitoring and forecasting crop production (i.e., crop acreage and yield) (Sadras et al., 2015) and estimating crop water use (Justice and Becker-Reshef, 2007) and water use efficiency (Bastiaanssen and Bos, 1999). Federal agencies and private businesses involved with food and feed production or crop insurance need alerts of impending crop failures and yield shortfalls to avoid human and livestock famine. Institutions in financial and development cooperation need reliable indicators to evaluate the outcome of their projects. Against this background, mapping the spatial extent and distribution of cropland / crop types is necessary, not only for near real-time crop production monitoring.

Cropland / crop type maps are a basic but essential layer of any agricultural monitoring system and it is a vital component in project evaluation. Remotely sensed data from Earth Observation (EO) satellites are the most cost-effective means for gathering spatially explicit, timely, detailed and reliable information over large land areas with high revisit frequency and also in past years (Atzberger, 2013).

This indicator uses remote sensing image classification to create annual maps of cropland / crop type, which is the basis for cropland / crop type acreage estimation and it allows assessing change in cropping intensity. This indicator is meant to measure outcome at local to regional level, the spatial focus is therefore single fields or – if not feasible – patches of cropland. This is fundamentally different from creating cropland statistics at the administrative or regional / country level. Therefore, the methods and based on medium to high resolution imagery.

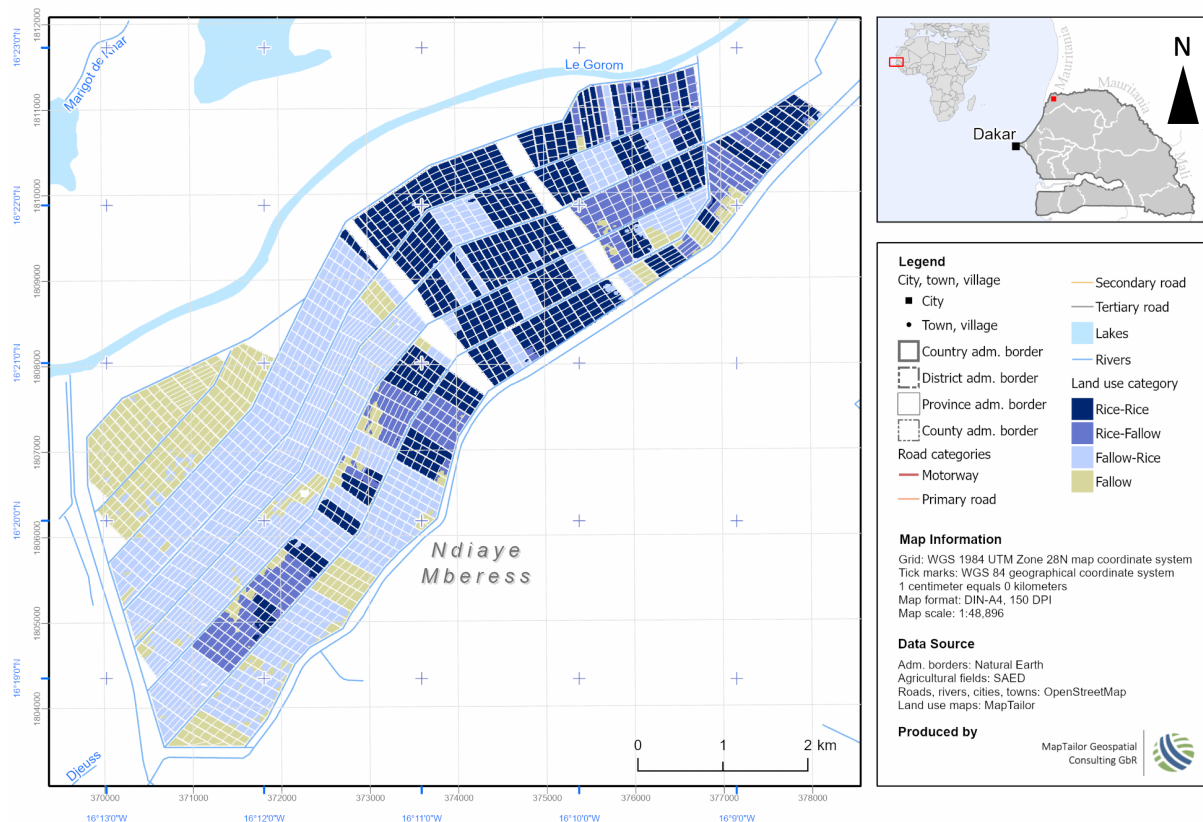


Figure 38: Example for crop type maps in different years in Senegal, which are the basis for quantifying crop specific area and change. Such maps are also the basis for other tasks in remote sensing, such as crop yield modelling. Source: MapTailor Geospatial Consulting GbR.

12.3. Definitions

The following definitions are from the World Program for the Census of Agriculture 2020⁷⁸:

- **Arable land:** Land that is used in most years for growing temporary (seasonal) crops, i.e. plowed and sown, as well as land lying fallow, e.g. due to soil regeneration purposes⁷⁹, or not sown for any unforeseen circumstances.
- **Cropland:** Total of arable land as well as land under permanent crops.
- **Agricultural land:** Total of cropland and permanent meadows and pastures.
- The term **crop type** describes a certain cultivar, such as rice or sorghum.

It might be helpful to consider the EO perspective (such as pixel size and minimum mapping units) to define these terms against the background of remote sensing workflows, which could be: "...annual cropland from a remote sensing perspective is a piece of land of minimum 0.25 ha (min. width of 30 m - considering pixel size) that is sowed/planted and harvestable at least once within the 12 months after the sowing/planting date. The annual cropland produces an herbaceous cover and is sometimes combined with some tree or woody vegetation..."

12.4. Analysis approach and tools

12.4.1. Name of the approach

⁷⁸ <http://www.fao.org/3/a-i4913e.pdf> (last access 03 December 2020)

⁷⁹ For example, in the Sahel, one of the largest dryland regions worldwide, crop-fallow rotation practices are widely used for soil fertility regeneration.

Broadly spoken, the workflow to map cropland / crop types consists of two phases (Figure 39) (i) identification and mapping of cropland (e.g. active and/or fallow), and (ii) distinguishing of different crop types (or fallow land) within the cropland mask. The method applied in both phases is called supervised image classification.

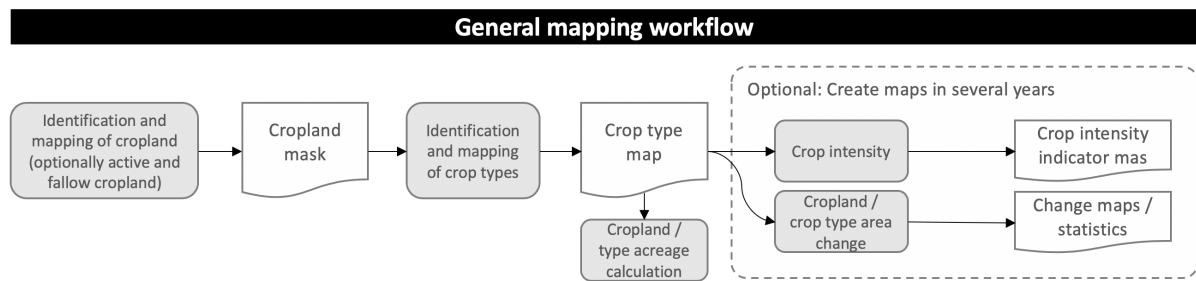


Figure 39: General mapping workflow, first, cropland is identified (this can be done by using a digital field cadastre, or an existing cropland mask, otherwise by supervised image classification), second, different crop types are mapped. When such maps are created in different years, indicators of crop intensity could be calculated to track changes in land use intensity.

12.4.2. The degree of processing to the desired product

The desired product consists of thematic maps showing the annual or seasonal spatial extent of cropland / crop type, i.e. maps containing information about where cropland and certain crop types occurred. It requires to analyse raw or pre-processed satellite data with machine learning algorithms. This in turn requires a reference data set to calibrate the machine learning algorithms ("supervised image classification") and to validate the maps. In case these cropland / crop type maps are created in different years, the relative change in cropland / crop type can be assessed and additional indicators of cropland intensity can be calculated.

12.4.3. Previous applications in the scientific context

Satellite image classification is a fundamental tool for many remote sensing applications. Indeed, remotely sensed image classification has been successfully applied to produce crop maps in homogeneous areas (Aguilar et al., 2018). Smallholder farms, which shape the predominate crop production systems – for example in Africa – present some mapping challenges compared to homogeneous agricultural areas (i.e., with intensive or commercial farms) (Debats et al., 2016). Smallholder farmers cultivate more than 80% of the cropland area available in Africa. The intrinsic characteristics of such farms include complex crop-planting patterns, and small fields (frequently less than 1 ha and with vaguely delineated boundaries) that are vaguely delineated⁸⁰. These characteristics pose challenges to mapping crops and fields from space (Lowder et al., 2016, 2014).

Creating an accurate inventory of cropland / crop type requires the selection of appropriate satellite data, the collection of quality ground information, the application of suitable pre- and post-processing methods and the implementation of robust methodologies. This is a challenge because cropping systems are often diverse and complex, and the types of crops grown and the timing of their growth vary from region to region, as do the management practices implemented. Consequently, the success of remote sensing approaches requires their adaptation to local cropping systems (e.g. by using cropping calendars, see below) and environmental conditions.

⁸⁰ Difficulties are not only in requiring high spatial resolution data, but also in the spectral identification of farm fields and crops because smallholder fields are irregularly shaped and their seasonal variation in surface reflectance is strongly influenced by irregular and variable farm practices in environmentally diverse areas.

Despite of these peculiarities, the production of reliable cropland / crop type maps from remotely sensed images is possible. Previous studies report high classification accuracies, e.g. the errors of omission and commission of cropland can be in the range of 10-15% in landscapes in sub-Saharan Africa, based on Sentinel-2 images (Sweeney et al., 2015; Vogels et al., 2019). For the entire African continent, the weighted overall accuracy of the GFSAD30 30m Cropland Extent product of Africa (Xiong et al., 2017b) was 94.5% with producer's accuracy of 85.9% (errors of omissions of 14.1%) and user's accuracy of 68.5% (errors of commissions of 31.5%) for the cropland class. Another study yielded cropland and fallow land user's accuracy of 73% and 91% and a producer's accuracy of 90% and 79%, respectively, with Sentinel-2 images (Tong et al., 2020). For crop types, accuracies can be in the range of 79% in Tanzania and 63% in Kenya (for maize/non-maize classifiers) (Jin et al., 2019) or 95% overall accuracy for maps that contain 7 crop type classes in Central Asia (Löw et al., 2017).

Fields of specific crops are “seen” differently by instruments of different resolving power (spatial resolution or “pixel size”). In the domain of crop classification, (Löw and Duveiller, 2014) investigated the question of determining the optimal pixel size as finding the coarsest acceptable pixel sizes. Building upon (Duveiller and Defourny, 2010), the authors defined three criteria (sample size, classification uncertainty, and accuracy) to identify the appropriate pixel size and purity. They demonstrate that there is no one-size-fits-all solution to the optimum pixel size problem: it is specific to the agricultural landscape under investigation. Results in a previous study (Waldner et al., 2016) confirm that, from a global mapping point of view, methods' performances vary from one agrosystem to another as a function of (i) their cropland fragmentation and (ii) other specific characteristics.

All aforementioned authors conclude that remote sensing from satellite Earth Observation is a convenient approach for producing these maps due to advantages in terms of cost, revisit time, and spatial coverage. A sensible strategy to improve the global cropland map would be to combine regionally selected methods according to their ability to perform accurately in specific landscapes. These studies also conclude that in most landscapes, freely available satellite images such as Sentinel-1/2 are sufficient to map cropland / crop types with a minimum mapping unit of circa 0.1 hectare (a homogeneous cropped area of roughly 3x3 sentinel pixels). All studies rely on reference data for the calibration of classifier algorithms.

Based on cropland / crop type maps from multiple seasons, various indicators can be computed that describe and quantify the status and changes in the intensity of cropland (Löw et al., 2017). See Table 18 for some examples.

Table 18: Set of potential indicators that can be computed based on seasonal and multi-seasonal cropland / crop type maps.

Temporality	Name	Description
One season	Cropland acreage	The acreage of cropland (active and/or fallow), irrespective of the cultivars
	Crop type acreage	Cultivar specific acreage
	Cropping diversity	Information about the spatial configuration of cultivars, can e.g. be used for assessing the efficiency of irrigation systems (Löw et al., 2017)
Multi-season	Land use mode and median	Most frequent land use type (irrigated, rainfed, or fallow) during the observation period
	Crop rotation	The temporal sequence of different crop cultivars, can for example be used to check the compliance with official crop rotation schemes (e.g. one-year rice followed by three years of legumes)
	Cropping frequency	The total number of years under which land was under cultivation (i.e., sown and harvested). The inverse corresponds to the fallow frequency (i.e. the number of years when land was not cultivated)
	Breakpoints	The year when major cropping system changed within the observation period., e.g. from rainfed to irrigated or vice versa

	Cropping frequency by epoch	Informs about the average number of harvests in two epochs, for example E1 = 2010-2014, E2 = 2015-2018
	Comparison of cropping frequency by epochs	Before-vs-after comparison of cropping intensity, i.e. number of harvests per year (for example: 2010-2012 vs. 2016-2018)

12.4.4. Brief technical and content description of a recommended workflow

12.4.4.1. Supervised image classification to create crop type maps

The proposed workflow consists of creating cropland / crop type maps in two or more growing seasons with the help of machine learning algorithms. To map changes in cropland / crop type, satellite images from several relevant growing seasons and some training data is required.

Some issues should be considered before acquiring the satellite images:

- First, they should fit the time period of the growing season of crops or a particular crop that is in the focus of the investigation. Selecting the proper timing of the image acquisition is imperative. Crop calendars can guide the process of proper image acquisition date selection (see chapter 12.4.7).
- Second, various studies demonstrate that using multi-temporal satellite images (i.e. several images in a grown season) is key in accurate cropland / crop type mapping.
- Third, the spatial resolution should be high enough for discerning single fields, especially when mapping small-holder farming systems is in the foreground, this can be a potentially limiting factor. With freely available satellite data, such as Sentinel-1 or 2, 10m data can be used. It should be considered that some satellite systems such as Sentinel-2 have multi-spectral bands with different spatial resolutions (here: 10m, 20m, and 60m, see Annex 1).
- Fourth, because cloud cover can limit the availability of multi-spectral images during the growing season, it is recommended to combine (fuse) them with SAR data, e.g. to combine Sentinel-1 and Sentinel-2 data.

The **complete** workflow applies the following steps in sequential fashion (see Figure 42) using freely available data and software (see Table 20). The overall workflow corresponds nearly to a classical, supervised image classification. It consists of pre-processing satellite images (e.g. removal of clouds), creating harmonized input data sets and the calculation of certain predictor variables such as vegetation indices, which characterize plant growth. A set of machine learning algorithms is calibrated to classify the input data and to create thematic maps of the major crop type categories. Some post-processing of the crop type maps is applied to improve the quality of the crop type maps further. An accuracy assessment informs the user about the quality (i.e. accuracy) of the created maps.

It must be noted that there can be different starting points to create crop type maps: if the user has a digital representation of all field parcels in the study area, then creation of a cropland mask can be omitted and the supervised image classification can focus on the separation of different crop types within the field parcels. This also has an impact on the amount and categories of reference data that is needed to calibrate the classifier algorithms, e.g. natural land covers "outside" the field parcels might not be needed in this case. Otherwise, the user has to separate agricultural from non-agricultural land uses, which requires to collect the corresponding reference data that contains all relevant categories (i.e., the crop type categories of interest and the most important non-agricultural land cover categories). An alternative could be using existing cropland maps (see 12.4.7) and to focus

the analysis to the locations within the cropland mask. This choice of the workflow is reflected in Figure 40.

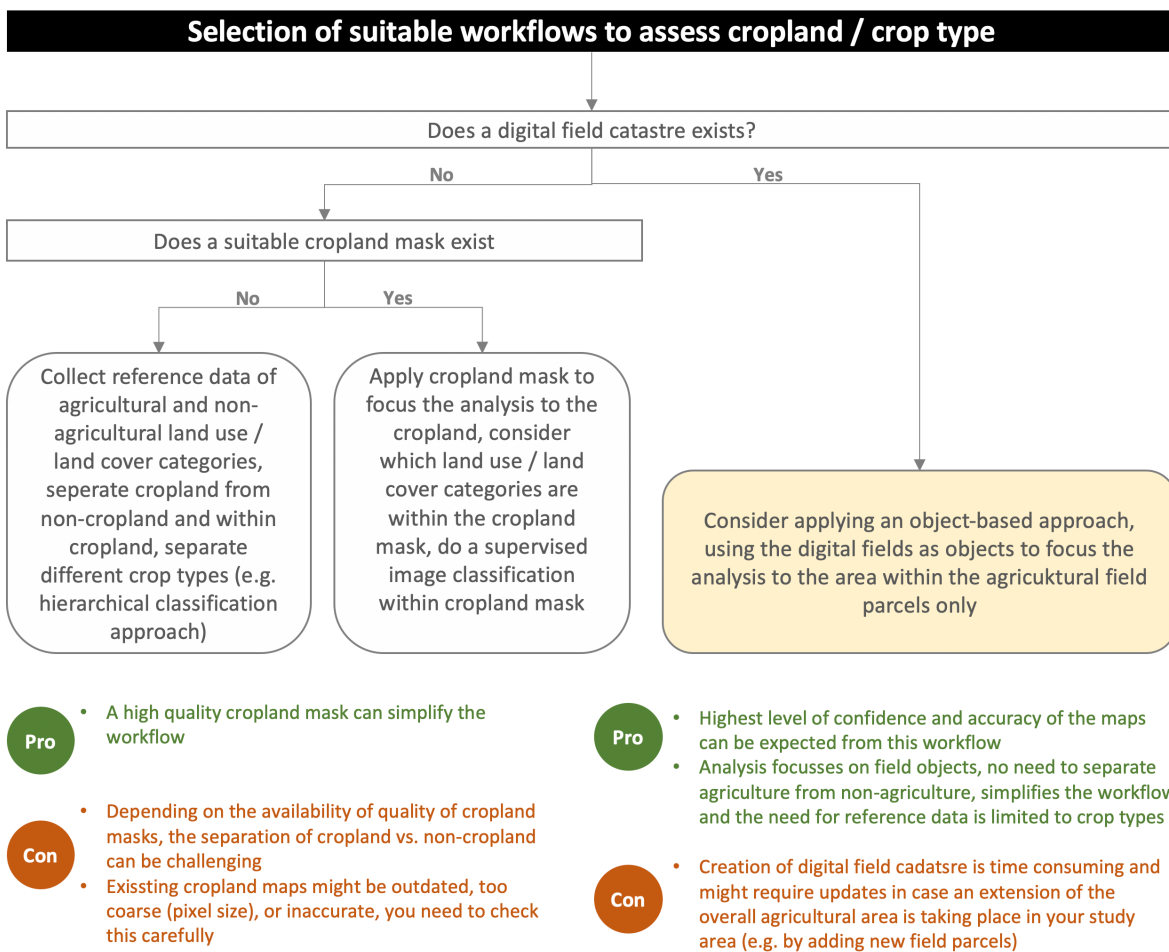


Figure 40: Guidance to select a proper workflow for assessing cropland / crop type acreage. The "gold standard" is highlighted in yellow colours.

The following workflow for crop type mapping can be implemented:

- Preparation of training data:** Provide training data as points (e.g. from GPS) or polygons in a common digital format, such as ESRI Shapefile, Geopackage, or Geojson. Training data consists of geolocated information about cropland presence / absence (e.g. binary, 1 = cropland, 0 = non-cropland) and/or crop types (e.g. 1=rice, 2=sorghum, 3=millet, 4=wheat, etc.).
- Imagery pre-processing** consists in the removal of clouds, cirrus, and cloud shadows in optical satellite images (e.g. Sentinel-2) using a cloud-score algorithm to mask contaminated pixels. It is recommended to use pre-processed satellite images from the data providers, such as Sentinel-2 Level 1B data or the Sentinel-1 GRD products. Although atmospherically corrected products are better for reliable spatial and temporal comparison, atmospheric correction is not always a pre-requisite for classification and change detection (Song et al., 2001), especially when working with normalized vegetation indices (see below). In addition, atmospherically corrected, Sentinel-2 level-2A products are not fully available yet in the repositories.

Therefore, the level-1C data can be used in case the Sentinel-2 Level 2A⁸¹ data are not available.

- **Temporal compositing** is the process of temporally aggregating satellite images into temporal “bins” of a certain period, e.g. quarterly or monthly. In the latter example, every available (and cloud masked) Sentinel-2 image within monthly periods are aggregated by calculating the average (or median) value of these images, resulting in 12 monthly Sentinel-2 image composites. This procedure closes gaps, which are caused by masking out cloudy pixels in each image, it reduced temporal-autocorrelation, and it creates a harmonized input data (in terms of having the same number of images per year). In addition, temporal compositing is applied to Sentinel-1 images to have the combined, multispectral and Radar based satellite data as input for the classifier algorithm.

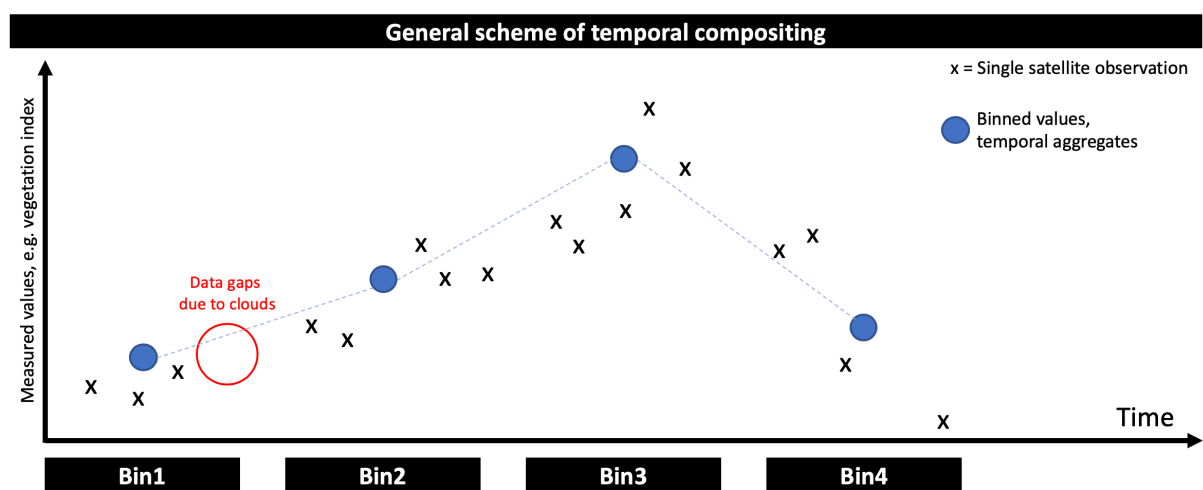


Figure 41: General scheme of temporal compositing.

- **Calculating multi-spectral predictor variables** for the classifier algorithm is the process of providing so-called “features” as input for the decision that the classifier algorithm will take. Next to the multi-spectral bands, mostly some vegetation indices such as the Normalized Difference Vegetation Index (NDVI) is computed (Rouse et al., 1974). To capture the phenological development of crops with optical remote sensing, different vegetation indices (VI) are calculated in addition to the multi-spectral bands, based on the monthly composites (see Table 19 for a selection of commonly used indices).

Table 19: Overview and description of some vegetation indices, that can be calculated based on the temporal aggregates and used as input for the classifier algorithm. The band names and the corresponding band identifier are at the example of Sentinel-2.

Sentinel-2 index	Name	Formula	References
NDVI	Normalized Difference Vegetation Index	$\frac{(NIR - Red)}{(NIR + Red)}$	(Rouse et al., 1974)
NGRDI	Normalized Difference Green/Red Edge Index	$\frac{(Red\ edge1 - Green)}{(Red\ edge1 + Green)}$	
GNDVI	Green NDVI	$\frac{(Water\ vapor - Green)}{(Water\ vapor + Green)}$	
NDRE	Normalized Difference Red Edge	$\frac{(Water\ vapor - Red\ edge1)}{(Water\ vapor + Red\ edge1)}$	

⁸¹ <https://sentinel.esa.int/web/sentinel/user-guides/sentinel-2-msi/product-types/level-2a> (last access 29 November 2020).

NDWI	Normalized Difference Water Index	$\frac{(Narrow\ NIR - SWIR1)}{(Narrow\ NIR + SWIR1)}$	(Gao, 1996)
NDYI	Normalized Difference Yellow Index	$\frac{(Green - Blue)}{(Green + Blue)}$	(Sulik and Long, 2016)

- **Calculating SAR predictor variables:** In addition to the multi-spectral bands, features based on SAR data should be computed. In case of Sentinel-1, this could be the VV and VH backscatter from the Sentinel-1 composites.
- **Calibrate** one or more classifier algorithms, such as Random Forest (RF)⁸² or Support Vector Machines (SVM), based on the reference data;
- Return the evaluation scores, confusion matrices (accuracy assessment) and trained classifiers;
- **Apply the classifier to the entire time series** and create a binary cropland map (i.e., 1=cropland vs. 0=non-cropland);
- **Decision fusion:** in case several classifier algorithms are calibrated, their results can be fused, e.g. by applying a simple majority voting.
- **Optionally**, create maps that show the a-posteriori classification probability;
- **Apply a post-classification** processing such as filtering to improve then maps;
- **Repeat these steps** or use the pre-calibrated classifier algorithm for every growing season to create a series of cropland/crop type maps.
- **Finally**, calculate the cropland / crop type area, change in area, and other indicators of interest as required (see Table 18 for some examples). Next to pixel counting, there are several methods, such as regression, calibration and small area estimators, that combine exhaustive but inaccurate information (from satellite images) with more accurate information on a sample (ground surveys). Consider the following methods for area estimation:
 - a. **Pixel counting:** after the input data is classified (see previous steps) the number of pixels under each category (e.g. cropland, or certain crop types) is multiplied by the pixel size to obtain the area⁸³.
 - b. **Calibration estimator:** The confusion matrix from the accuracy assessment provides information on the accuracy of the map (commission and omission errors). This information can be used to correct the bias in the area estimation by the pixel counting approach and for estimating the area of classes, such as the area of cropland, and their standard errors. In this regard, the reference data can be used to adjust the area estimate as obtained from the map (Olofsson et al., 2014; Stehman, 2009). Confusion matrices should be computed on a sample of test samples that have not been used as training for the image classification. Both sets, training and test, should be spatially uncorrelated and the confusion matrix has to be computed using ground information on a statistical sample of points or segments (area elements). This method is recommended, given that these pre-conditions about the test data apply.
 - c. **Regression estimator**

⁸² Random Forest (RF) is a machine-learning algorithm, which consists of an ensemble of decision trees (Breiman, 2001). RF reduces the prediction variance by using a large number of decision trees (Breiman et al., 1984).

⁸³ Note that no map is 100% accurate and the bias of area estimation by using the pixel counting approach is approximately the difference between the commission error and the omission error (Gallego et al., 2008).

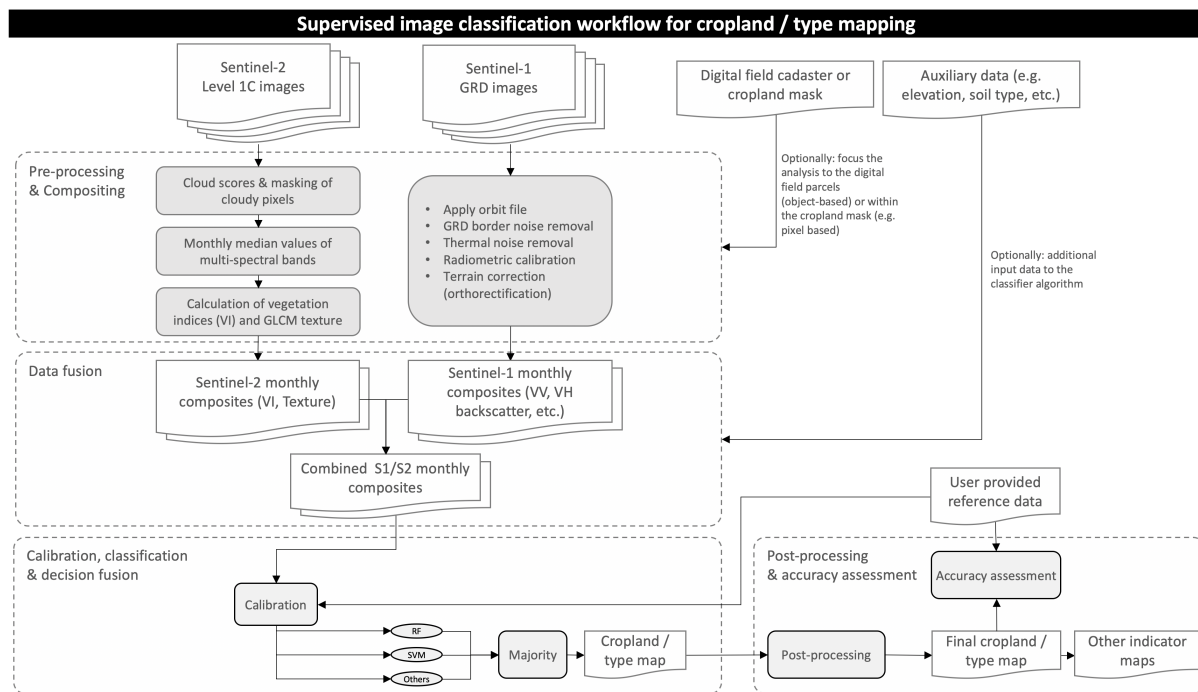


Figure 42: Detailed flow chart and visualization of the major processing steps to derive cropland and crop type maps based on supervised image classification.

Table 20: Freely available software and tools that is suitable for calculating indicator #8 "Cropland / crop type mapping" – Supervised image classification workflow.

Name	Purpose	Most important functions
Orfeo Toolbox QGIS ⁸⁴	incomplete workflow can readily be implemented using existing functions in QGIS, but the preprocessing of satellite images would be quite time consuming	<ul style="list-style-type: none"> Train a classifier with features Object Based and Pixel Based Image Classification Validating classification Majority voting for the fusion of classifications
R	Complete workflow can readily be implemented using existing functions in R, data download would have to be managed	<ul style="list-style-type: none"> Raster processing: R package 'raster' Optionally: Image segmentation: R package 'SegOptim' Image classification: R package 'randomForest' or 'caret'
Google Earth Engine (GEE) ⁸⁵	Complete workflow can readily be implemented using existing functions in GEE, not data download needed, processing in the cloud	<ul style="list-style-type: none"> median() sampleRegions() ee.Classifier.smileRandomForest() or ee.Classifier.libsvm() classify() ee.ConfusionMatrix()

12.4.5. What expertise is required?

12.4.5.1. Further statistics?

Spatial aggregation (such as the area of cropland / crop type per project region or administrative unit) of information requires some knowledge to assess and understand statistics of central tendencies.

⁸⁴ <https://www.orfeo-toolbox.org/CookBook/recipes/pbclassif.html> last access 30 November 2020)

⁸⁵ https://developers.google.com/earth-engine/api_docs (last access 30 November 2020)

cy. The guidelines proposed by (Olofsson et al., 2014, 2013) and detailed in Annex 4 should be understood and applied.

12.4.5.2. Geodata processing and/or handling GIS?

It is mandatory to handle at least a graphical user interface (GUI) based GIS like QGIS⁸⁶. For fast geo-data processing, it is advisable to work in GEE, which requires JavaScript programming⁸⁷, or other statistical programming languages with raster processing capabilities, such as R⁸⁸ or Python⁸⁹.

12.4.5.3. Technical expertise remote sensing?

Advanced understanding of remote sensing image analysis, including experience in supervised image classification with multi-temporal satellite data, is mandatory for creating new cropland / crop type maps. A potential alternative for the cropland mapping (not crop types) is visual interpretation of VHR images and on-screen digitization in GIS, which requires a solid understanding of image interpretation and a good knowledge about cropping practises in the study region.

12.4.5.4. Programming knowledge?

Statistical programming languages with raster processing capabilities, such as R⁹⁰ or Python⁹¹. For the implementation of the workflow, it is advisable to also consider working in GEE, which requires JavaScript programming⁹². The methods can also be implemented without programming in QGIS (using GRASS GIS and Orfeo Toolbox), but the pre-processing of the satellite images can become very time and computer resource consuming, due to data size.

12.4.6. How to validate the indicator maps?

The workflow creates maps of cropland / crop type, which can be evaluated by an accuracy assessment. For the validation of the maps, a set of independent (i.e., not used in the training / calibration) reference locations need to be considered.

The good practices outlined by (Olofsson et al., 2014, 2013) should be considered to assess the map accuracy and to calculate error-corrected acreage estimates of cropland / crop type. The reference data can be used to adjust the area estimate as obtained from the map. In addition, a well-documented and good overview of this subject was prepared by FAO (FAO, 2016). See Annex 4 of the MAPME Open Source Guide for more details on this issue.

12.4.7. Required input data

12.4.7.1. Which data sources are suitable for the approach?

Running the above workflows to implement a supervised image classification method crop mapping croplands / crop types requires various basic data inputs (see also **Figure 3**).

⁸⁶ <https://www.qgis.org/en/site/> (last access 19 August 2019).

⁸⁷ <https://developers.google.com/earth-engine/tutorials> (last access 19 August 2019).

⁸⁸ <https://www.r-project.org/> (last access 19 August 2019).

⁸⁹ <https://www.python.org/> (last access 19 August 2019).

⁹⁰ <https://www.r-project.org/> (last access 19 August 2019).

⁹¹ <https://www.python.org/> (last access 19 August 2019).

⁹² <https://developers.google.com/earth-engine/tutorials> (last access 19 August 2019).

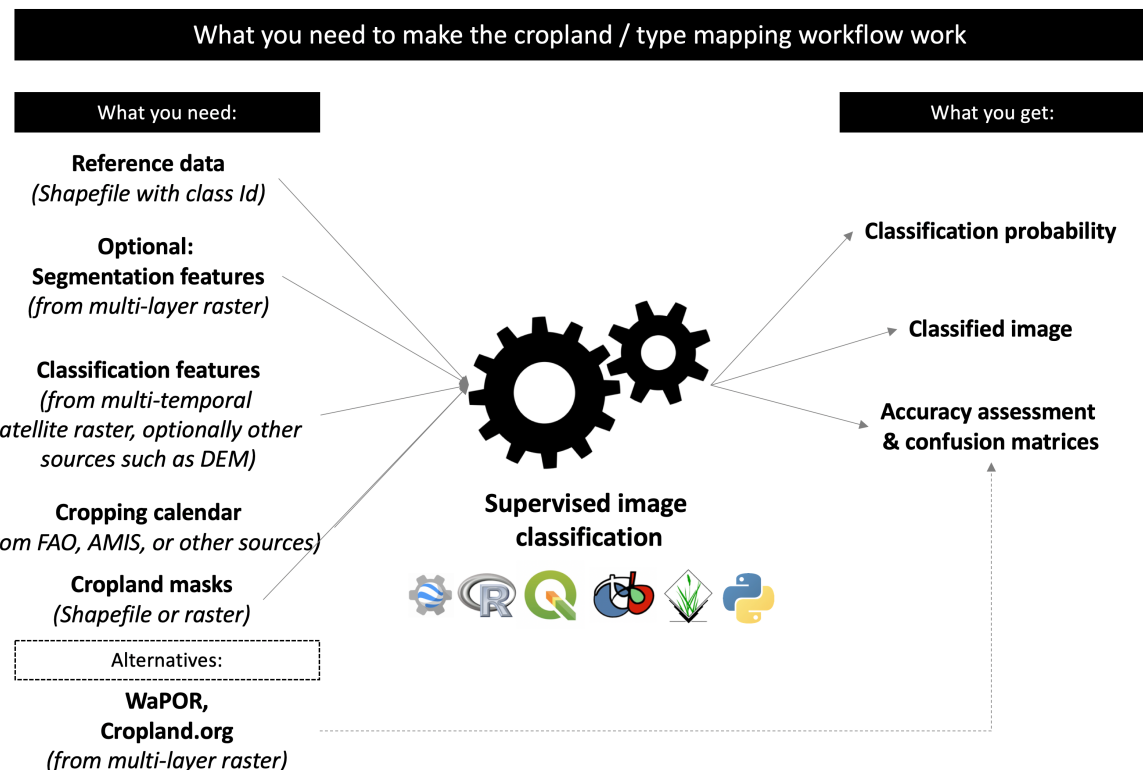


Figure 43: Overview of required data sets and information in supervised image classification.

Reference data: Traditionally, ground data used in crop classification have been collected via crop field surveys. In this approach, experts visit fields and record information about the cultivated crop – such as crop type, cultivar, growth stage, vegetation cover, etc. – along with the GPS location of that observation. The objective of this type of field surveying is to sample the diversity of crop types within the region of interest as representatively as possible. Doing so requires that a sufficient number of samples be collected for each target class. The timing of field surveys is usually determined by the local crop calendar (see below under "Auxiliary data").

The reference data is then converted into a suitable format, e.g. as an ESRI Shapefile or GeoPackage, or a single-layer raster dataset containing samples for calibrating (training) a classifier. The labels, classes or categories should be coded as integers {0,1} for single-class problems (i.e. cropland vs. non-cropland), or, {1,2,...,n} for multi-class problems, i.e. different crop types.

As a rule of thumb, the minimum sampling density to validate land cover maps should reach 30 samples for the least represented land use class (e.g. 30 per crop type category).

Remote sensing data: Typically, a multi-layer raster dataset, recorded on one several acquisition dates per growing season (multi-temporal imagery) from freely available satellite systems such as Sentinel-1, Sentinel-2 and Landsat-8 (see Annex 1). The most commonly used file format is GeoTIFF. Satellite data is the basis for extracting classification features, which is typically a multi-layer raster dataset with features such as spectral bands, spectral indices, texture, terrain elevation, etc.

Table 21: Overview of some satellite system properties and crop mapping requirements. See Annex 1 for a detailed description of individual satellite systems.

Spatial	Type	Examples	Data costs	Revisit frequency	Application examples
---------	------	----------	------------	-------------------	----------------------

resolution					Cropland	Crop type	Crop intensity
< 10m	Optical, SAR	SPOT, Terra SAR-X, RapidEye	See Annex 1	Only a few per years, or tasking new acquisitions	Yes, including very small fields < 1.5 ha	Yes, including very small fields < 1.5 ha	Yes, including very small fields < 1.5 ha
10-60m	Optical, SAR	Sentinel-1, Sentinel-2, Landsat-8	None	Weekly, sufficient to create 1-3 monthly composites	Yes	Yes	Yes
100-500	Optical	MODIS, VIIRS, Sentinel-3	None	Daily if cloud free	Yes	Only for large fields, e.g. > 10-15 hectares	Only for large fields, e.g. > 10-15 hectares

Auxiliary data: The timing of field surveys and the timing of satellite images (that cover a growing season) is usually determined by the local crop calendar. Crop calendars describe when the major growing phases of particular crops occur each year (see Table 4). For best results, site visits should coincide with the period in crop growth during which the crop type can most easily be identified.

Other auxiliary data and information come from sources other than remote sensing, and can be used to improve classification accuracy. This adds additional context features that can be integrated with remote sensing-based classification features at various stages during the image classification process (e.g. as input for the classifier algorithm, or to do some post-classification improvements). These variables may include, but are not limited to, elevation, slope, aspect, hydrology, geology, soils, transportation networks, etc. The context variables would have to be converted into the same format as the remote sensing data, e.g. GeoTIFF, and projected into the same coordinate system.

Existing digital field cadasters or cropland masks (see chapter 12.4.8) can be used to focus the analysis to the area of interest, which can largely simplify the workflow and reduce the need to have reference data of other, non-crop-type related categories in the map.

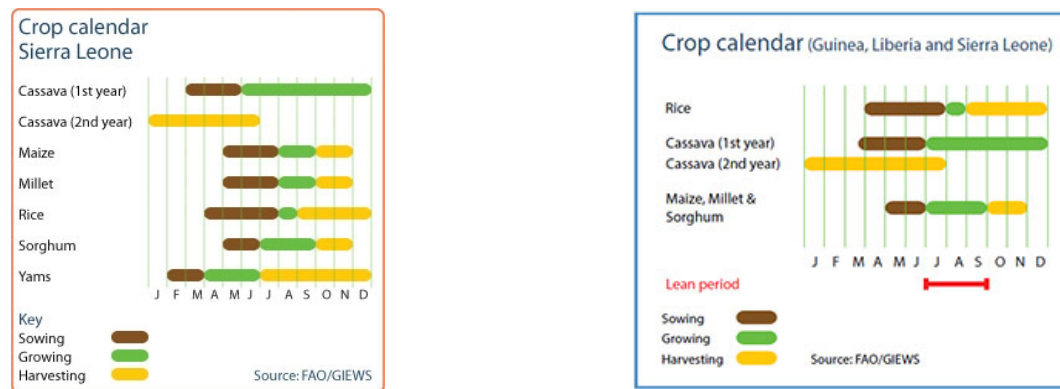


Figure 44: Examples of crop calendars by FAO.

12.4.7.1.1. What limitations must be expected without in-situ data, and to what extent are other data sources suitable as substitutes for in-situ data?

Although field validation is recommended, the biggest disadvantage is that they are labour-intensive, time-consuming and challenging when the goal is to acquire representative data at national and regional scales. Without in-situ data, other reliable sources of data must usually be considered to supplement ground surveys (or replace them entirely). These sources include data collected by local,

regional or national government agencies or, more informally, through crowdsourcing. Some potential, crowd-sourcing based platforms (see Table 22) and tools (see Table 23) can be considered. These platforms represent online applications that guide the visual interpretation of VHR images⁹³, which is efficiently augmented by – for example – the NDVI temporal signatures of the observed locations (see Figure 45).

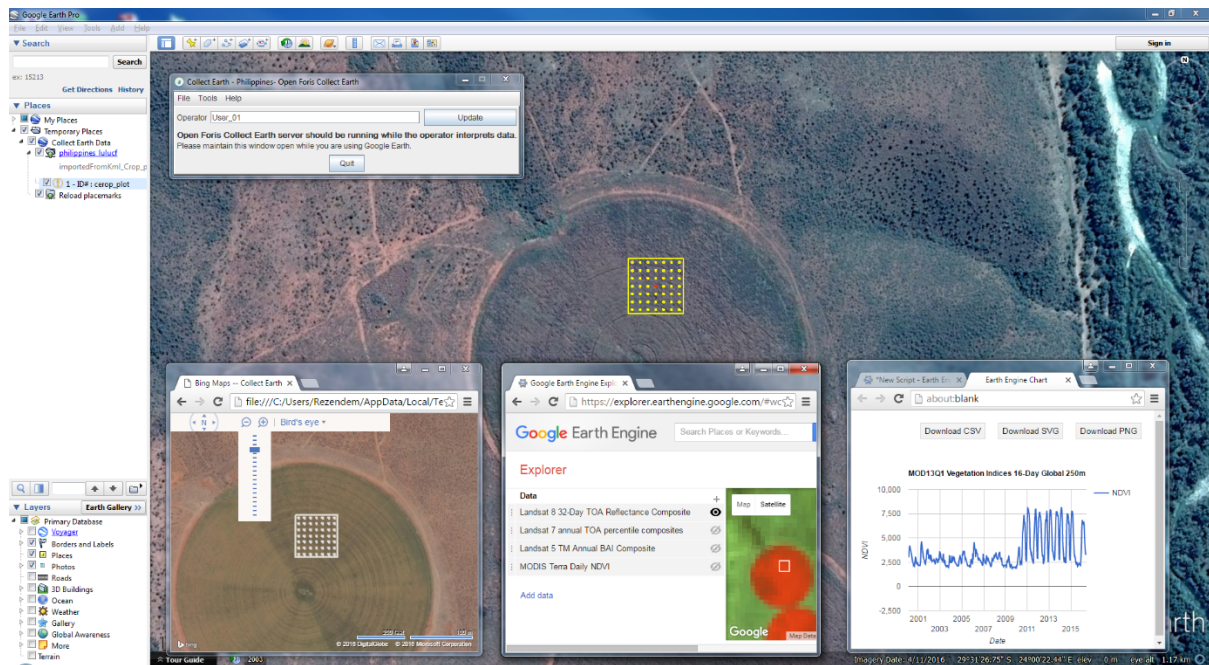


Figure 45: Examples of the Collect Earth platform used to collect reference data. Source: <http://www.openforis.org/tools/collect-earth/case-study.html>.

Table 22: Examples for crowd-sourced and/or freely available reference data sets (cropland and/or crop type specific)

Name	Description	Source / Reference
croplands.org	A platform that presents freely available cropland (and partly crop type) maps and reference data.	https://croplands.org/app/data/classify (Xiong et al., 2017a)
Geo-Wiki	A global reference data set on cropland was collected through a crowdsourcing campaign using the Geo-Wiki crowdsourcing tool. 36,000 sample units, focussing on cropland identification.	http://www.geo-wiki.org/ (Laso Bayas et al., 2017)

Table 23: Examples for tools potentially suitable for on-screen collection of reference data.

Name	Description	Source / Reference
Collect Earth	Collect Earth Online is a custom built, open-source, satellite image viewing and interpretation system developed by SERVIR - a joint NASA and USAID program in partnership with regional technical organizations around the world - and the FAO as a tool for use in projects that require land cover and/or land use reference data. Contains, amongst others, publicly available reference data about cropland / crop type, but only in certain regions / years.	https://collect.earth (Saah et al., 2019)

⁹³ The acquisition date of these VHR images might, however, deviate from the year of observation. This is therefore quite efficient for the most stable land cover types but should not be used for crop type for instance as they might change annually.

Geo-Wiki	A global reference data set on cropland was collected through a crowdsourcing campaign using the Geo-Wiki crowdsourcing tool. 36,000 sample units, focussing on cropland identification. (Laso Bayas et al., 2017)
----------	---

Without any reference data at all, crop type maps can usually neither be created (missing calibration data for the classifier algorithm for such specific classes such as crop types) nor validated.

12.4.8. Cost-benefit:

Good practice recommendation: Gather reference data, at best in-situ, and pre-process combined optical and SAR data, e.g. Sentinel1/2 and optionally Landsat-8 data in addition. Create an accurate map of cropland (e.g. using pixel or object based, supervised image classification), and within the cropland mask, apply supervised image classification to create a crop type map, if required. VHR images in at least two periods. Assess and quantify land cover change, based on the annual maps. Report accuracy metrics and calculate land cover area statistics corrected for accuracy and provide a second map showing a-posteriori classification probabilities.

Alternatives and trade-offs: Try existing cropland / crop type maps (see chapter 12.4.7.1 or **Annex 2**) exist. Existing, value-added data sets (cropland maps) are available and can be considered to assess indicator#8 or to cross-check your own maps. Most notably, for Africa (and partly middle East) the platform WaPOR⁹⁴ (only Africa and middle east) and ACMA (Xiong et al., 2017a) do provide cropland and crop type maps. A high resolution (30m) cropland map was released for Africa in 2017 (Xiong et al., 2017b) and ESA is preparing a prototype high resolution land cover map with 20m spatial resolution over Africa based on 1 year of Sentinel-2A observations from December 2015 to December 2016⁹⁵. Similar land use / land cover maps, which contain the category "cropland", do exist in other regions or even globally. The platforms <https://croplands.org/> or <https://wapor.apps.fao.org> provides some of these aforementioned products.

Yet, keep in mind that these products are either relatively coarse (in terms of pixel size), which means that they don't allow for small-scale assessments such as smallholder farming systems. And they usually do not contain the crop categories under investigation.

⁹⁴ https://wapor.apps.fao.org/home/WAPOR_2/1 (last access 01 December 2020).

⁹⁵ <http://2016africalandcover20m.esrin.esa.int> (last access 01 December 2020).

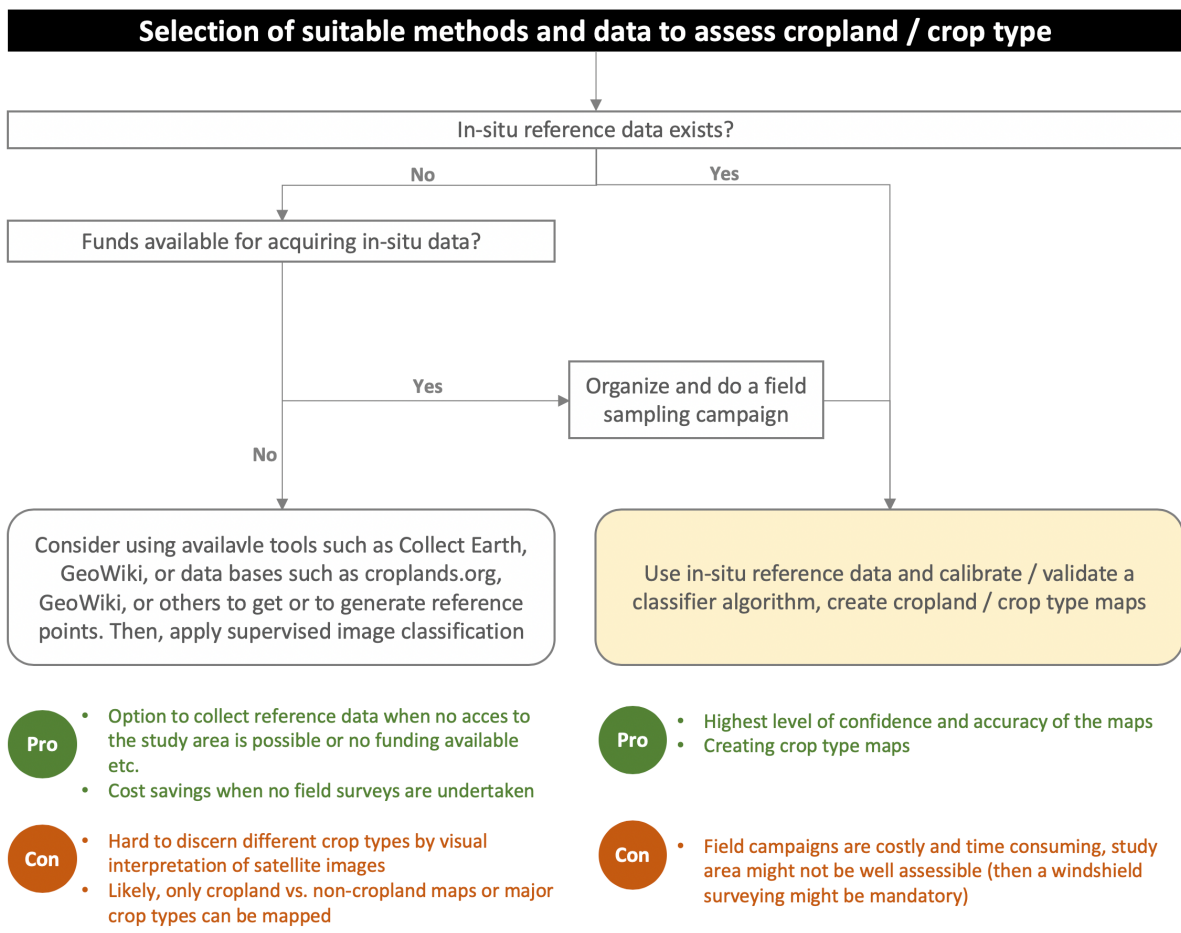


Figure 46: Guidance to select proper and methods for assessing cropland / crop type acreage. The "gold standard" is highlighted in yellow colours.

13.General conclusion and recommendations

This study provides the basis for good practice guidelines for using remote sensing to assess six distinct success indicators for evaluating forest-related projects ex post. An attempt was made to highlight potential “gold standard” workflows, which however tend rely on costly VHR and in-situ data. Hence, “quick win” alternatives based on freely available data and workflows that are as simple as possible have been presented. Please note that the recommendations in this document are meant to be a guideline but should in no way be seen as exclusive. This document should also be viewed in the context of steadily evolving technologies (e.g. DL) and increasing availability of higher resolution VHR data (e.g. future Sentinel missions) and computational power (cloud computing). The following recommendations are also partly illustrated in Figure 47 and Figure 48:

Reference data:

Remote sensing is advancing quickly, but the importance of (in-situ) ground truthing cannot be overstated. All indicators require some sort of reference data, such as for the training of classifier algorithms (indicators #1, #3 and #7), calibrating and fine-tuning image segmentation (indicators #1, #5 and #6) and for validation of indicator maps. In-situ data from field surveys is the most accurate type of reference. However, the large scale of study regions and costs for organising field surveys can make field visits an expensive proposition. Previous studies showed that – for each indicator – reference data can, in principle, be acquired from existing VHR data (e.g. satellite images shown in Google Earth or newly acquired VHR data).

Spatial dimension of remote sensing data:

Most of the indicators in this document can be quantified or at least proxied from MR data. This allows cost savings for data acquisition, but not for data analysis. The need to monitor small-scale phenomena, such as selective logging (indicator #1), individual tree crowns (indicator #5) or seedlings (indicator #7) limit its use. VHR data is generally recommended for assessing indicators #1 and #7 and strongly encouraged for indicators #5 and #6, because the detection of ITCs, initial gully erosion, or individual seedlings is heavily affected by mixed pixels or even impossible using MR data. Still, most of the indicators allow approximation with freely available, moderate remote sensing data. The trade-offs, for example in terms of accuracy, are described in each indicator section.

Multi-spectral dimension of remote sensing data:

LiDAR data is strongly recommended for indicators #5 and #6, but also possible using VHR optical data (multispectral or hyperspectral). It must be taken into consideration that the primary source for LiDAR data is ALS or drones. A combination of multitemporal, satellite-based optical and radar should be preferred for assessing indicator #1 (if optical VHR data is not an option) and #3.

Temporal dimension of remote sensing data:

Using multitemporal data sets (i.e. having several consecutive images in a vegetation season) is recommended for indicators #1 (#2) and #3, because it enhances classification accuracy. For indicator #4 it is mandatory. If mono-temporal VHR images are used to assess indicators, the timing must be selected with care (e.g. to consider off-leaf seasons).

Methods and workflows:

Generally speaking, workflows for assessing indicators #1, #2, #3, and #7 consist of classifying VHR or MR remote sensing data to create thematic maps. Supervised image classification (pixel or object-based) should be based on the use of non-parametric machine learning algorithms (e.g. RF or SVM), or Deep Learning methods (indicator #5 and #7). Image segmentation (OBIA) is advisable for indicators #1 (with VHR data), #5, #6, and #7, which can be combined with image classification to further enhance the accuracy of the indicator maps.

Validation strategies:

All indicator maps can and should be validated to inform users about the reliability of the maps. For indicator maps #1 and #3, the accuracy assessment based on confusion matrices including confidence intervals and error-corrected area estimates should be provided. The validation of indicator map #2 could be substituted by informing the user about the accuracy of the forest cover maps (indicator #1). Indicator maps #5 and #6 can be validated using reference polygons. The segmentation accuracy could be evaluated using the percentage of ITCs classified as correctly detected regarding the total number of ITCs tested. It is very unlikely that an automatically delineated crown exactly matches a manually delineated one. **As a general note of caution, it is strongly suggested that any important policy and management decision or conclusion in project evaluation should not be based on maps alone that have not been either sufficiently validated (at best with in reliable situ information) or cross-checked, or evaluated in terms of their detection sensitivity in the manner described here.**

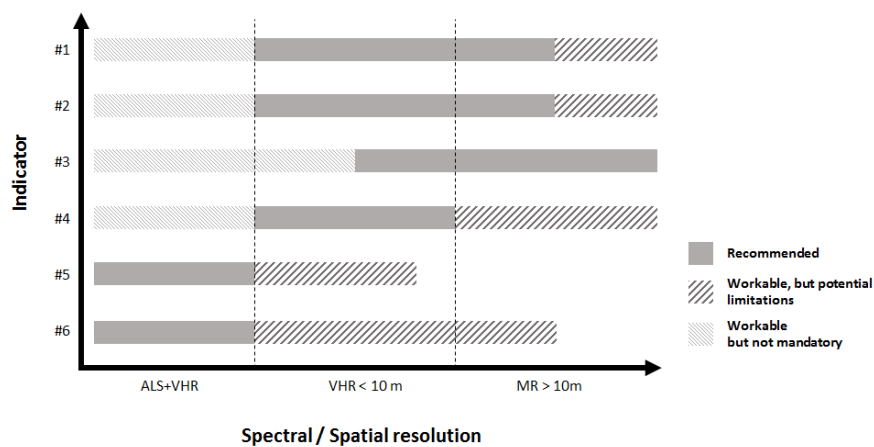


Figure 47: Suitability of different spatial resolution systems for assessing six forest indicators.

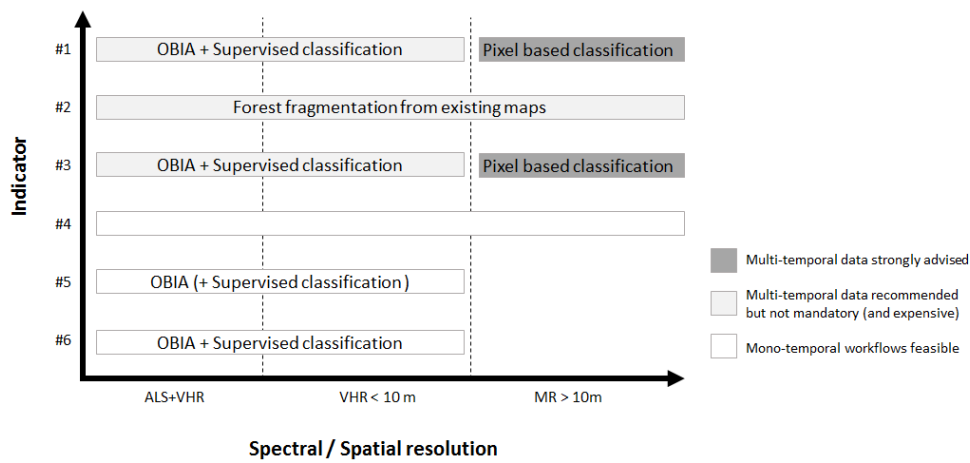


Figure 48: Recommended workflows and data sets regarding observation frequency.

14. References

- Achard, F., Beuchle, R., Mayaux, P., Stibig, H.J., Bodart, C., Brink, A., Carboni, S., Desclée, B., Donnay, F., Eva, H.D., Lopi, A., Raši, R., Seliger, R., Simonetti, D., 2014. Determination of tropical deforestation rates and related carbon losses from 1990 to 2010. *Glob. Chang. Biol.* 20, 2540–2554. <https://doi.org/10.1111/gcb.12605>
- Achard, F., Defries, R., Eva, H., Hansen, M., Mayaux, P., Stibig, H.J., 2007. Pan-tropical monitoring of deforestation. *Environ. Res. Lett.* 2. <https://doi.org/10.1088/1748-9326/2/4/045022>
- Aguilar, R., Zurita-Milla, R., Izquierdo-Verdiguier, E., de By, R.A., 2018. A cloud-based multi-temporal ensemble classifier to map smallholder farming systems. *Remote Sens.* 10. <https://doi.org/10.3390/rs10050729>
- Akike, S., Samanta, S., 2016. Land Use/Land Cover and Forest Canopy Density Monitoring of Wafi-Golpu Project Area, Papua New Guinea. *J. Geosci. Environ. Prot.* 4, 1–14. <https://doi.org/10.4236/gep.2016.48001>
- Andreoli, R., 2018. Modeling Erosion Risk Using the RUSLE Equation. *QGIS Appl. Water Risks* 4, 245–282.
- Asner, G.P., Kellner, J.R., Kennedy-Bowdoin, T., Knapp, D.E., Anderson, C., Martin, R.E., 2013. Forest Canopy Gap Distributions in the Southern Peruvian Amazon. *PLoS One*. <https://doi.org/10.1371/journal.pone.0060875>
- Asner, G.P., Knapp, D.E., Broadbent, E.N., Oliveira, P.J.C., Keller, M., Silva, J.N., 2005. Selective logging in the Brazilian Amazon. *Science (80-.).* 310, S1–S28. <https://doi.org/10.1126/science.1118051>
- Atzberger, C., 2013. Advances in remote sensing of agriculture: context description, existing operational monitoring systems and major information needs. *Remote Sens.* 5, 949–981. <https://doi.org/10.3390/rs5020949>
- Axelsson, A., Lindberg, E., Olsson, H., 2018. Exploring multispectral ALS data for tree species classification. *Remote Sens.* 10. <https://doi.org/10.3390/rs10020183>
- Bastiaanssen, W.G.M., Bos, M.G., 1999. Irrigation performance indicators based on remotely sensed data: A review of literature. *Irrig. Drain. Syst.* 13, 291–311.
- Benavidez, R., Jackson, B., Maxwell, D., Norton, K., 2018. A review of the (Revised) Universal Soil Loss Equation ((R)USLE): with a view to increasing its global applicability and improving soil loss estimates. *Hydrol. Process.* 22, 6059–6086.
- Blaschke, T., 2010. Object based image analysis for remote sensing. *ISPRS J. Photogramm. Remote Sens.* 65, 2–16. <https://doi.org/10.1016/j.isprsjprs.2009.06.004>
- Breidenbach, J., Næsset, E., Lien, V., Gobakken, T., Solberg, S., 2010. Prediction of species specific forest inventory attributes using a nonparametric semi-individual tree crown approach based on fused airborne laser scanning and multispectral data. *Remote Sens. Environ.* 114, 911–924. <https://doi.org/10.1016/j.rse.2009.12.004>
- Broadbent, E.N., Asner, G.P., Keller, M., Knapp, D.E., Oliveira, P.J.C., Silva, J.N., 2008. Forest fragmentation and edge effects from deforestation and selective logging in the Brazilian Amazon. *Biol. Conserv.* 141, 1745–1757. <https://doi.org/10.1016/j.biocon.2008.04.024>
- Congedo, L., 2016. Semi-Automatic Classification Plugin User Manual. <https://doi.org/10.13140/RG.2.1.1219.3524>
- Curtis, P.G., Slay, C.M., Harris, N.L., Tyukavina, A., Hansen, M.C., 2018. Classifying drivers of global forest loss. *Science (80-.).* 361, 1108–1111. <https://doi.org/10.1126/science.aau3445>
- Dalagnol, R., Phillips, O.L., Gloor, E., Galvão, L.S., Wagner, F.H., Locks, C.J., Aragão, L.E.O.C., 2019. Quantifying canopy tree loss and gap recovery in tropical forests under low-intensity logging using VHR satellite imagery and airborne LiDAR. *Remote Sens.* 11, 1–20. <https://doi.org/10.3390/rs11070817>
- Dalponte, M., Ørka, H.O., Ene, L.T., Gobakken, T., Næsset, E., 2014. Tree crown delineation and tree species classification in boreal forests using hyperspectral and ALS data. *Remote Sens. Environ.* 140, 306–317. <https://doi.org/10.1016/j.rse.2013.09.006>
- Debats, S.R., Luo, D., Estes, L.D., Fuchs, T.J., Caylor, K.K., 2016. A generalized computer vision

- approach to mapping crop fields in heterogeneous agricultural landscapes. *Remote Sens. Environ.* 179, 210–221. <https://doi.org/10.1016/j.rse.2016.03.010>
- Demina, N., Karpov, A., Voronin, V., Lopatin, E., Bogdanov, A., 2018. Possible use of remote sensing for reforestation processes in Arctic zone of European Russia. *Arct. Environ. Res.* 18, 106–113. <https://doi.org/10.3897/issn2541-8416.2018.18.3.106>
- Duarte, L., Teodoro, A.C., Gonçalves, J.A., Soares, D., Cunha, M., 2016. Assessing soil erosion risk using RUSLE through a GIS open source desktop and web application. *Environ. Monit. Assess.* 188, 351.
- Duveiller, G., Defourny, P., 2010. A conceptual framework to define the spatial resolution requirements for agricultural monitoring using remote sensing. *Remote Sens. Environ.* 114, 2637–2650. <https://doi.org/10.1016/j.rse.2010.06.001>
- Eeckhaut, M., Van Den, Kerle, N., Herva's, J., Supper, R., 2011. Mapping of Landslides Under Dense Vegetation Cover Using Object-Oriented Analysis and LiDAR Derivatives. *Miet. Proc. Second World Landslide Forum* 1–6. <https://doi.org/10.1007/978-3-642-31325-7>
- Ellis, P., Griscom, B., Walker, W., Gonçalves, F., Cormier, T., 2016. Mapping selective logging impacts in Borneo with GPS and airborne lidar. *For. Ecol. Manage.* <https://doi.org/10.1016/j.foreco.2016.01.020>
- Ene, L., Næsset, E., Gobakken, T., 2012. Single tree detection in heterogeneous boreal forests using airborne laser scanning and area-based stem number estimates. *Int. J. Remote Sens.* 33, 5171–5193.
- FAO, 2016. *Map Accuracy Assessment and Area Estimation: A Practical Guide.*
- Fensholt, R., Rasmussen, K., Kaspersen, P., Huber, S., Horion, S., Swinnen, E., 2013. Assessing Land Degradation/Recovery in the African Sahel from Long-Term Earth Observation Based Primary Productivity and Precipitation Relationships. *Remote Sens.* 5, 664–686. <https://doi.org/10.3390/rs5020664>
- Francipane, A., Mussomè, F., Cipolla, G., Noto, L., 2018. Object-Based Image Analysis Technique for Gully Mapping Using Topographic Data at Very High Resolution (VHR) 3, 725–718. <https://doi.org/10.29007/shdh>
- Frankl, A., Nyssen, J., Adgo, E., Wassie, A., Scull, P., 2019. Can woody vegetation in valley bottoms protect from gully erosion? Insights using remote sensing data (1938–2016) from subhumid NW Ethiopia. *Reg. Environ. Chang.* <https://doi.org/10.1007/s10113-019-01533-4>
- Funk, C., Peterson, P., Landsfeld, M., Pedreros, D., Verdin, J., Shukla, S., Husak, G., Rowland, J., Harrison, L., Hoell, A., Michaelsen, J., 2015. The climate hazards infrared precipitation with stations—a new environmental record for monitoring extremes. *Sci. Data* 2, 150066. <https://doi.org/10.1038/sdata.2015.66>
- Fynn, I.E.M., Campbell, J., 2019. Forest fragmentation analysis from multiple imaging formats. *J. Landsc. Ecol.* 12, 1–15. <https://doi.org/10.2478/jlecol-2019-0001>
- Gallego, J.F., Craig, M., Michaelsen, J., Bossyns, B., Fritz, S., 2008. Best practices for crop area estimation with remote sensing. *Ispra: Joint Research Center. Ispra.* <https://doi.org/10.2788/31835>
- Gao, B.-C., 1996. NDWI A Normalized Difference Water Index for Remote Sensing of Vegetation Liquid Water From Space. *Remote Sens. Environ.* 58, 257–266.
- Gerlein-Safdi, C., Keppel-Aleks, G., Wang, F., Frolking, S., Mauzerall, D.L., 2020. Satellite Monitoring of Natural Reforestation Efforts in China's Drylands. *One Earth* 2, 98–108. <https://doi.org/10.1016/j.oneear.2019.12.015>
- Gibbs, H.K., Salmon, J.M., 2015. Mapping the world's degraded lands. *Appl. Geogr.* 57, 12–21. <https://doi.org/10.1016/j.apgeog.2014.11.024>
- Giles, P.T., Burgoyne, J.M., 1993. Tropical deforestation and habitat fragmentation in the Amazon: satellite data from 1978 to 1988. *Science (80-.).* 260, 1905–1910. <https://doi.org/10.1127/0309133308096755>
- Hansen, M.C., Potapov, P. V., Moore, R., Hancher, M., Turubanova, S.A., Tyukavina, A., Thau, D., Stehman, S. V., Goetz, S.J., Loveland, T.R., Kommareddy, A., Egorov, A., Chini, L., Justice, C.O., Townshend, J.R.G., 2013. High-resolution global maps of 21st-century forest cover change.

- Science (80-). 342, 850–853. <https://doi.org/10.1126/science.1244693>
- Hao, P., Löw, F., Biradar, C., 2018. Annual cropland mapping using reference Landsat time series-A case study in Central Asia. *Remote Sens.* 10. <https://doi.org/10.3390/rs10122057>
- Hasan, A.F., Laurent, F., Messner, F., Bourgoin, C., Blanc, L., 2019. Cumulative disturbances to assess forest degradation using spectral unmixing in the northeastern Amazon. *Appl. Veg. Sci.* 22, 394–408. <https://doi.org/10.1111/avsc.12441>
- Hermosilla, T., Wulder, M.A., White, J.C., Coops, N.C., Hobart, G.W., 2017. Updating Landsat time series of surface-reflectance composites and forest change products with new observations. *Int. J. Appl. Earth Obs. Geoinf.* 63, 104–111. <https://doi.org/10.1016/j.jag.2017.07.013>
- Hermosilla, T., Wulder, M.A., White, J.C., Coops, N.C., Pickell, P.D., Bolton, D.K., 2019. Impact of time on interpretations of forest fragmentation: Three-decades of fragmentation dynamics over Canada. *Remote Sens. Environ.* 222, 65–77. <https://doi.org/10.1016/j.rse.2018.12.027>
- Hesselbarth, M.H.K., 2019. R Package "landscapemetrics."
- Hethcoat, M.G., Edwards, D.P., Carreiras, J.M.B., Bryant, R.G., França, F.M., Quegan, S., 2019. A machine learning approach to map tropical selective logging. *Remote Sens. Environ.* 221, 569–582. <https://doi.org/10.1016/j.rse.2018.11.044>
- Higginbottom, T., Symeonakis, E., 2014. Assessing Land Degradation and Desertification Using Vegetation Index Data: Current Frameworks and Future Directions. *Remote Sens.* 6, 9552–9575. <https://doi.org/10.3390/rs6109552>
- Ibrahim, Y.Z., Balzter, H., Kaduk, J., Tucker, C.J., 2015. Land degradation assessment using residual trend analysis of GIMMS NDVI3g, soil moisture and rainfall in Sub-Saharan West Africa from 1982 to 2012. *Remote Sens.* 7, 5471–5494. <https://doi.org/10.3390/rs70505471>
- INPE, 2008. Monitoramento da cobertura florestal da Amazônia por Satélites. Sistemas PRODES, DETER, DEGRAD E QUEIMADAS 2007-2008. São José dos Campos.
- Jakubowski, M.K., Li, W., Guo, Q., Kelly, M., 2013. Delineating individual trees from lidar data: A comparison of vector- and raster-based segmentation approaches. *Remote Sens.* 5, 4163–4186. <https://doi.org/10.3390/rs5094163>
- Jin, Z., Azzari, G., You, C., Di Tommaso, S., Aston, S., Burke, M., Lobell, D.B., 2019. Smallholder maize area and yield mapping at national scales with Google Earth Engine. *Remote Sens. Environ.* 228, 115–128. <https://doi.org/10.1016/j.rse.2019.04.016>
- Jones, H.G., Vaughan, R.A., 2010. Remote sensing of vegetation: Principles, techniques, and applications. Oxford University Press, New York.
- Jung, M., 2016. LecoS - A python plugin for automated landscape ecology analysis. *Ecol. Inform.* 31, 18–21. <https://doi.org/10.1016/j.ecoinf.2015.11.006>
- Justice, C., Becker-Reshef, I., 2007. Report from the workshop on developing a strategy for global agricultural monitoring in the framework of Group on Earth Observations (GEO), 16–18 July 2007, FAO, Rome. University of Maryland: College Park, MD, USA, p. 67.
- Kendall, M.G., 1938. A New Measure of Rank Correlation. *Biometrika* 30, 81–93. <https://doi.org/10.2307/2332226>
- Kim, M., Madden, M., Warner, T.A., 2009. Forest Type Mapping using Object-specific Texture Measures from Multispectral Ikonos Imagery : Segmentation Quality and Image Classification Issues. *Photogramm. Eng. Remote Sens.* 75, 819–829.
- Langner, A., 2018. ΔrNBR (Google Earth Engine) - Manual. Jt. Res. Cent.
- Langner, A., Miettinen, J., Kukkonen, M., Vancutsem, C., Simonetti, D., Vieilledent, G., Verhegghen, A., Gallego, J., Stibig, H.J., 2018. Towards operational monitoring of forest canopy disturbance in evergreen rain forests: A test case in continental Southeast Asia. *Remote Sens.* 10, 1–21. <https://doi.org/10.3390/rs10040544>
- Laso Bayas, J.C., Lesiv, M., Waldner, F., Schucknecht, A., Duerauer, M., See, L., Fritz, S., Fraisl, D., Moorthy, I., McCallum, I., Perger, C., Danylo, O., Defourny, P., Gallego, J., Gilliams, S., Akhtar, I.U.H., Baishya, S.J., Baruah, M., Bungnamei, K., Campos, A., Changkakati, T., Cipriani, A., Das, Krishna, Das, Keemee, Das, I., Davis, K.F., Hazarika, P., Johnson, B.A., Malek, Z., Molinari, M.E., Panging, K., Pawe, C.K., Pérez-Hoyos, A., Sahariah, P.K., Sahariah, D., Saikia, A., Saikia, M., Schlesinger, P., Seidacaru, E., Singha, K., Wilson, J.W., 2017. A global reference database of

- crowdsourced cropland data collected using the Geo-Wiki platform. *Sci. Data* 4, 1–10.
<https://doi.org/10.1038/sdata.2017.136>
- Leeuwen, W.J.D. Van, 2008. Monitoring the Effects of Forest Restoration Treatments on Post-Fire Vegetation Recovery with MODIS Multitemporal Data. *Sensors* 8, 2017–2042.
- Li, J., Hu, B., Woods, M., 2015. A Two-Level Approach for Species Identification of Coniferous Trees in Central Ontario Forests Based on Multispectral Images. *IEEE J. Sel. Top. Appl. Earth Obs. Remote Sens.* 8, 1487–1497. <https://doi.org/10.1109/JSTARS.2015.2423272>
- Lima, T.A., Beuchle, R., Langner, A., Grecchi, R.C., Griess, V.C., Achard, F., 2019. Comparing Sentinel-2 MSI and Landsat 8 OLI imagery for monitoring selective logging in the Brazilian Amazon. *Remote Sens.* 11, 1–21. <https://doi.org/10.3390/rs11080922>
- Liu, C.C., Chen, Y.H., Wu, M.H.M., Wei, C., Ko, M.H., 2019. Assessment of forest restoration with multitemporal remote sensing imagery. *Sci. Rep.* 9, 1–19. <https://doi.org/10.1038/s41598-019-43544-5>
- Liu, Y., Gong, W., Hu, X., Gong, J., 2018. Forest type identification with random forest using Sentinel-1A, Sentinel-2A, multi-temporal Landsat-8 and DEM data. *Remote Sens.* 10, 1–25.
<https://doi.org/10.3390/rs10060946>
- Löw, F., Biradar, C., Dubovik, O., Fliemann, E., Akramkhanov, A., Narvaez Vallejo, A., Waldner, F., 2017. Regional-scale monitoring of cropland intensity and productivity with multi-source satellite image time series. *GIScience Remote Sens.* 55, 1–29.
<https://doi.org/10.1080/15481603.2017.1414010>
- Löw, F., Duveiller, G., 2014. Defining the Spatial Resolution Requirements for Crop Identification Using Optical Remote Sensing. *Remote Sens.* 6, 9034–9063. <https://doi.org/10.3390/rs6099034>
- Lowder, S.K., Skoet, J., Raney, T., 2016. The Number, Size, and Distribution of Farms, Smallholder Farms, and Family Farms Worldwide. *World Dev.* 87, 16–29.
<https://doi.org/10.1016/j.worlddev.2015.10.041>
- Lowder, S.K., Skoet, J., Singh, S., 2014. What do we really know about the number and distribution of farms and family farms in the world ? Background paper for "The State of Food and Agriculture 2014, ESA Working Paper No. 14-02.
- Maltamo, M., Næsset, E., Vauhkonen, J., 2014. Forestry applications of airborne laser scanning. *Concepts case Stud. Manag Ecosys* 27, 460.
- McGarigal, K., Cushman, S.A., Neel, M.C., Ene, E., 2015. FRAGSTATS: spatial pattern analysis program for categorical maps.
- Mohan, M., Silva, C.A., Klauberg, C., Jat, P., Catts, G., Cardil, A., Hudak, A.T., Dia, M., 2017. Individual tree detection from unmanned aerial vehicle (UAV) derived canopy height model in an open canopy mixed conifer forest. *Forests* 8, 1–17. <https://doi.org/10.3390/f8090340>
- Olofsson, P., Foody, G.M., Herold, M., Stehman, S. V., Woodcock, C.E., Wulder, M.A., 2014. Good practices for estimating area and assessing accuracy of land change. *Remote Sens. Environ.* 148, 42–57. <https://doi.org/10.1016/j.rse.2014.02.015>
- Olofsson, P., Foody, G.M., Stehman, S. V., Woodcock, C.E., 2013. Making better use of accuracy data in land change studies: Estimating accuracy and area and quantifying uncertainty using stratified estimation. *Remote Sens. Environ.* 129, 122–131.
<https://doi.org/10.1016/j.rse.2012.10.031>
- Ottosen, T.-B., Petch, G., Hanson, M., Skjøth, C.A., 2020. Tree cover mapping based on Sentinel-2 images demonstrate high thematic accuracy in Europe. *Int. J. Appl. Earth Obs. Geoinf.* 84, 101947. <https://doi.org/10.1016/j.jag.2019.101947>
- Paneque-Gálvez, J., McCall, M.K., Napoletano, B.M., Wich, S.A., Koh, L.P., 2014. Small drones for community-based forest monitoring: An assessment of their feasibility and potential in tropical areas. *Forests* 5, 1481–1507. <https://doi.org/10.3390/f5061481>
- Panlasigui, S., Rico-Straffon, J., Pfaff, A., Swenson, J., Loucks, C., 2018. Impacts of certification, uncertified concessions, and protected areas on forest loss in Cameroon, 2000 to 2013. *Biol. Conserv.* 227, 160–166. <https://doi.org/10.1016/j.biocon.2018.09.013>
- Pasquarella, V.J., Holden, C.E., Woodcock, C.E., 2018a. Improved mapping of forest type using spectral-temporal Landsat features. *Remote Sens. Environ.* 210, 193–207.

- <https://doi.org/10.1016/j.rse.2018.02.064>
Pasquarella, V.J., Holden, C.E., Woodcock, C.E., 2018b. Improved mapping of forest type using spectral-temporal Landsat features. *Remote Sens. Environ.* 210, 193–207.
<https://doi.org/10.1016/j.rse.2018.02.064>
- Persson, M., Lindberg, E., Reese, H., 2018. Tree species classification with multi-temporal Sentinel-2 data. *Remote Sens.* 10, 1–17. <https://doi.org/10.3390/rs10111794>
- Poortinga, A., Tenneson, K., Shapiro, A., Nquyen, Q., Aung, K.S., Chishtie, F., Saah, D., 2019. Mapping plantations in Myanmar by fusing Landsat-8, Sentinel-2 and Sentinel-1 data along with systematic error quantification. *Remote Sens.* 11, 1–19. <https://doi.org/10.3390/rs11070831>
- Reeves, M.C., Winslow, J.C., Running, S.W., 2001. Mapping Weekly Rangeland Vegetation Productivity Using MODIS Algorithms. *J. range Manag.* 54, 0.
- Reeves, M.C., Zhao, M., Running, S.W., 2005. Usefulness and limits of MODIS GPP for estimating wheat yield. *Int. J. Remote Sens.* 26, 1403–1421.
<https://doi.org/10.1080/01431160512331326567>
- Riitters, K., Wickham, J., O'Neill, R., Jones, B., Smith, E., 2000. Global-scale patterns of forest fragmentation. *Ecol. Soc.* 4.
- Röder, A., Udelhoven, T., Hill, J., del Barrio, G., Tsiorliris, G., 2008. Trend analysis of Landsat-TM and -ETM+ imagery to monitor grazing impact in a rangeland ecosystem in Northern Greece. *Remote Sens. Environ.* 112, 2863–2875. <https://doi.org/10.1016/j.rse.2008.01.018>
- Rouse, J.W., Haas, R.H., Schell, J.A., Deering, D.W., 1974. Monitoring vegetation systems in the Great Plains with ERTS, in: Freden, S.C., Mercanti, E.P., Becker, M.A. (Eds.), *Proceedings of the Earth Resources Technology Satellite Symposium NASA SP-351*. NASA, Washington, DC, p. 309–317.
- Saah, D., Johnson, G., Ashmall, B., Tondapu, G., Tenneson, K., Patterson, M., Poortinga, A., Markert, K., Quyen, N.H., San Aung, K., Schlichting, L., Matin, M., Uddin, K., Aryal, R.R., Dilger, J., Lee Ellenburg, W., Flores-Anderson, A.I., Wiell, D., Lindquist, E., Goldstein, J., Clinton, N., Chishtie, F., 2019. Collect Earth: An online tool for systematic reference data collection in land cover and use applications. *Environ. Model. Softw.* 118, 166–171.
<https://doi.org/10.1016/j.envsoft.2019.05.004>
- Sadras, V.O., Cassman, K.G.G., Grassini, P., Hall, A.J., Bastiaanssen, W.G.M., Laborte, A.G., Milne, A.E., Sileshi, G., Steduto, P., 2015. Yield gap analysis of field crops, Methods and case studies. FAO Water Reports 41. FAO: Rome, Italy..
- Sannier, C., Makaga, E.M.K., Fichet, L.V., Mertens, B., Huynh, F., 2011. Monitoring of forest cover change in the Republic of Gabon between 1990, 2000 and 2010 following IPCC guidelines, in: ISPRS.
- Schepaschenko, D., See, L., Lesiv, M., Bastin, J.-F., Mollicone, D., Tsendbazar, N.-E., Bastin, L., McCallum, I., Laso Bayas, J.C., Baklanov, A., Perger, C., Dürauer, M., Fritz, S., 2019. Recent Advances in Forest Observation with Visual Interpretation of Very High-Resolution Imagery. *Surv. Geophys.* 40, 839–862. <https://doi.org/10.1007/s10712-019-09533-z>
- Senf, C., Pflugmacher, D., Wulder, M.A., Hostert, P., 2015. Characterizing spectral-temporal patterns of defoliator and bark beetle disturbances using Landsat time series. *Remote Sens. Environ.* 170, 166–177. <https://doi.org/10.1016/j.rse.2015.09.019>
- Shen, W., Li, M., Huang, C., Tao, X., Li, S., Wei, A., 2019. Mapping annual forest change due to afforestation in Guangdong Province of China using active and passive remote sensing data. *Remote Sens.* 11, 1–21. <https://doi.org/10.3390/rs11050490>
- Shruthi, R.B.V., Kerle, N., Jetten, V., Abdellah, L., Machmach, I., 2015. Quantifying temporal changes in gully erosion areas with object oriented analysis. *Catena*.
<https://doi.org/10.1016/j.catena.2014.01.010>
- Song, C., Woodcock, C.E., Seto, K.C., Pax-Lenney, M., Macomber, S.A., 2001. Classification and change detection using Landsat TM data: When and how to correct atmospheric effects? *Remote Sens. Environ.* 75, 230–244.
- Souza, C.M., Siqueira, J. V., Sales, M.H., Fonseca, A. V., Ribeiro, J.G., Numata, I., Cochrane, M.A., Barber, C.P., Roberts, D.A., Barlow, J., 2013. Ten-year landsat classification of deforestation and forest degradation in the brazilian amazon. *Remote Sens.* 5, 5493–5513.

- <https://doi.org/10.3390/rs5115493>
- Soverel, N.O., Coops, N.C., White, J.C., Wulder, M.A., 2010. Characterizing the forest fragmentation of Canada's national parks. *Environ. Monit. Assess.* 164, 481–499.
<https://doi.org/10.1007/s10661-009-0908-7>
- Stehman, S. V., 2009. Model-assisted estimation as a unifying framework for estimating the area of land cover and land-cover change from remote sensing. *Remote Sens. Environ.* 113, 2455–2462.
<https://doi.org/10.1016/j.rse.2009.07.006>
- Stocking, M.A., Murnaghan, N., 2013. A handbook for the field assessment of land degradation. Routledge.
- Sulik, J.J., Long, D.S., 2016. Spectral considerations for modeling yield of canola. *Remote Sens. Environ.* 184, 161–174. <https://doi.org/10.1016/j.rse.2016.06.016>
- Sweeney, S., Ruseva, T., Estes, L., Evans, T., 2015. Mapping cropland in smallholder-dominated savannas: Integrating remote sensing techniques and probabilistic modeling. *Remote Sens.* 7, 15295–15317. <https://doi.org/10.3390/rs71115295>
- Tapia-Armijos, M.F., Homeier, J., Espinosa, C.I., Leuschner, C., De la Cruz, M., 2015. Deforestation and Forest Fragmentation in South Ecuador since the 1970s – Losing a Hotspot of Biodiversity. *PLoS One* 1–18. <https://doi.org/10.1371/journal.pone.0133701>\r10.5061/dryad
- Taubert, F., Fischer, R., Groeneveld, J., Lehmann, S., Müller, M.S., Rödig, E., Wiegand, T., Huth, A., 2018. Global patterns of tropical forest fragmentation. *Nature* 554, 519–522.
<https://doi.org/10.1038/nature25508>
- Thorne, C.R., Zevenbergen, L.W., Grissinger, E.H., Murphrey, J.B., 1985. Calculator programme and nomograph for on-site predictions of ephemeral gully erosion.
- Tochon, G., Féret, J.B., Valero, S., Martin, R.E., Knapp, D.E., Salembier, P., Chanussot, J., Asner, G.P., 2015. On the use of binary partition trees for the tree crown segmentation of tropical rainforest hyperspectral images. *Remote Sens. Environ.* 159, 318–331.
<https://doi.org/10.1016/j.rse.2014.12.020>
- Tong, X., Brandt, M., Hiernaux, P., Herrmann, S., Rasmussen, L.V., Rasmussen, K., Tian, F., Tagesson, T., Zhang, W., Fensholt, R., 2020. The forgotten land use class: Mapping of fallow fields across the Sahel using Sentinel-2. *Remote Sens. Environ.* 239.
<https://doi.org/10.1016/j.rse.2019.111598>
- Torbick, N., Ledoux, L., Salas, W., Zhao, M., 2016. Regional mapping of plantation extent using multisensor imagery. *Remote Sens.* 8. <https://doi.org/10.3390/rs8030236>
- Unesco, 1978. Tropical forest ecosystems : a state-of-knowledge report / prepared by Unesco, UNEP, FAO, Natural resources research ; 14. Unesco, Paris.
- VanDerWal, J., Falconi, L., Januchowski, S., Shoo, L., Storlie, C., 2019. SDMTools - Species Distribution Modelling Tools: Tools for processing data associated with species distribution modelling exercises.
- Verhegghen, A., Eva, H., Achard, F., 2015. Assessing forest degradation from selective logging using time series of fine spatial resolution imagery in Republic of Congo, in: International Geoscience and Remote Sensing Symposium (IGARSS). <https://doi.org/10.1109/IGARSS.2015.7326202>
- Vieilledent, G., Grinand, C., Rakotomalala, F.A., Ranaivosoa, R., Rakotoariajaona, J.R., Allnutt, T.F., Achard, F., 2018. Combining global tree cover loss data with historical national forest cover maps to look at six decades of deforestation and forest fragmentation in Madagascar. *Biol. Conserv.* 222, 189–197. <https://doi.org/10.1016/j.biocon.2018.04.008>
- Vogels, M.F.A., de Jong, S.M., Sterk, G., Douma, H., Addink, E.A., 2019. Spatio-temporal patterns of smallholder irrigated agriculture in the horn of Africa using GEOBIA and Sentinel-2 imagery. *Remote Sens.* 11. <https://doi.org/10.3390/rs11020143>
- Waldner, F., De Abelleyeira, D., Veron, S.R., Zhang, M., Wu, B.F., Plotnikov, D., Bartalev, S., Lavreniuk, M., Skakun, S., Kussul, N., Le Maire, G., Dupuy, S., Jarvis, I., Defourny, P., 2016. Towards a set of agrosystem-specific cropland mapping methods to address the global cropland diversity. *Int. J. Remote Sens.* 37, 3196–3231. <https://doi.org/10.1080/01431161.2016.1194545>
- Weinstein, B.G., Marconi, S., Bohlman, S., Zare, A., White, E., 2019. Individual tree-crown detection in rgb imagery using semi-supervised deep learning neural networks. *Remote Sens.* 11, 1–13.

<https://doi.org/10.3390/rs11111309>

- Wessels, K.J., Bergh, F. Van Den, Scholes, R.J., van den Bergh, F., Scholes, R.J., 2012. Limits to detectability of land degradation by trend analysis of vegetation index data. *Remote Sens. Environ.* 125, 10–22. <https://doi.org/10.1016/j.rse.2012.06.022>
- Wessels, K.J., Prince, S.D., Malherbe, J., Small, J., Frost, P.E., VanZyl, D., 2007. Can human-induced land degradation be distinguished from the effects of rainfall variability? A case study in South Africa. *J. Arid Environ.* 68, 271–297. <https://doi.org/10.1016/j.jaridenv.2006.05.015>
- White, J.C., Wulder, M.A., Varhola, A., Vastaranta, M., Coops, N.C., Cook, B.D., Pitt, D., Woods, M., 2013. A best practices guide for generating forest inventory attributes from airborne laser scanning data using an area-based approach, *Forestry Chronicle*.
<https://doi.org/10.5558/tfc2013-132>
- Xiong, J., Thenkabail, P.S., Gumma, M.K., Teluguntla, P., Poehnelt, J., Congalton, R.G., Yadav, K., Thau, D., 2017a. Automated cropland mapping of continental Africa using Google Earth Engine cloud computing. *ISPRS J. Photogramm. Remote Sens.* 126, 225–244.
<https://doi.org/10.1016/j.isprsjprs.2017.01.019>
- Xiong, J., Thenkabail, P.S., Tilton, J.C., Gumma, M.K., Teluguntla, P., Oliphant, A., Congalton, R.G., Yadav, K., Gorelick, N., 2017b. Nominal 30-m cropland extent map of continental Africa by integrating pixel-based and object-based algorithms using Sentinel-2 and Landsat-8 data on google earth engine. *Remote Sens.* 9, 1–27. <https://doi.org/10.3390/rs9101065>
- Xu, H., Hu, X., Guan, H., Zhang, B., Wang, M., Chen, S., Chen, M., 2019. A remote sensing based method to detect soil erosion in forests. *Remote Sens.* 11. <https://doi.org/10.3390/rs11050513>
- Zenkevich, J., Aksenov, D., Loshkareva, A., Gluskhov, I., Tikhomirova, O., Sementsova, M., 2015. Developing of remote sensing monitoring system for logging activities in CarBi monitoring area. Moscow.
- Zhang, C., Zhou, Y., Qiu, F., 2015. Individual tree segmentation from LiDAR point clouds for urban forest inventory. *Remote Sens.* 7, 7892–7913. <https://doi.org/10.3390/rs70607892>
- Zhang, Q., Hakkenberg, C.R., Song, C., 2018. Evaluating the Effectiveness of Forest Conservation Policies with Multitemporal Remotely Sensed Imagery: A Case Study From Tiantangzhai Township, Anhui, China, *Comprehensive Remote Sensing*. Elsevier Inc.
<https://doi.org/10.1016/b978-0-12-409548-9.10435-x>
- Zhen, Z., Quackenbush, L.J., Zhang, L., 2016. Trends in automatic individual tree crown detection and delineation-evolution of LiDAR data. *Remote Sens.* 8, 1–26. <https://doi.org/10.3390/rs8040333>

15. Annex (external documents)

Annex 1: Overview of very high and medium resolution satellite systems and their properties.

Annex 2: Overview of existing, value-added data sets such as forest maps and their properties.

Annex 3: Characteristics of selected medium and very high-resolution remote sensing systems.

Annex 4: Assessing the classification accuracy of indicator maps.

*Annex 5: Brief guideline for the collection of in-situ reference data or mapping land use /land cover (especially *prosopis juliflora*) with satellite image classification.*

Annex 6: Brief summary of useful guidelines for the collection of in-situ reference data in forestry applications.

[End of document]





Open Source Guide to Earth Observation in Development Corporation
Methods and guidance from the joint initiative MAPME

More Information on the project homepage (<https://mapme-initiative.org>)
or contact us: contact@mapme-initiative.org



MAPME
maps for planning,
monitoring & evaluation